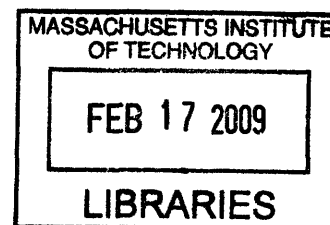# Improved Filtration Membranes through Self-Organizing Amphiphilic Comb Copolymers

by

Ayse Asatekin Alexiou

B.S. Chemical Engineering
Middle East Technical University, 2002
B.S. Chemistry
Middle East Technical University, 2003

Submitted to the Department of Chemical Engineering in Partial Fulfillment of the
Requirements for the Degree of

Doctor of Philosophy in Chemical Engineering

at the

Massachusetts Institute of Technology

February 2009

Signature of Author: _____

Ayse Asatekin Alexiou
Department of Chemical Engineering
January 2009

Certified by: _____

Anne M. Mayes
Toyota Professor of Materials Science and Engineering
Thesis Supervisor

Certified by: _____

Michael F. Rubner
TDK Professor of Polymer Materials Science and Engineering
Thesis Supervisor

Accepted by: _____

William M. Deen
Professor of Chemical Engineering
Chairman, Committee for Graduate Students

1

Improved Filtration Membranes through Self-Organizing Amphiphilic Comb Copolymers

by

Ayse Asatekin Alexiou

Submitted to the Department of Chemical Engineering in partial fulfillment of the requirements for the degree of Doctor of Philosophy in Chemical Engineering

Abstract

The operating cost of a membrane filtration system is generally determined by two major factors: the permeability of the membrane to water, and the lifetime of the membrane. Both of these are strongly affected by the chemical structure and surface properties of the membrane. Hence, the development of novel membrane materials that improve these two properties would make membrane treatment of water streams cheaper. One of the most important reasons for low permeability and short membrane life is fouling, which makes it one of the most important challenges faced in membrane operations, especially in processes where the feed has high concentrations of biomolecules, such as wastewater treatment, and in food and biochemical industries.

In this thesis, the self-organization of amphiphilic comb copolymers is employed to develop improved membranes for aqueous filtration. The use of self-assembling copolymers leads to the desired properties (surface chemistry, selectivity) without additional processing steps.

One aspect of this thesis focuses on the development of size-selective nanofiltration (NF) membranes that can fractionate small molecules by size through the microphase separation of the amphiphilic comb copolymers. This size scale corresponds to a "missing link" in the separations currently offered by commercial membranes. Such membranes formed by coating a porous support membrane with the comb copolymer poly(vinylidene fluoride)-*graft*-poly(ethylene oxide methacrylate) (PVDF-*g*-POEM) were first introduced by Akthakul *et al.* (Macromolecules 37 (2004) 7663-7668). The microphase separation of the comb copolymer results in the formation of interconnected effective "nanochannels" of the hydrophilic poly(ethylene oxide) (PEO) side-chains, which allow water permeability and size selectivity. This thesis includes work that characterizes the fouling resistance of these membranes in more detail, including their performance in the presence of various foulants as well as in the context of membrane bioreactor (MBR) operation for wastewater treatment. In each of these cases, PVDF-*g*-POEM thin film composite (TFC) NF membranes were shown to resist irreversible fouling completely, recovering their initial flux upon cleaning with water. The mechanism of this exceptional resistance to adsorptive fouling was attributed to net steric repulsion forces between the PEO brush formed on the membrane surface and the foulant molecule, based on interaction force measurements. The ability to fine-tune the pore size

of these membranes by feed properties such as temperature, pressure, and ionic strength was also studied in this thesis. The degree of swelling of the PEO chains in the feed determines the effective diameter of the nanochannels, and the variations in selectivity and water flux can be related with the phase diagram of PEO/water mixtures as predicted. The combination of these properties make PVDF-g-POEM TFC NF membranes very promising for the food and pharmaceutical industries, where different and fine-tuned separations are needed at different stages of the production process, and feeds have large concentrations of biomolecules that lead to severe fouling.

Another objective of this study was to extend the size-selective NF membranes to different copolymer chemistries. Such membranes were prepared and characterized from the comb copolymer polyacrylonitrile-*graft*-poly(ethylene oxide) (PAN-g-PEO). This copolymer is synthesized using free radical copolymerization, a method with simpler scale-up and good control over copolymer composition, both of which posed difficulties in the use of PVDF-g-POEM. PAN-g-PEO TFC NF membranes also showed high fluxes, size-based selectivity, and complete resistance to irreversible fouling.

Amphiphilic comb copolymers with PEO side-chains have also been used to impart fouling resistance to ultrafiltration (UF) membranes. The comb copolymer is added to the casting solution during the manufacture of the membrane by phase inversion, and segregates to the polymer surface during coagulation to form a fouling-resistant PEO brush on the polymer/water interface (Hester *et al.,* Macromolecules 32 (1999) 1643-1650). This thesis introduces PAN-based UF membranes prepared by this method, using PAN-g-PEO as an additive. Such membranes were shown to exhibit significantly enhanced flux. Furthermore, PAN/PAN-g-PEO blend UF membranes resist irreversible fouling completely, recovering their initial flux completely upon a water rinse or backwash. This property is exceptional, and has not been reported for any other polymeric porous membrane system, to the author's knowledge. The fouling resistance of these membranes arises from a steric repulsion of foulant molecules by the PEO brush. The performance of these membranes in the context of the filtration of oily wastewaters, a process severely impacted by fouling, has also been demonstrated in this thesis. PAN/PAN-g-PEO blend UF membranes promise to cut costs and energy use significantly in several UF applications limited by fouling, including municipal and industrial wastewater treatment, MBRs, and separations in the food and pharmaceutical industries.

Overall, this thesis was instrumental in extending, developing and understanding the use of the self-organization of amphiphilic comb copolymers in the manufacture of better filtration membranes, and bringing this method closer to industrial application. This approach can be extended to design different comb copolymer chemistries for applications such as heavy metal removal, affinity filtration, and desalination.

3

Table of Contents

5

List of Figures

List of Tables

Acknowledgements

First and foremost, I would like to thank Professor Anne Mayes, who supervised the work presented in this thesis from the beginning, and guided me and supported me through this process. She has been a true mentor and teacher to me, and I learned much more than science from her: I admire her creative and inspired way of thinking, her brilliant scientific vision, her excitement in research, her energy in teaching, her effort to direct her work towards environmentally sensitive subjects, and her endless enthusiasm that carried me through when I lost motivation. I am truly grateful for all her help and support, which she didn't give up even while going through difficult times herself. I appreciate her guidance and mentorship as I am trying to start an academic career myself, and the way she trained me through my doctorate for that purpose. I will do my best to be worthy of her faith and trust in me.

I would also like to thank Professor Michael Rubner, who supervised me at the later stages of my project. He was also the person who led me to Professor Mayes while I was searching for a thesis subject. His support and help allowed me to keep working on my research without worrying about funding and bureaucracy. His wisdom, advice and feedback were influential throughout these few years when I was lucky to work for him.

I would also like to acknowledge my thesis committee, Professor Paula Hammond and Professor William Deen, whose advice has been very helpful in directing my research. I appreciate the teaching opportunities I had during my time here. For that, I am thankful to Professor Hammond and Professor Gregory Rutledge, as well as Professor Christopher Love, Professor John Lienhard and Doctor Jean-Francois Hamel.

I had the opportunity to work with and learn from so many great people at MIT, especially in Mayes group. Professor Metin Acar and Sebnem Inceoglu taught me a lot about synthesis starting the moment I arrived here, while Caitlin Devereux and Ariya Akthakul taught me about membranes. I am thankful for the caring friendship and unselfish and patient help and teaching of Juan Gonzalez, William Kuhlman, Elsa Olivetti, Sang Woog Ryu, Ikuo Taniguchi, and Nathan Lovell. Nathan deserves additional thanks for being there for me to the end, and keeping me company and the Mayes lab together even when only the two of us were left. I would also like to send additional thanks to Juan for teaching me all about the DSC and being a true friend, Will for his endless knowledge in chemistry and chromatography and his cheerful sarcasm, Elsa for all the TEM she did for me and her never fading smile, and Sang Woog for teaching me many things about polymer synthesis. Two undergraduate students who I had the opportunity to work with, Emily Guilotti and Jennifer Gagner, have also been very helpful in the course of this project. I am also grateful to all other Mayes group members, who taught me so much and made Mayes lab like family: Ozge Akbulut, Ikuo Taniguchi, Solar Olugebefola, Jong Hak Kim, Long Hua Lee, Sheldon Hewlett, Sarah Ibrahim, Simon Mui, and Jane Park. I would also like to thank Elizabeth Shaw for patiently teaching me about XPS, and Dr. Anthony Garratt-Reed for training me to use the SEM. The members of Rubner and Cohen groups, who are too many to list here, also

This work would not have been possible without the love and support of many people who are very close to my heart, who kept me going, kept me sane, and were there in days of happiness, sadness, frustration and celebration alike.

I would first like to thank my sweet husband, Alexander Alexiou. Meeting him was one of the best things that ever happened to me. I am thankful to him for always being there for me, for always having the right words, for encouraging me when I am frustrated, calming me down when I am upset and cheering for me when things are going well. He is my love, my true friend, my sanctuary from the craziness of the world, the one that makes everything feel right at the end of the day.

I would like to deeply thank Sezen Buell, who has been my best friend and my companion in life in so many ways. As we sailed through many life experiences together, similar in so many ways and different in many others, we became like each other's family across an ocean from our home country. I am very lucky to have her, and I wish her the best of luck for her own doctorate.

I also would like to thank many friends at MIT who have made these years worthy of every effort, and never left me alone, including Nebibe Varol, Yasemin Sancak, Ulas Ziyan, Serena Povia, Jorge Vieyra, Pinar Kurt, and many others. I send my thanks to my long time friends, Filiz Toprak, Cem Kayaligil, Gozde Kilic and Cihan Oguz, who were there for me even though they were far away geographically.

Many members of my family also deserve my thanks. My late grandfather, Sevki Kaptanoglu, was the engineer in the family and I wish he got to see this. I also thank my grandmother, Sabahat Kaptanoglu, for all her love and support, as well as my grandfather Halil Asatekin, my uncles Cuneyt Kaptanoglu and Selcuk Asatekin, my aunts Selda Kaptanoglu and Aysegul Asatekin, and my cousins Caner, Engin, Ahmet and Sinem. I also appreciate the support of my parents-in-law Alice and Nick Alexiou, my brother-in-law Joseph Alexiou, and my grandmother-in-law Esther Sparberg.

My sister, Cigdem Asatekin, also deserves my thanks for being an amazing friend to me, for sharing everything with me, for her honesty, sweetness and craziness, and for motivating me to be a good person all my life. She influenced the person I became very much. I send her all my love, and I hope she follows her heart and finds success in what she truly wants to do, like me.

Last but not the least, deepest thanks go to my parents, Gul and Mehmet Asatekin, who have brought me up to be the person I am and inspired me all my life. They have always supported me even when they missed me a lot, just as I missed them, so I can be the best at what I really want to do. They have also inspired me to go into academia, and were role models to me in many ways. They were always there for me when I needed guidance and support. I would not be the person I am without them. I cannot thank them enough for all they did.

Chapter 1:

Scope and overview

1.1. Scope

This thesis explores the development of new water filtration membranes with improved properties based on the self-assembly of amphiphilic comb copolymers. Membrane-based separations have been studied since the 1960s. During this time, membranes improved to a great extent, and penetrated into many industries including food and biotechnology, in addition to becoming much more widely used in water treatment applications. Today, as issues such as pollution, sustainability and water shortage have become part of the mainstream debate, membrane technologies are gaining even more importance [1, 2].

The feasibility of a membrane operation is often determined by the cost in comparison to conventional systems. This cost is generally determined by two major factors: the permeability of the membrane to water, and the lifetime of the membrane. Both of these are strongly affected by the chemical structure and surface properties of the membranes. Hence, the development of novel membrane materials that improve these two properties would make membrane treatment of water streams cheaper.

One of the most important reasons for low permeability and short membrane life is fouling, which is a decline in membrane permeability due to the narrowing and blocking of its pores by components in the feed, such as solutes and particulates. The feed streams in most membrane operations contain large amounts of organic molecules and macromolecules that adsorb on the membrane surface and clog its pores, resulting in the organic fouling of the membrane. This type of fouling is generally not reversible by physical methods such as rinsing and backwashing. Chemical cleanings, often involving strong agents such as caustic and acidic solutions, are needed to recover the flux, but these chemicals often also degrade the membrane material. Hence, a membrane that will

resist organic fouling would have the potential to both maintain high permeabilities and to last a longer time, as fewer cleanings are needed [1, 2]. One premise of this thesis was to develop such membranes, in order to improve existing membrane operations and open new fields of application.

The self-organization abilities of copolymers of various blocky architectures offer many possibilities in developing functional membrane materials that incorporate desired qualities of high permeability and fouling resistance. Mayes and coworkers have generally focused on the amphiphilic comb (or graft) copolymer architecture for membrane applications in past efforts [3-12], and molecules with this basic structure, are also central to this thesis.

One component of this work will build off the approach pioneered by Hester *et al.* using surface-segregating comb copolymers to create surface modified ultrafiltration (UF) membranes based on poly(vinylidene fluoride) (PVDF) [3-7], and extended to polysulfone-based UF membranes by Park *et al.* [8, 9]. This thesis employs the same approach for polyacrylonitrile (PAN) based membranes using a new amphiphilic comb chemistry, and describes their exceptional performance in different applications [13-16]. These novel PAN membranes appear unique in the published literature on UF membranes in their ability to completely resist irreversible fouling by organic molecules.

Another issue encountered in the membrane market is the absence of size-selective membranes with pore sizes below 2 nm, or a molecular weight cut-off (MWCO) below 10,000 g/mol. This size scale is too small to achieve effective separations by UF membranes. Nanofiltration.(NF) membranes, defined by their effective pore size between 0.5-2 nm, are generally charged and do not perform size-selective separations. Hence, there is essentially a "missing link" in the separations that can be obtained with the membranes available today. Development and improvement of such membranes is another objective of the work in this thesis.

This latter portion of the effort makes use of the natural tendency for comb/graft copolymers to form bicontinuous structures upon microphase separation of the hydrophobic backbone and hydrophilic side-chains [5, 10-12] The side-chains of such a

copolymer form effective "nanochannels" that allow the permeation of water as well as molecules that can fit through them. This property was first exploited by Akthakul *et al.* to make membranes that can fractionate small molecules and nanoparticles by size while resisting fouling [10-12]. These membranes, prepared by solution coating a porous UF support membrane with the copolymer poly(vinylidene fluoride)-*graft*-poly(oxyethylene methacrylate) (PVDF-*g*-POEM), were further analyzed as a part of this thesis. Their fouling resistance properties in a variety of applications were studied, as well as the mechanism of their fouling resistance [17]. The responsive properties of such membranes, arising from the tunable swelling of the side-chains lining the nanochannels, were also demonstrated [18]. This capability would be very useful in fine tuning the selectivity of these membranes to the separation desired. Finally, NF membranes founded on the same mechanism of microphase separation were developed in a PAN-based chemistry. These membranes were prepared by coating a porous base membrane with the new comb copolymer, polyacrylonitrile-*graft*-poly(ethylene oxide) (PAN-*g*-PEO). This copolymer is synthesized by free radical copolymerization, a method that offers significantly better composition control and easier scale-up, bringing these NF systems a step closer to industrial implementation.

1.2. Overview

Chapter 2 is a general overview of membrane technology, with a special focus on concepts that are of importance in the later chapters. It starts with the historical development of membrane technology, and gives background information on aqueous membrane filtration processes. It also includes definitions of key performance parameters such as flux and retention. Finally, it introduces mechanisms involved in membrane fouling and details state-of-the-art approaches to preventing it.

Chapter 3 focuses on further development of poly(vinylidene fluoride)-based size-selective nanofiltration (NF) membranes developed previously in our group. The ability of these membranes to resist fouling is explored in the context of application to membrane bioreactors. Atomic force microscopy (AFM) experiments that measure the interaction between model foulants and the membrane surface give some insight into the

mechanism of fouling resistance. In addition, the ability to adjust the effective pore size of these membranes with process parameters such as temperature, pressure and ionic strength is demonstrated.

Chapter 4 introduces novel composite NF membranes based on polyacrylonitrile-*graft*-poly(ethylene oxide) (PAN-*g*-PEO). The synthesis and characterization of the copolymer and the manufacture of the membranes are described. The ability of these membranes to perform size-based separations is demonstrated. Moreover, it is shown that these membranes resist irreversible protein fouling completely.

Chapter 5 focuses on ultrafiltration (UF) membranes that are prepared using PAN-*g*-PEO as a surface-segregating additive to prevent fouling. These novel membranes exhibit complete resistance to irreversible fouling by various foulants, and can recover their initial flux by a water rinse. The additive also improves the flux and wettability. These properties show great promise for better economics for membrane processes that involve feeds with high fouling potential, by decreasing energy, cleaning and membrane replacement costs significantly.

Chapter 6 demonstrates a specific application of the membranes based on PAN-*g*-PEO, described in Chapters 4 and 5. The oil industry produces large amounts of wastewater that is difficult to treat due to large degrees of oil contamination. This chapter compares the performance of a commercial UF membrane with PAN-*g*-PEO containing UF and NF membranes in the treatment of three samples of oil industry wastewater. Both UF membranes show similar retention properties, while the NF membranes show only slightly higher organics removal. However, PAN-*g*-PEO containing UF and NF membranes show significantly better resistance to fouling, maintaining a higher portion of their initial fluxes during filtration and recovering their initial fluxes by a backwash even with these demanding feeds. This shows promise in improving the economics of membrane processes for this application.

Finally, Chapter 7 includes a summary of conclusions, and an outlook of the implications of this research, including future research opportunities.

Chapter 2:

Background: Polymeric membranes for water filtration

2.1. Introduction & Historic Development

A membrane can broadly be defined as a discrete interface that regulates the permeation of species in contact with it [1]. This very general definition applies to a wide variety of interfaces, including biological membranes such as the cell membrane, as well as synthetic membranes used in industry for a variety of separations.

Membrane phenomena have been studied since the 18th century. The first discovery in this area was the description of osmosis by Nollet. Early investigators used diaphragms such as animal bladders as laboratory tools through the 19th and early 20th centuries, and the use of such membranes contributed to important physical and chemical theories, including the van't Hoff equation and the kinetic theory of gases [1].

Membrane science and technology entered a new phase in 1907, when Bechhold developed nitrocellulose membranes that could be prepared with different permeabilities reproducibly. Zsigmondy and Bachman, as well as other researchers, used these membranes to separate macromolecules and fine particles from aqueous solution [19]. In 1937, nitrocellulose membranes became commercially available. The first significant application of the membranes was in testing drinking water safety during World War II [1].

A milestone in membrane technology was the development of high-flux, asymmetric cellulose acetate membranes by Loeb and Sourirajan in 1962 [20]. These membranes have a thin, dense skin layer supported by a thicker, microporous substructure, a morphology that results naturally from the immersion precipitation process used in their

fabrication. This discovery transformed membrane separation from a laboratory tool to an industrial process, and made reverse osmosis practical. Soon, synthetic polymers such as polyacrylonitrile and polysulfone were being made into porous membranes using the same process [19]. Another breakthrough was the invention of interfacially polymerized composite membranes for reverse osmosis by Cadotte in 1972 [21]. Improvements in membrane stability and the development of better membrane modules followed. By 1980, microfiltration, ultrafiltration, reverse osmosis and electrodialysis were all established processes [1].

The market for cross-flow filtration membrane modules and equipment was estimated to be $6.8 billion in 2005, and $7.6 billion in 2006 [22, 23]. Tightening environmental regulations were a contributor to this growth, as well as falling membrane costs making them competitive with conventional processes such as sand filtration for wastewater remediation. Increasing energy costs also resulted in reverse osmosis membrane systems being preferred over distillation for desalination. Membrane markets are expected to continue their strong growth trajectory, with cross-flow systems alone becoming a $10 billion business by 2010 worldwide [22, 23].

2.2. Classification of Aqueous Membrane Separations by Pore Size

Membranes, as well as the filtration processes in which they are used, are often classified according to their effective pore size. This is both because membrane applications are mostly determined by the separation desired (i.e., what needs to be retained, and what needs to be allowed through), and because membranes whose selectivities are similar often have morphological similarities. The most typical classes of membranes used in liquid filtration are, in order of decreasing effective pore size, microfiltration (MF), ultrafiltration (UF), nanofiltration (NF) and reverse osmosis (RO). The range of pore sizes for each of these membrane classes, along with the characteristic sizes of species of interest in water-based applications, are shown in Figure 2.1. Of these membrane types, UF and NF are described in more detail here due to their relevance in this thesis.
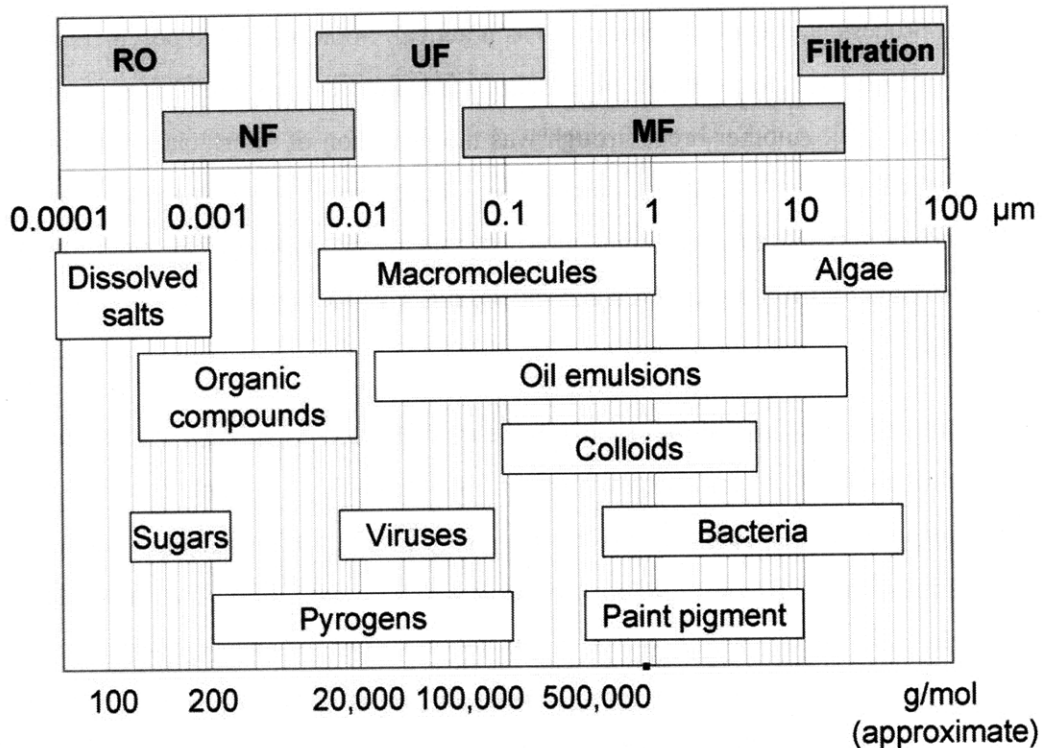
Figure 2.1. Membrane separation spectrum for water-based filtrations.

2.2.1. Microfiltration

Microfiltration (MF) membranes retain suspended particles with diameters between 0.1 to 10 μm. Their most common application arises from their ability to retain microorganisms. The first application of MF membranes was in the culture of microorganisms in drinking water to monitor water supply contamination during World War II in Germany [1]. MF membranes are still used for cell culture. MF membranes that retain all viable bacteria are used in the pharmaceutical industry for sterile filtration to produce injectable drug solutions [24]. Cold sterilization of beer and wine is also done with MF membranes [25]. Finally, MF cartridges are frequently used in the polishing of ultrapure water, and in drinking water treatment [1, 26].

2.2.2. Ultrafiltration

Ultrafiltration (UF) membranes retain macromolecules and colloids, while allowing water and small molecules through. Their pore size is between 2 -100 nm [2]. The first UF plant was installed in 1969 to recover electrocoat paint from automobile paint shop rinse water. The food industry began using UF processes shortly thereafter for protein separation from milk whey and for apple juice clarification [2]. UF is also used in wastewater treatment, especially for oily streams [27] and in cases where the component to be recovered is valuable. In the biotechnology industry, UF is employed for a range of separations in enzyme production, cell harvesting, and virus production [2, 24]. It's also used to pretreat water for desalination by reverse osmosis [28], and in membrane bioreactors (MBRs), which combine suspended microbial treatment of wastewater with membrane-based separation [29, 30]. In essentially all of these applications, membrane fouling is the most severe obstacle to wider use [31, 32].

Most ultrafiltration membranes have an asymmetric morphology, with a thin, finely porous skin layer supported by a thick, more open support layer. Figure 2.2 shows scanning electron micrographs of the surface (a) and cross-section (b) of a commercial asymmetric membrane, manufactured of polyacrylonitrile for ultrafiltration applications. The selectivity of the membrane is determined by the thin top layer, typically 0.1-2 μm in thickness (seen in Figure 2.2a, and facing downward in Figure 2.2b), while the microporous bottom layer provides the needed mechanical support. Such membranes are naturally formed by so-called "phase inversion" techniques [20]. There are also some commercial examples of asymmetric UF membranes with a more gradual pore size gradient from top to bottom, as well as symmetric UF membranes.
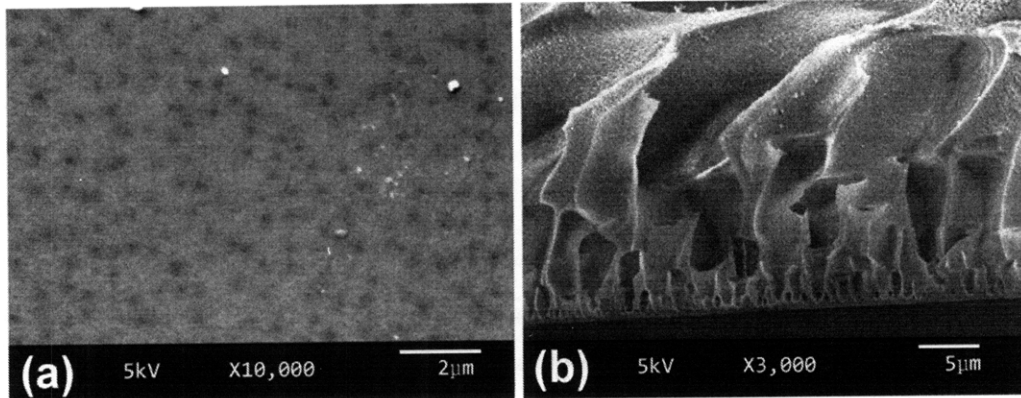
Figure 2.2. Scanning electron microscopy (SEM) images of a PAN-400 ultrafiltration membrane, manufactured by Sepro Membranes, Inc.: (a) selective layer surface; (b) cross-section with the selective layer facing downward.

Common materials for UF membranes include polyethersulfone (PES), polysulfone (PSf), poly(vinylidene fluoride) (PVDF), polyacrylonitrile (PAN), poly(etherimide) (PEI), and cellulose acetate (CA) [2]. Selection of membrane materials is based on the temperature and pressure of filtration as well as feed characteristics such as pH, oil content, and fouling potential. PES and PSf membranes are resistant to extreme pH levels, and have good thermal stability. However, their hydrophobic nature limits their wettability and makes them susceptible to fouling. PVDF has exceptional chemical resistance and good thermal stability up to 140°C. It is more resistant to a range of solvents than PSF and PES, but still suffers from high fouling tendency due to hydrophobicity. PEI membranes can be used at higher temperatures than PVDF, but suffer from poorer chemical stability [2]. PAN is a relatively hydrophilic membrane material in comparison with the others above, but it is still subject to fouling, and is less resistant to high temperatures or drying [33]. Cellulosic membranes resist fouling better, but are subject to degradation by microorganisms [34].

2.2.3. Nanofiltration

Nanofiltration (NF) membranes were developed after reverse osmosis membranes (RO), for applications in the range between RO and UF. Commercial NF membranes are

typically of similar chemistry and structure to RO membranes, but with nominal pore size of around 1 nm [1], which provides for generally higher fluxes compared with RO. NF membranes have NaCl rejections between 20-80%, high retention of doubly charged ions including hard components, and molecular weight cut-offs for dissolved organic components of 200-1000 Daltons [35]. NF membranes are often used in the softening of groundwater [34, 35], and the purification of surface water for drinking water production [35, 36]. In these applications where feed quality can fluctuate drastically over time, membranes have great advantage in the maintenance of effluent quality. The application of NF membranes in wastewater treatment has also been studied, particularly for wastewater from the textile industry to enable water reuse, and for MBR treatment of wastewater [17, 37], due to their ability to remove trace contaminants such as endocrine disrupting agents and pharmaceuticals [1, 34].

NF membranes generally have a thin film composite (TFC) structure, consisting of a porous support layer of one polymer covered with an ultra-thin layer of a second polymer that determines the selectivity properties of the membrane. It is very similar to phase inversion membranes with a completely non-porous selective layer. However, the composite structure has one major advantage: it allows the use of polymers for the selective layer that cannot be processed to form a porous membrane structure, such as cross-linked polymers or charged polymers with poor solubility in common solvents. Such polymers can be formed as selective layers *in situ* using interfacial polymerization, a common method for the manufacture of NF membranes [34].

The rejection of solutes by NF membranes is complex, having contributions from pore transport and solution-diffusion mechanisms, as well as Donnan exclusion of charged species in feed solutions due to charged groups (usually negative) on the membrane surface [34]. Overall, the size cut-off of the membrane is in the range of small molecules. Most NF membranes will retain oligosaccharides, partially retain di- and tri-saccharides, and allow the passage of glucose [34]. NF membranes capable of size-based separation with sub-nanometer resolution could attract significant markets in the chemical, pharmaceutical and food industries. Such membranes will be described and investigated further in this thesis in Chapters 3 and 4.

As with other membrane classes, today's commercial NF membranes exhibit substantial fouling. In their widest current application of surface and ground water treatment, a chief foulant is natural organic matter (NOM): matter that is created by the degradation of biological organisms in the ground and leached into water. NOM contains mostly humic substances such as humic and fulvic acids, and can cause severe and irreversible fouling, especially in the presence of calcium ions. Each divalent calcium ion can complex with two carboxyl groups on humic acid molecules, resulting in the formation of a gel layer on the membrane surface. Negative charges often present on the membrane itself cause the gel to adhere to the surface as well, making it difficult to remove [38, 39]. Extensive research is ongoing in the area of fouling-resistant membranes [35], which is a major focus of the work presented in Chapters 3, 5 and 6 of this thesis.

2.2.4. Reverse osmosis

Reverse osmosis (RO) was the first polymer membrane filtration process to be employed on a commercial scale, after the development of phase inversion membranes [2, 20]. RO membranes retain essentially all solutes in water, including small ions such as sodium and chlorine. The most prominent application of RO is in the desalination of brackish and sea water to produce drinking water. It is also widely used in the production of ultrapure water for the electronic and pharmaceutical industries [1]. RO is considered to be promising for wastewater treatment applications, but currently, it is only economical in cases where the components to be recovered are valuable, such as the recovery of nickel from nickel-plating rinse tanks [1].

The effective pore size of a RO membrane is in the range of 3 to 5 Å. This is in the range of the thermal motion of the polymer chains, so the selective layer of a RO polymer membrane is generally non-porous. Separation in reverse osmosis membranes occurs due to the preferential dissolution of molecules in this layer combined with differences in the diffusion rates, known as the solution-diffusion model [2]. To enable reasonable fluxes while maintaining a non-porous selective layer, RO membranes have an asymmetric structure. Cellulose acetate (CA) membranes with nonporous selective layers made by the phase inversion process once dominated the RO market, but the majority of RO

membranes in use today are thin film composite (TFC) membranes with an ultra-thin selective layer [34] formed by interfacial polymerization in situ on top of a porous support membrane. The selective layer is generally a cross-linked, charged aromatic polyamide while the substrate is often an asymmetric PSF or PES UF membrane [1, 34].

2.3. Membrane Fabrication

Polymeric membranes are manufactured by several main methods depending on the structure desired, which varies with application. In this section, two membrane preparation methods that have been employed in this project are described: Phase inversion, used to prepare UF membranes described in Chapter 5, and membrane coating, used in the preparation of the NF membranes described in Chapters 3 and 4.

The phase inversion process, also termed immersion precipitation, is the most common method of preparing porous membranes from polymers. The technique was first described by Loeb and Sourirajan in 1962 [20]. To precipitate the polymer membrane from a film of solution, the Loeb-Sourirajan method uses immersion into a non-solvent for the polymer, such as water, that also removes the solvent from the system [40-42]. RO membranes cast by this method have a completely dense top skin layer, with an underlying microporous support structure. UF and MF polymer membranes are also largely produced by this method, and have a similarly anisotropic structure, as shown in Figure 2.2b. However, the skin layer in these membranes is very finely microporous (Figure 2.2a), while the porous support structure is often more open. Allowing a drying time for the deposited polymer solution film before coagulation can aid in the formation of a skin layer [41].

Figure 2.3 shows a schematic diagram of an industrial system for membrane manufacture using this method. The casting solution is poured onto a substrate, often including a non-woven backing fabric, and formed into a film of 50-200 μm thickness by a doctor blade. The film is then immersed into the coagulation bath, often consisting mostly of water. It might also contain additives to regulate membrane morphology and pore size. To avoid the creation of defects and unevenness in the membrane, the immersion must be done under carefully controlled conditions, at a constant speed, and at an angle to prevent

waves from forming on the bath surface. The membrane develops as the polymer precipitates in the coagulation bath. After the coagulation step, there is sometimes a heat treatment step where the membrane is annealed in a heated water bath to refine the morphology.
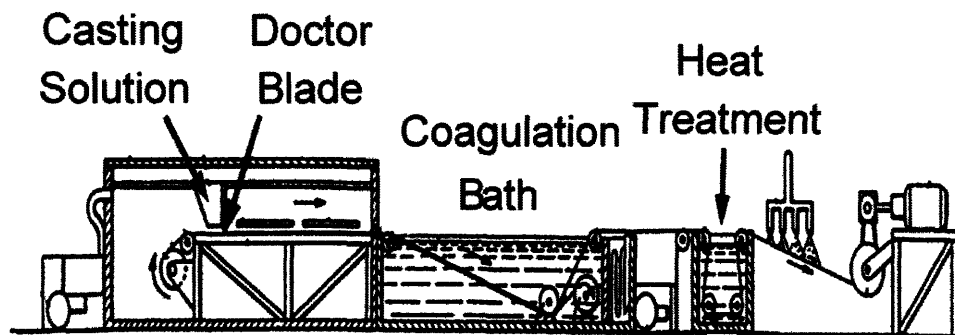
Figure 2.3. Schematic diagram of an industrial phase inversion casting operation.

In the phase inversion process, tailoring of the membrane morphology, pore size, and degree of porosity is achieved by altering the phase separation kinetics and/or thermodynamics involved in the process [1]. One of the most significant parameters is the composition of the casting solution, including the choice of solvent, the concentration of polymer, and use of pore forming additives such as poly(ethylene glycol) (PEG) and poly(vinyl pyrrolidone) (PVP), water-soluble small molecules like glycerol, or salts like zinc chloride [1, 41, 43]. Some portion of these components, especially the polymeric additives, may remain trapped in the membrane even after precipitation and rinsing, making it more hydrophilic. Casting bath parameters also have a strong effect on final membrane structure. The pore size and morphology of the membrane is strongly affected by the temperature of the coagulation bath, as well as the addition of organic solvents and other additives [40, 41].

The phase separation that takes place upon immersion of the polymer solution film into the casting bath is a complicated process involving the diffusion of solvent and non-solvent, liquid-liquid demixing, gelation, and vitrification or crystallization of the

26

polymer [40, 41]. While there exists a general understanding of how parameters such as chemistry and temperature affect final membrane morphology, attempts to model the process emphasize qualitative rather than quantitative prediction [1]. Even today, the design of a new membrane is very much a trial-and-error process. Membrane manufacturers guard closely their proprietary formulas and methods, and most experts still describe the process of membrane design as a black art [1, 41].

Membranes prepared by the phase inversion method have the advantage of high porosity, reaching up to 90% through their cross-section (their selective layer porosities are substantially lower). The pore structures in the support layer are generally highly interconnected [1, 44]. The combination of these two factors results in high intrinsic permeabilities. One drawback of this manufacturing method, however, is that the resulting pore size distribution is often broad [45, 46]. This polydispersity prevents sharp permeate size cut-offs. Membranes that combine the high flux of phase inversion membranes with the narrow pore size distribution of track-etched membranes are an active area of research [12, 47, 48].

Porous membranes formed by phase inversion often serve as a support layer for TFC membranes, where the selective layer is a thin, dense coating covering the membrane surface. While most thin film composite membranes are formed by interfacial polymerization in situ, they can alternately be prepared by dip coating a microporous support membrane into a polymer solution, prepared with a volatile solvent, to create a liquid layer 50-100 μm thick. The membrane is then dried, leaving a selective film layer 0.5-2 μm thick [34, 49]. For this process to create defect-free membranes, the microporous support must be clean, low in defects and very finely microporous at the surface. As the selective layer is very thin, the permeability of the support can significantly affect that of the final membrane [1, 34, 50]. Because the selective layer of most TFC membranes is very thin and delicate, often a protective layer of a water-soluble polymer such as poly(vinyl alcohol) (PVA) is coated onto the membrane to prevent damage by mechanical abrasion until use [34, 49].

2.4. Parameters Quantifying Membrane Performance

The most important property of membranes is their ability to control the rate of transport of different species. Therefore, certain permeation-related parameters of membranes are routinely checked, as they are considered representative of their performance. Some of these are flux, permeability, rejection of specific solutes and molecular weight cut-off. These terms, used routinely in the following chapters, are defined below.

2.4.1. Flux and permeability

The flux J_i of component i through a membrane is defined as the flow rate Q_i of that component through the area A of membrane used:

$$J_i = \frac{Q_i}{A}$$

(2.1)

For a membrane to be effective, the flux for the component that is desired to pass through the membrane (such as water) should be high, and the flux for the component to be retained (such as suspended oil) should be low. Fluxes in liquid filtrations are typically reported in units of $L/m^2\,h$ (LMH) or gal/ft^2 day (gfd). Typical fluxes vary between 10-1000 $L/m^2\,h$ for MF and UF membranes, 30-150 $L/m^2\,h$ for NF membranes, and 25-50 $L/m^2\,h$ for RO membranes [1, 2, 32, 34, 35, 49, 51, 52].

For pressure-driven filtration processes, flux is an indicator of the hydraulic resistance the membrane exhibits to flow of that component through it. However, flux measurements depend on the pressure at which the measurement is made as well as the feed solution used. For liquid filtrations, flux is directly proportional to the effective pressure difference ΔP_{eff} between the feed and the effluent:

$$J_i = P_m . \Delta P_{eff}$$

(2.2)

In this equation, the proportionality constant P_m is termed the permeability of the membrane. The pure water permeability (PWP), measured with pure water as the feed solution, is an important parameter that can be used to compare different membranes for

28

an application. A higher PWP indicates that a smaller applied pressure will yield the flow rates needed, and that the membrane is more energy efficient. Permeability values are reported in units of $L/m^2 h$ MPa (LMH/MPa) in this thesis. Other common units of PWP include $L/m^2 h$ bar (LMH/bar) and gal/ft^2 day psi (gfd/psi).

The effective pressure difference ΔP_{eff} is the driving force for flow. In most MF and UF processes, ΔP_{eff} is essentially equal to the applied pressure difference, ΔP. However, if there is a significant osmotic pressure difference $(\Delta\Pi)$ between the feed and the permeate, then the concentration difference causes a decrease in the driving force:

$$\Delta P_{eff} = \Delta P - \sigma\Delta\Pi \tag{2.3}$$

where σ is the Staverman reflection coefficient, which is a measure of the permselectivity of the membrane [19]. For UF and MF membranes, which allow the permeation of salts, σ is generally zero and osmotic pressure effects negligible. For RO membranes, which retain salts essentially completely, σ is close to 1, and overcoming the osmotic pressure becomes a significant issue. In seawater RO, the osmotic pressure difference is often over 2.5 MPa (25 bars or 360 psi), and the pressure needed to drive permeation can be very high. Seawater RO operations generally employ pressure differences of 5.5-10 MPa, compared with 1-3 MPa for brackish water RO [2, 34, 53-56].

2.4.2. Rejection and molecular weight cut-off

The function of a membrane lies in its ability to separate different components of the feed. This ability to separate, however, can be defined in a number of ways, depending on the application. When the main objective of the process is to remove a component, such as salt, from a stream, rejection (also termed retention) of a specific component is the main separation parameter. This is generally the case for RO and NF, and is also relevant in UF and MF. The percent rejection of component i describes how much of that component is prevented by the membrane from passing into the permeate stream, and is defined as:

$$R_i = \left(1 - \frac{c_{i,permeate}}{c_{i,feed}}\right).100 \tag{2.4}$$

29

where $c_{i,permeate}$ is the concentration of component i in the permeate, and $c_{i,feed}$ is the concentration of that component in the feed.

For cases where the separation is based on the size of the solute, it is desirable to have a parameter that can be used to estimate if a solute will pass through the membrane, or if it will be retained. This is especially relevant for UF membranes, where the size of the surface pores determines selectivity. It can also be relevant for NF membranes, especially those aimed at molecular fractionation. However, the pores in the selective layer of a UF membrane are not monodisperse. As a result, such membranes do not exhibit a sharp size cut-off. Instead, a diffuse cut-off is observed for most membranes, where the rejection changes from 0 to 100% in a gradual way over a range of molecule or particle sizes. Of course, this range is desired to be as narrow as possible to achieve efficient separations.

The molecular weight cut-off (MWCO) of a membrane is defined as the molecular weight of a solute for which the rejection is 90% by that membrane. As a metric of comparison, MWCO should be viewed cautiously, especially since there can be great differences in the sizes of two macromolecules of the same molecular weight. Hence, when a MWCO value is stated, it is essential to include the information regarding what kind of reference molecules were used, as well as the pressure, concentration and other process parameters. Some common reference molecules used for the determination of the MWCO of UF membranes are dextrans of varying molecular weights, globular proteins, and water-soluble polymers such as poly(ethylene oxide) [49]. MWCO also does not give information regarding the width of the cut-off. Therefore, these nominal values are a good guideline, but each membrane should be evaluated specifically for the application under consideration.

2.5. Membrane Fouling

Membrane fouling is the blocking of flow through the membrane due to the adsorption and accumulation of feed components on the membrane. Fouling is a key obstacle to the wider use of membrane processes, particularly in water filtration systems, due to its economic implications [31, 32, 57-59]: the accumulation of foulants results in either a decrease in flow through the membrane (Figure 2.4), or in cases where the flow rate is

30

kept constant, an increase in the pressure needed to maintain the flux. This results in a much higher energy demand per volume of filtrate, driving up energy costs significantly. To recover the permeability at least partially, cleaning steps are often performed, resulting in down time. Cleaning can involve a simple backwash, where the direction of applied pressure is reversed briefly to dislodge foulants held by physical interactions. When that is not sufficient, chemical cleanings are performed, which often involve the use of aggressive chemicals. Severe fouling thus shortens the lifetime of membranes, resulting in high membrane replacement costs. In some cases, the feed may require pretreatment steps to remove major foulants at least partially. This drives up both capital and operating costs of the system, and increases the complexity of operation. Therefore, fouling mitigation is a major focal point in membrane research and development, encompassing subjects ranging from the underlying mechanisms of fouling to the design of membranes and modules that resist fouling [32, 57, 60].
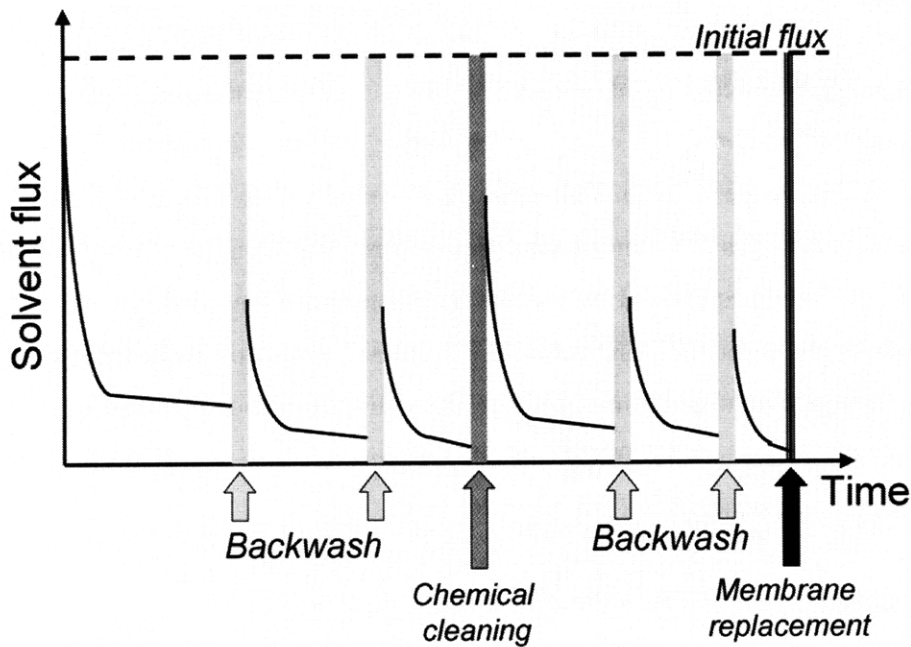
Figure 2.4. A representative plot of flux versus time in a membrane filtration system, demonstrating fouling.

2.5.1. Concentration polarization

Although concentration polarization is a mechanism distinct from membrane fouling, it has the same result: flux decline during the filtration of a solute. Furthermore, it exacerbates fouling. Concentration polarization is a local increase in the concentration of solutes in the feed, especially the ones that are retained, near the surface of the membrane [1, 31, 32, 57, 61]. This concentration gradient occurs due to the preferential passage of solvent (e.g., water molecules) through the membrane. As a result, the layer of fluid immediately adjacent to the membrane surface is depleted of the solvent, and a boundary layer is formed. The local decrease in solvent concentration in turn reduces the driving force for diffusion. This causes a decrease in flux, and poorer selectivity. Furthermore, as the concentration of the solute near the membrane is higher than the bulk concentration, there is an increased driving force for the solute to adsorb onto the membrane surface and cause fouling. Concentration polarization is noted to be most problematic for UF systems, though the effect is still significant in all other membrane processes [1, 31, 32, 57].

The only way to prevent concentration polarization is to design membrane systems and modules to prevent the formation of a boundary layer. Addition of spacers that create turbulence [62, 63], systems with high cross-flow velocity [64, 65], and continuous mixing of the feed solution are some general approaches taken [1, 31, 32, 49, 57]. Using shorter membrane modules divided by spacers that disturb the flow regime, rather than one long module, is also helpful, preventing the full development of the boundary layer. Some other methods that are aimed at fouling prevention, such as back-pulsing, ultrasound and use of air bubbles in UF and MF systems, are also useful in minimizing concentration polarization [60].

2.5.2. Fouling mechanisms in aqueous filtration

Membrane fouling is a complex physicochemical phenomenon. Usually, several mechanisms are involved simultaneously. In fact, improving our understanding of membrane fouling, including better ways to predict, characterize and image it, is an active research area [31].

Main mechanisms of membrane fouling include the adsorption of feed components, clogging and blocking of pores, cake (or gel) layer formation, scaling, and bacterial growth [31]. Concentration polarization also contributes to flux decline. These mechanisms are important to different extents, depending on the membrane operation as well as the feed characteristics.

Adsorption of biomolecules on the membrane surface, termed organic or adsorptive fouling, is one of the most important mechanisms involved in membrane fouling, mainly because it is often a first step in other fouling phenomena such as biological fouling and pore blockage. Feed water often contains organic molecules, including oils, greases, proteins, polysaccharides, humic substances, and other macromolecules [27, 66, 67]. During filtration these components are driven to the membrane-water interface, where they adsorb. This can occur within the internal pores of the membrane as well as on the membrane surface. The driving force is stronger for membranes with hydrophobic surfaces, causing more severe fouling. This is explained by the fact that macromolecules of biological origin, such as proteins and humic substances, often contain both hydrophilic and hydrophobic domains. By organizing at hydrophobic membrane surfaces like a surfactant, the interfacial energy of the membrane-water interface is reduced [66, 68]. Once a monolayer of foulant molecules is adsorbed, foulant-foulant interactions result in build-up that narrows and blocks pores. This process causes a significant decrease in flux. If the membrane is microporous, as in the case of UF membranes, a notable decrease in the effective pore size also occurs, lowering the MWCO [68]. This is the most important obstacle in the application of membranes to the size-based fractionation of proteins and other biomolecules.

Feed solution chemistry often has a strong effect on biomolecule adsorption. Factors such as pH, ionic strength, and the presence of divalent ions alter the fouling potential of a feed [26, 39]. For example, each calcium ion can complex with two carboxylic acid groups, forming linkages between macromolecules that contain acid groups such as humic substances and some polysaccharides [68]. This has been shown to significantly increase the fouling rate. Process parameters, such as applied pressure and surface shear, also influence the extent of fouling, since they change the concentration of foulants at the

33

membrane surface [68]. Finally, membrane properties such as hydrophobicity, roughness and surface charge density all influence the degree of fouling [31, 68]. Adsorptive fouling is generally not reversible by physical methods such as back-washing [31]. Chemical cleaning methods that will break down the foulant are necessary.

If the feed contains fine particulates, colloids and precipitated materials, then cake fouling (or the formation of a gel layer) becomes significant, especially in the later stages of filtration. As in the case of concentration polarization (which also aggravates the fouling process), particles and colloids are driven to the membrane surface and accumulate there to form the cake layer, which compacts gradually. Cake fouling is especially significant in UF and MF, where the feeds contain more particulates and the cake resistance is comparable in magnitude with the hydraulic resistance of the membrane [27]. A similar problem is observed in the filtration of oily streams, where oil droplets coalesce on the membrane surface to form a resistance layer very quickly [31]. Most cake fouling is held together by physical forces, and can be removed with relative ease by methods like back-washing, ultrasound treatment, or rinsing of the membrane at high shears [31].

Bacterial fouling of a membrane, also termed biofouling, is commonly observed in RO systems as well as membrane bioreactors (MBRs), and wastewater treatment systems [31, 58, 59, 69]. It is highly interrelated with adsorptive and cake fouling described above [59]. Biofouling is characterized by the formation of a biofilm on the membrane surface, which occurs in three main steps: the transport of microorganisms to the membrane surface, attachment to the membrane, and growth of the biofilm. In addition to flux decline due to fouling, biofilms can result in the degradation of the membrane due to attack by microorganisms. This is an especially important problem in the case of cellulose acetate membranes [1, 70].

The mechanism of flux decline in biofouling involves cake formation and pore blockage by microorganisms, but in most UF and NF systems, the chief contribution to fouling is macromolecules produced by the microorganisms, termed extracellular polymeric substances (EPS). EPS contains a wide range of organic macromolecules, including

proteins, polysaccharides and humic substances. Adsorptive fouling by EPS is considered the major contributor to biofouling, rather than the blocking of pores by attached cells [67, 71].

2.5.3. Prevention methods

Fouling prevention starts with designing a membrane that resists adsorption, a major objective of this thesis. Extensive research has shown that hydrophilic membranes are less susceptible to fouling [32], since the driving force for the adsorption of dissolved biomolecules at a water-polymer interface is stronger when the surface is hydrophobic. However, hydrophilic membrane materials (such as cellulose acetate) typically exhibit inferior mechanical and chemical stability. Therefore, much research aims to create membranes that have hydrophilic surfaces on more resilient hydrophobic bulk materials. This can be achieved through various strategies [32], such as plasma treatment [72, 73], surface graft polymerization [74, 75], surface immobilization [76, 77], application of hydrophilic coatings such as hydrogels [78, 79], or use of surface-segregating additives [4-6, 13].

Plasmas are ionized gases that consist of electrons, positively charged ions, and neutral atoms or molecules or both. A plasma is a highly reactive state of matter that can form a variety of chemical groups on exposed surfaces, depending on the chemical make-up of both the surface and the plasma [73]. Plasmas can be used to generate hydrophilic groups on the membrane surface, thereby increasing its wettability and fouling resistance [73, 80]. In addition, plasmas are sometimes used to initiate the polymerization of hydrophilic monomers [72, 80] in surface graft polymerization practices.

Surface graft polymerization is a common method of surface modification used commercially. In this process, the surface of the membrane is activated to create reactive sites. This may be accomplished by chemical treatment, plasma treatment, or irradiation with UV light, high-energy electrons or gamma-rays [74]. Free radicals or ions generated at the polymer surface act as initiator sites, causing polymer chains to grow from the surface when exposed to monomer solution or vapor. This method allows for a wide choice of hydrophilic monomers available for grafting [74, 75, 81]; examples are

hydroxyethyl methacrylate, *N*-vinyl pyrrolidone, acrylic acid and 4-vinyl pyridine. This approach also holds the advantage of generating dense surface coverages of grafted chains [74]. However, the activation step is often costly, and the polymerization can be poorly controlled, especially if chain transfer reactions are prominent. High levels of ungrafted homopolymer are sometimes encountered that may leach from the membrane surface during use, increasing susceptibility to fouling.

Surface immobilization is an alternate method for grafting hydrophilic polymers to a membrane surface. This process generally involves chemical activation of the surface to form reactive groups. The surface is then exposed to a solution of a hydrophilic polymer having complement groups (usually end groups) that can react with the surface sites. At the completion of the reaction, the hydrophilic chains are attached to the membrane, forming a fouling-resistant coating [32, 77, 80]. While this approach is more controlled than surface-initiated polymerization, the density of grafted chains tends to be lower, due to the steric obstruction of the surface as grafted coils begin to overlap. This is undesirable, as high grafting densities are correlated with enhanced resistance to biomolecule adsorption [82, 83].

Coating a membrane with a layer of crosslinked, hydrophilic polymer can prevent the adsorption of foulants on the membrane surface as well as their introduction into membrane pores, thus preventing fouling [32, 78, 79, 84, 85]. Gels of poly(ethylene oxide) or poly(vinyl alcohol) are good candidates for such coatings [78, 79, 85]. The coatings are usually applied on the base membrane as a thin layer of prepolymer solution that is later crosslinked [78, 85]. Delamination of the coating layer during use can be avoided by allowing the prepolymer to partially penetrate the pores of the membrane prior to crosslinking, thereby physically hooking the coating to the membrane [85]. Although the permeability of such membranes is often decreased in pure water filtration tests, most of the time there are significant gains in flux during the filtration of foulant solutions [79]. This method also has the cost disadvantage of an additional fabrication step, however.

A promising more recent approach to UF membrane surface modification involves the addition of an amphiphilic block or graft copolymer to the membrane casting solution along with the base material [4-6, 8, 13, 16, 86-89]. During precipitation in a water-based coagulation bath, the additive acts as a macromolecular surfactant, segregating to all polymer-water interfaces, and self-assembling to form a hydrophilic "brush" layer [4-6, 8, 13, 86] covering all membrane surfaces. The coverage extends throughout the internal pores of the membrane, thus preventing internal pore fouling by biomolecules that permeate the membrane. The method has several unique advantages in requiring no additional processing steps, yielding substantially higher pure water fluxes than in the absence of additive [4-6, 13], and, in some cases, providing a "self-healing" surface via the segregation of residual additive from the membrane matrix [4]. This method will be studied further in Chapters 5 and 6 of this thesis.

Chapter 3:

Nanofiltration membranes with PVDF-*g*-POEM as selective layer: Fouling resistance and responsive pore size

3.1. Introduction

Nanofiltration (NF) membranes are defined by an effective pore size between 0.5-2 nm [1]. Currently, commercial NF membranes can be described more as "loose reverse osmosis (RO) membranes", because of their chemical and structural similarity combined with lower salt retentions and higher fluxes [34]. NF membranes that have more well-defined selectivity, good fouling resistance, and high flux are highly desirable in the industry. A pore size that can be fine tuned to a specific application would also enhance the appeal of such membranes. This chapter of this thesis explores membranes that combine these properties, making use of the self-assembly of an amphiphilic comb copolymer.

3.1.1. NF membranes with subnanometer size selectivity

Membranes that have size cut-offs in the nanometer range and can fractionate molecules whose sizes differ by less than a nanometer have great potential for high-end molecular separations. Especially the pharmaceutical [90], chemical [91, 92] and biochemical [56, 93] industries would benefit from such technologies. Such molecular sieve type membrane processes would be easier to scale up than competing technologies such as electrophoresis and chromatography [94]. Commercial NF membranes are generally unsuited for this purpose, due to their ionic charge [2, 34] which largely controls retention.

A number of researchers have aimed to manufacture membranes whose selectivity is in the small molecule range and is based on size. Martin and coworkers have employed a polycarbonate track-etched membrane with 30 nm pores as a template and used an electroless plating technique to deposit gold in the pores, producing nanotubules [95, 96] (Figure 3.1a). With long enough deposition times, the internal diameter of the nanotubules can be reduced to less than 1 nm, in the range of molecular dimensions. These membranes are able to perform size-based separation of molecules [95] and proteins [96]. However, they are expected to have very low fluxes, as the initial track-etched membrane porosity is only 2-3% of the surface [1].
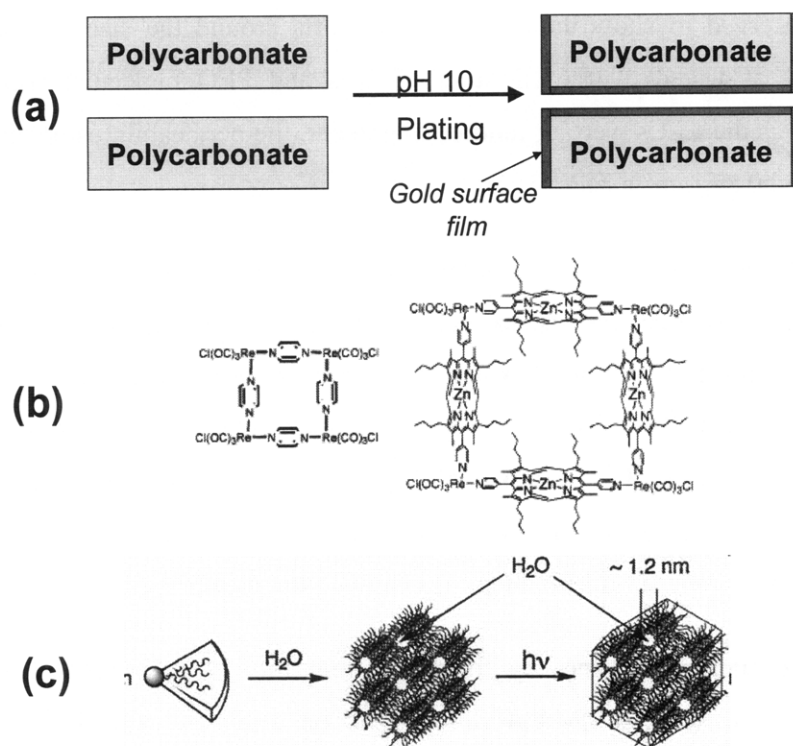
Figure 3.1. Schematic illustration of published approaches to preparing molecular filters. (a) Gold nanotubule membranes through electroless plating of track-etched membranes [95] (b) Two chemical structures of molecular squares used as membrane selective laI yer [97] (c) Crosslinked hexagonal lyophilic liquid crystals [98]

Another approach involves thin film composite (TFC) membranes with molecular squares as the selective layer [97, 99]. The cavities in such structures range between 3 Å and 18 Å in size. Two such structures that lie at the extremes of this cavity size distribution are shown in Figure 3.1b. Simple diffusion studies and molecular simulations indicated the existence of intermolecular channels ~6 Å in diameter for the smaller squares and 18-20 Å for the larger ones that allow size-based selectivity [97].

Gin and coworkers also developed TFC structures, using polymerized lyotropic liquid crystal (LLC) assemblies as the selective layer [98, 100, 101]. LLCs in the inverted hexagonal phase form lipid microtubules filled with water. Cross-linking enabled the structure to resist the high pressures experienced in NF [100] (Figure 3.1c). These membranes were observed to show molecular size cut-offs around the size of phase separation (1.2 nm), as tested by the filtration of dyes and PEO molecular weight standards. However, as the LLCs were of random alignment, the permeabilities obtained were very low, around 0.87 L/m^2 h MPa [101].

Another approach to form size-selective membranes involves the self-assembly of copolymers of various architectures. Block copolymers that phase-separate to form hexagonally packed cylinders have been exploited for membrane applications [47, 48, 102, 103]. In these studies, the microphase separated block copolymer serves as the selective layer of the membrane. This results in highly monodisperse pore size combined with high surface porosity. It is crucial that the cylinders are continuous and aligned perpendicular to the membrane surface to allow flux through the membrane.

Yang *et al.* prepared such membranes by forming a thin film of polystyrene-*block*-poly(methyl methacrylate) (PS-*b*-PMMA)/PMMA blend on a silicon oxide layer that aligns the nanodomains. The film was then removed by etching the silicon oxide with hydrofluoric acid and moved the film onto a support membrane. PMMA homopolymer was removed by a solvent wash, leaving behind pores 15 nm in size [47, 103]. Phillip *et al* studied the separation properties of extruded monoliths of the terpolymer polylactide-*block*-poly(dimethylacrylamide)-*block*-polystyrene   (PLA-*b*-PDMA-*b*-PS).   This

terpolymer formed hexagonally packed cylinders of the PLA phase, which was etched to leave behind pores approximately 15 nm in diameter [48].

In both of these cases, the membrane formation involves complex processes that would be difficult to scale-up. Peinemann *et al.* formed membranes that exhibited hexagonally ordered cylindrical pores on its surface by phase inversion casting of polystyrene-*block*-poly(4-vinylpyridine) (PS-*b*-P4VP). In this process, the use of a volatile solvent in the casting solution that evaporates during the drying time was crucial. The diameter of the surface pores was approximately 40 nm [102].

Each of these approaches employed the concept of microphase separation to form membranes with sharp size selectivity. However, the size scale of microphase separation in block copolymers is typically in the UF range of pore sizes (10-40 nm in the studies listed above). Hence, these cylindrical block copolymer membrane structures could not be used as molecular filters.

Another issue is the alignment of the cylindrical domains in the membrane structure. This is often difficult to realize in industrial systems that are not as controlled as the laboratory environment. Even in the study of Peinemann *et al.*, where aligned domains were achieved by a commercially relevant process [102], local fluctuations in process conditions can cause uneven structures upon scale-up. A bicontinuous structure would be more robust, and allow for more flexibility.

Graft copolymer structures form bicontinuous phases in a much broader composition range than block copolymers [104, 105]. The nanodomains formed are also finer, and the size scale of microphase separation can be in the range necessary for molecular sieving [5, 104, 105]. In the Mayes group, new thin film composite NF membranes comprised of a commercial polyvinylidene fluoride (PVDF) UF membrane coated with the amphiphilic graft copolymer poly(vinylidene fluoride)-*graft*-poly(oxyethylene) methacrylate, PVDF-*g*-POEM were developed by Akthakul [11, 12]. The chemical structure of this copolymer is given in Figure 3.2a. Microphase separation of the PVDF backbone and short (9 unit) polyethylene oxide (PEO) side chains results in an interconnected network of hydrophilic, charge-neutral "nanochannels" ~2 nm in diameter (Figure 3.2b). This phase allows the

passage of water as well as other molecules smaller in size than its domain size. It retains all molecules larger than its domain size, leading to a sub-nanometer precision size cut-off. This has been studied by Akthakul et al. using rigid positively and negatively charged dyes as probes. The membranes were able to fractionate two like-charged dye mixtures, brilliant blue R / congo red (anionic) and alcian blue (pyridine variant) / rhodamine B (cationic) mixtures [12]. Gold nanoparticles protected with self-assembled monolayers in toluene were also used as probes. The PVDF-g-POEM coated membranes having 23 ethylene oxide unit side-chains retainebd nanoparticles around 3.2 nm in core diameter [11].

(a)   (b)
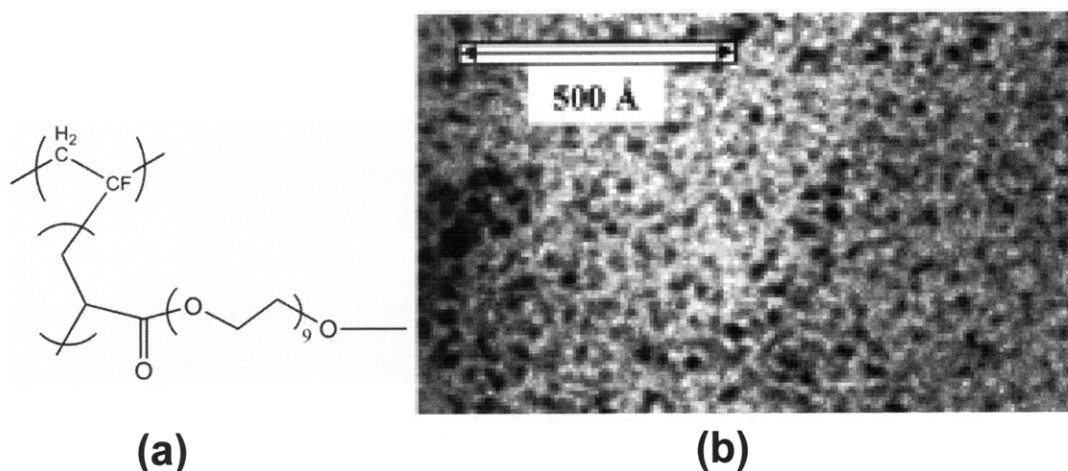
Figure 3.2. (a) Chemical structure of PVDF-g-POEM (b) TEM micrograph of PVDF-g-POEM stained with ruthenium tetroxide. The stained POEM microdomains appear as darker regions in the image [5].

3.1.2. NF membranes with tunable pore size

One objective of this project was to develop ways of fine-tuning the size cut-off of PVDF-g-POEM TFC NF membranes. This could be very useful for applications in the pharmaceutical, biochemical and food industries [106, 107] which currently lack methods for low-cost, high-throughput fractionation of molecules.

Filtration membranes whose flux and selectivity can be modulated with different process parameters have been studied extensively [108, 109]. Researchers have developed

membranes that respond to various stimuli, including pH [7, 110-112], temperature [113-118], ionic strength [112, 113], light [119], and the presence of solvents such as ethanol [120]. Most of this research focuses on membranes whose size cut-off is in the ultrafiltration (UF) or microfiltration (MF) ranges [7, 110-113, 118-120].

Studies on responsive NF membranes are much more limited. For example, temperature-responsive, TFC membranes with size cut-off in the NF range were developed by Lopez and coworkers, using a hybrid gel of poly(N-isopropylacrylamide) (PNIPAAM) and silica [116] as a mesoporous selective layer, and employing surfactants as structure forming agents during casting [121]. PNIPAAM has a lower critical solution temperature (LCST) in water (nominally ~32°C): polymer chains are soluble in water below this temperature. When the temperature is raised above the LCST, the polymer becomes insoluble in water and chains collapse, resulting in a decrease in the size of polymer coils and consequently, pore enlargement. In centrifugal filtration experiments, membranes prepared with the above method were found to be essentially impermeable to water at low temperatures, whereas at 40°C, they were permeable to water, with a molecular weight cut-off (MWCO) of 7850 g/mol based on poly(ethylene oxide) (PEO) standards. Similarly, Nykanen *et al.* used triblock copolymers of poly(styrene) (PS)-*b*-PNIPAAM-*b*-PS that form spherical and gyroid structures to make membranes whose water permeability changed drastically with temperature [114]. However, the retention of solutes was not observed to change significantly in that study.

Inoue and coworkers used graft copolymers with a vinyl backbone and polypeptide side-chains to prepare membranes whose permeability to various small molecules changes according to pH [122-124]: The side-chains are negatively charged at high pH, which results in a high degree of swelling and increased permeability to small molecules. At lower pH levels, the carboxyl groups on the polypeptide chains are protonated, and the membrane substantially loses its hydrophilicity, resulting in lower permeabilities. The addition of doubly charged salts such as calcium and copper also cause a decrease in permeability due to ionic cross-linking of carboxyl groups [125]. Because of the charges present, separations employing these membranes are likely to involve both size-based and charge-based (Donnan) exclusion mechanisms.

PVDF-*g*-POEM TFC NF membranes have the potential for exhibiting tunable and responsive pore size. The selectivity of these membranes is determined by the chain density within the PEO-lined nanochannels. This is in turn affected by two major factors: the length scale of the microphase separation that creates the nanochannels, and the conformation of the PEO chains. The former can be influenced by controlling manufacturing conditions such as the composition of the copolymer or the coagulation bath. The latter can be changed during use by modifying the solvent quality of the feed for PEO. Akthakul *et al.* first demonstrated this ability for PVDF-*g*-POEM TFC NF membranes in the context of filtration of gold nanoparticles in different solvents. In that study, the size cut-off for a polydisperse nanoparticle solution was seen to shift significantly when the filtration was performed in toluene, ethanol, and water [11]. The current study focuses on process parameters that can be varied more readily in an industrial process, such as temperature, pressure, ionic strength, and ethanol content, all of which alter the swelling of PEO chains in solution [126-141]. Such capability is highly desirable, as it would allow a single membrane to be used for a range of molecular sieving operations by fine-tuning the effective pore size to the separation desired.

3.1.3. Fouling resistant NF membranes for membrane bioreactor (MBR) applications

A second objective of this study was to investigate the fouling behavior of PVDF-*g*-POEM/PVDF TFC NF membranes, and the possibility of their implementation in membrane bioreactors (MBRs), systems that combine conventional biological wastewater treatment using suspended biomass with membrane separation. They are an attractive alternative to conventional activated sludge treatment using secondary sedimentation. MBRs offer the advantages of higher product water quality and reduced footprint [69]. However, the widespread application of MBRs is constrained by membrane fouling [30, 69].

Membranes employed in MBRs are typically porous ultrafiltration (UF) membranes. To improve effluent quality while substantially eliminating internal pore fouling, NF membranes offer a potential alternative to UF membranes for MBRs [37, 142, 143]. NF MBR systems, unlike UF-based ones, have the potential for rejecting low molecular

weight contaminants such as endocrine disrupting chemicals, pharmaceuticals, and pesticides that can be hazardous to human health [143]. In their study of NF MBRs, Choi et al. [37, 142] noted that high flux NF membranes with high organic matter rejection and low salts rejection are needed to improve the practicability of such systems. Because of the high rejection of organics in NF MBR systems, they can further reduce fouling of RO membranes when used in advanced wastewater reclamation in place of UF MBRs.

A variety of constituents in waters can lead to membrane fouling, including dissolved inorganic or organic compounds, colloids, bacteria, and suspended solids (see Chapter 2) [35]. Biofouling is largely attributable to accumulated extracellular materials, rather than individual bacterial cells or microbial flocs [144-146]. These extracellular materials, including soluble microbial products (SMP) and extracellular polymeric substances (EPS), consist mainly of polysaccharides, proteins, and natural organic matter (NOM) [71, 147-150].

Proteins are a significant source of fouling, because of their strong tendency to adsorb on surfaces from aqueous solution [151, 152]. In addition to MBR systems [69, 71, 148], they are present in many processes that membranes are used extensively for, including wastewater treatment [71, 153], and separations in the food [154-157], paper and pulp [158], and biotechnology [24, 155] industries.

Polysaccharides are another class of important foulants in NF [158]. Sodium alginate, a polysaccharide, is also known to be a component of EPS observed in the presence of microorganisms in the feed [71, 148], and a significant contributor to biofouling [159].

In addition to contributing to biofouling, NOM has been described as one of the major membrane fouling agents in NF of surface waters [38, 39, 160-163]. Its major component, humic acid (HA) [160], is a degradation product of lignin, carbohydrate and protein. It is present in soil and is leached out into surface waters [164]. The fouling characteristics of humic acid are highly dependent on solution chemistry [26, 39, 165, 166]. Membrane fouling by humic acid has been found to increase with the presence of divalent cations, particularly Ca^{2+}. Complexation of Ca^{2+} ions with the carboxyl groups of humic acid

leads to intermolecular linkages that result in the formation of a compact cake layer that significantly reduces flux.

The fouling resistance of PVDF-g-POEM TFC NF membranes was investigated employing bovine serum albumin, sodium alginate, and humic acid as representatives of the three important classes of biomolecule foulants in MBRs: proteins, polysaccharides and NOM, respectively [148-150]. Fouling behavior was characterized in 10-day filtration studies using 1000 mg/L feed solutions. Filtration studies using activated sludge from an aerobic MBR as the feed solution were also performed by our collaborators at University of Illinois at Urbana-Champaign. The PVDF-g-POEM coated membranes were shown to completely resist irreversible fouling, defined as fouling that cannot be recovered by a pure water rinse, while providing substantially improved effluent quality over the PVDF UF base membrane control.

The mechanism of this exceptional behavior was investigated by atomic force microscope (AFM) colloid probe measurements, performed by our collaborators at Yale University. These experiments showed long-range steric repulsive forces between the membrane surface and the foulant, responsible for preventing biomolecule adsorption.

3.2. Experimental Methods

3.2.1. Materials

Poly(vinylidene fluoride) (PVDF, $M_n \sim 107$ kg/mol), poly(ethylene glycol) methyl ether methacrylate (POEM, $M_n = 475$ g/mol), N-methyl pyrrolidone (NMP), 4-methoxyphenol (MEHQ), N,N,N',N",N"-pentamethyldiethylenetriamine (PMDETA), bovine serum albumin (BSA, 66.5 kDa), and all dyes were purchased from Sigma-Aldrich (St. Louis, MO). Copper (I) chloride (CuCl), basic-activated alumina, poly(ethylene glycol) (PEG, $M_n = 600$ g/mol), N,N-dimethyl formamide (DMF), hexane, ethanol, tetrahydrofuran (THF), deuterated dimethyl sulfoxide (DMSO-d_6), humic acid, calcium chloride (CaCl$_2$), phosphate buffered saline (PBS) concentrate (10x), sodium chloride and sodium alginate were purchased from VWR (West Chester, PA). All chemicals and solvents were reagent grade, and were used as received. PVDF400 ultrafiltration membranes, purchased from

Sepro Membranes Inc. (Oceanside, CA), were used as the base membrane. Deionized water was produced from a Millipore Milli-Q unit.

The molecular weights of sodium alginate and humic acid were measured by static light scattering (Wyatt MiniDawn). The experiments were performed using solutions in water at three different concentrations, and measurements at three different angles. The weight-average molecular weight of sodium alginate was found to be 29,000 g/mol, and that of humic acid was calculated to be 17,000,000 g/mol. The unusually high molecular weight measured for humic acid indicates the formation of aggregates in water [167].

The activated sludge used in this study was cultured within an aerobic membrane bioreactor having a porous liner manufactured into its walls through which fluid is passed by gravity [168]. The liner consists of filter grade porous polyethylene (Atlas Minerals & Chemicals, Mertztown, PA) with a thickness of 0.48 cm and a nominal pore size of approximately 25 μm. The reactor had a diameter of 9 inches (22.86 cm), a volume of 9.4 liters and was configured into a standard reactor geometry according to Holland and Chapman [169]. Mixing was accomplished with a three-inch (7.62 cm) diameter Rushton impellor at a speed of 150 revolutions per minute (rpm).

The reactor was operated with a hydraulic retention time of 18 hours and a solids retention time of 28 days. The influent consisted of 150 mg/L of ammonia nitrogen and acetate at a concentration of 350 mg/L chemical oxygen demand (COD) resulting in a mixed liquor volatile suspended solids (MLVSS) concentration of approximately 1800 mg/L VSS. COD and MLVSS were measured according to [170]. Ammonia nitrogen was measured using a microtiter-based method [171].

3.2.2. Synthesis of PVDF-g-POEM

POEM was grafted to PVDF following a slightly modified version of the atom transfer radical polymerization (ATRP) approaches previously published [5, 172]. PVDF (5 g) was dissolved in NMP (50 mL) in a conical flask at 50°C. The solution was cooled to room temperature and transferred to a 250 mL Schlenk flask. POEM (50 mL), CuCl (0.04 g), and PMDETA (0.26 mL) were added to the reaction vessel, which was subsequently

sealed. Nitrogen gas was bubbled through the reaction mixture for 20 minutes. After a total reaction time of one hour, MEHQ (2.5 g), dissolved in approximately 10 mL of THF, was added to the reaction mixture, which was then diluted with approximately 100 mL of THF. This mixture was passed through a column of basic-activated alumina and precipitated in a 10:3 mixture of hexane and ethanol. The product was redissolved and reprecipitated twice, then dried in a vacuum oven overnight. POEM content of the copolymer was determined by ^{1}H Nuclear Magnetic Resonance (NMR) spectroscopy in deuterated DMSO using a Bruker DPX 400 spectrometer as described previously [5] to be 48 wt% (Appendix A).

3.2.3. Fabrication of TFC membranes

For the preparation of TFC membranes used in fouling studies, the coating solution was prepared by dissolving 1 g of PVDF-g-POEM copolymer and 1 g of PEG in 4 mL DMF at approximately 50°C. No PEG was added into the coating solution in the preparation of the membranes used in studying the responsive pore size properties of PVDF-g-POEM TFC NF membranes. The coating process was identical from this point on. The coating solution was passed through a 1-μm syringe filter (Whatman) and degassed under vacuum for approximately one hour. Membranes were coated using a control coater (Testing Machines Inc., Ronkonkoma, NY). The PVDF400 base membrane was fixed onto the coater, and the coating bar (number 4, nominal film thickness 40 μm) inserted. The coating solution was poured onto the base membrane to form a thin line about 0.5 cm from the coating bar, and the coater was used to move the bar at a constant reproducible speed (speed level 4 on the instrument). After 5 minutes, the membranes for fouling studies were immersed in a bath of ethylene glycol for 30 minutes, then rinsed in an isopropanol bath for 10 minutes and air dried. The membranes for responsive pore size studies were immersed in isopropanol for 10 minutes and air dried.

Membrane morphology was characterized using a JEOL 5910 Scanning Electron Microscope (SEM) operating at 5 kV. The membranes were fractured in liquid nitrogen for cross-sectional observation, and sputter coated with gold-palladium for SEM imaging.

3.2.4. Fouling experiments

Circular pieces were cut from the membrane, and hydrated for at least 30 minutes before testing. Fouling experiments were performed on 25 mm diameter membranes using an Amicon 8010 stirred, dead-end filtration cell (Millipore) with a cell volume of 10 mL and an effective filtration area of 4.1 cm^2, attached to a 3.5-L dispensing vessel. Permeate was collected at fixed time intervals using a FRAC-100 fraction collector (Pharmacia) and weighed to determine trans-membrane flux. Solute rejection was determined by UV spectroscopy.

Filtration cells were stirred at 500 rpm using a stir plate to minimize concentration polarization. Deionized (DI) water was first passed through the membrane until the flux remained stable over at least a half hour (2 h minimum DI water filtration). The end of the stabilization period was taken to be the zero time point in the filtration plots. The cell was then emptied and refilled with the model foulant solution. Protein solutions comprised 1000 mg/L BSA in PBS. NOM fouling studies used 1000 mg/L humic acid and 10 mM $CaCl_2$ in DI water. Polysaccharide fouling experiments were performed with 1000 mg/L sodium alginate in DI water. A sample of the permeate was collected after 1 hour of filtration. Foulant retention values were obtained by measuring the foulant concentration in this sample by UV-visible spectroscopy using a Cary 500i UV-Vis-NIR dual-beam spectrophotometer. The concentrations were quantified using UV absorbance at 280 nm for BSA and 200 nm for sodium alginate and humic acid. During the fouling experiments, a build-up of foulant concentration was observed within the filtration cell, due to the retention of the foulant coupled with the small size of the filtration cell compared with the total volume of solution that was filtered. This can be regarded, in a way, as concentration polarization. This also allowed is to test the fouling resistance of the membranes at foulant concentrations, which could be calculated by a material balance. After each fouling test, the filtration cell was rinsed 5-7 times with DI water and then refilled with DI water as a feed to determine the reversibility of fouling.

Flux decline experiments using activated sludge were performed by Adrienne Menniti at the University of Illinois at Urbana-Champaign following the same approach as described

above, but with a different experimental setup. Filtration was performed using an Amicon stirred cell model 8200 (Millipore, Billerica, MA). The Amicon cell was mixed at 175 rpm for all sludge experiments. Flux measurements were performed by weighing permeate at fixed time intervals on a top loading balance (Model PB3002-S, Mettler Toledo, Columbus, OH) assuming a permeate density of 1 g/mL. Automatic collection of permeate data was performed using the software WinWedge (TAL Technologies, Philadelphia, PA). Clean water flux and hydraulic recovery measurements were performed using NANOpure ultrapure water (Barnstead, Dubuque, IA). Activated sludge concentrations for dead-end filtration experiments using TFC or base membranes were approximately equal at 1745 and 1855 mg/L MLVSS, respectively. Membrane retention was characterized based on total COD measured in the filtrate and the retentate.

The PVDF UF base membrane served as the control in filtration experiments, as UF membranes are commonly employed in MBRs. The fouling properties of commercial TFC NF membranes have been documented in other studies [39, 66, 166].

3.2.5. Responsive pore size experiments

Circular pieces 49 mm in diameter were cut from coated membranes and wetted in water for at least 15 minutes before performing filtration experiments. The experiments were performed using a Sepa stirred, dead-end filtration cell (Osmonics) with an effective filtration area of 16.9 cm^2 and a liquid capacity of 300 mL. The filtration cell was placed in a water bath with a temperature controller that kept the system at the desired temperature with an accuracy of $\pm2°C$. The cell was stirred at 400 rpm using a stir plate to minimize concentration polarization.

Membrane permeability was determined by collecting the filtrate for a known period of time, weighing it and normalizing by the membrane area and pressure difference, the latter measured by an electronic pressure gauge.

The effective pore size of the membrane was also probed by the permeation of rigid dye molecules. Two dyes were used in this study: Brilliant Blue R (calculated molecular diameter: 11.1 Å) was used in observing the effect of ethanol addition to the feed, and

Reactive Red 120 (calculated molecular diameter: 9.8 Å) was used to observe the effects of temperature, pressure and ionic strength. The chemical structures and three dimensional molecular models of these dyes are given in Figure 3.3. The diameters were calculated using Molecular Modeling Pro software (ChemSW, Fairfield, CA) by calculating the molecular volume of the dye from its chemical structure and fitting this value to a sphere of equal volume.

Brilliant Blue R   Reactive Red 120
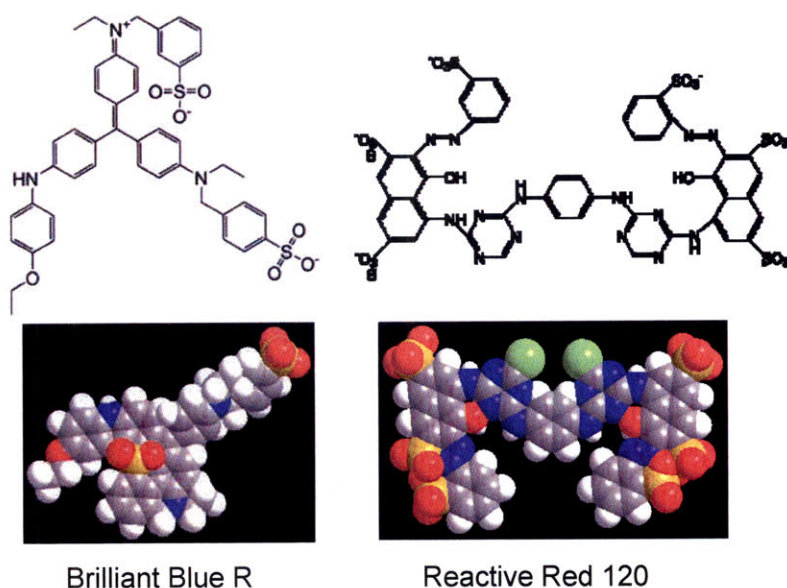
Figure 3.3. Chemical structures and molecular models of the dyes used in pore size tuning experiments

The effect of ethanol content in the feed was investigated by filtering a series of solutions of Brilliant Blue R (100 mg/L) in mixtures of ethanol and water, at a pressure of 150 psi (1.03 MPa). First, the ethanol/water mixture without the dye was passed through the membrane for at least 40 minutes. Then the feed was replaced with the dye solution. After the color of the filtrate stabilized (at least 1 hour), a sample was collected. The concentration was determined by UV-visible spectroscopy at 555 nm.

The dependence of membrane permeability on temperature and pressure was investigated. Deionized (DI) water or salt solution was passed through the membrane at room

temperature and 200 psi (1.38 MPa) until the flux stabilized (at least one hour). Permeate was collected for 15 minutes and weighed to determine the permeability. The pressure was then decreased to 150 psi (1.03 MPa), and the flux was allowed to stabilize for 30 minutes. Another sample was collected and weighed. This was repeated at 100 psi (0.69 MPa) and 50 psi (0.34 MPa). Then the temperature was increased, first to 50°C and then to 70°C, and after a stabilization period of one hour, the above procedure was repeated at each temperature. This procedure was subsequently repeated with a feed of 0.1 M NaCl solution.

The permeation of Reactive Red 120 at different temperatures and pressures was also tested. For these experiments, the membrane was first allowed to stabilize by passing either DI water or 0.2 M NaCl solution through at 25°C for one hour. The initial feed solution was then replaced with the dye solution and filtration was performed similar to the method described above, increasing first the pressure and then the temperature step by step, and allowing the system to stabilize before collecting each sample. At the end of this period, the cell was rinsed with DI water, and DI water at 75°C was subsequently filtered through the membrane at 200 psi for 1 hour to clean the membrane. The dye concentrations of the feed and permeate were determined by UV-visible spectroscopy at 525 nm.

3.2.6. Atomic force microscopy (AFM) measurements

Atomic force microscopy (AFM) was used to characterize the interfacial forces between the membrane and organic foulants. The force measurements were performed by Dr. Seoktae Kang at Yale University using a MultiMode AFM connected to a Nanoscope IIIa controller (Veeco Metrology Group, Santa Barbara, CA). A carboxylate modified latex (CML) particle (Interfacial Dynamics Corp., Portland, OR) was used for making the AFM colloid probe because the model organic foulants used in this study (BSA, alginate, and humic acid) contain predominantly carboxylic functional groups. The CML particle (3.0 μm in diameter) was attached by Norland optical adhesive (Norland Products, Inc., Cranbury, NJ) to a tipless SiN cantilever having a spring constant of 0.06 N/m (Veeco Metrology Group, Santa Barbara, CA) and cured under UV light for 20 min. A fluid cell

was used to allow force measurements in desired solution chemistries, with the membrane being located on the bottom of the fluid cell.

The fluid cell was first rinsed with DI water before injecting test solution to fully displace the DI water in the fluid cell. The force measurements were conducted at four different locations on the membrane, and 10 force measurements were taken at each location. Details on the procedures of using an AFM colloid probe to determine the intermolecular adhesion forces in membrane fouling are given in recent work [166, 173, 174].

According to Derjaguin's approximation, the interaction force between a sphere and a flat surface is related to the interaction energy per unit area [175]:

$$F(h) = 2\pi R W(h) \tag{3.1}$$

where $F(h)$ is the interaction force between a sphere and a flat surface separated by a distance h, R is the radius of the spherical particle, and $W(h)$ is the interaction energy per unit area between two flat surfaces separated by a distance h. According to equation 3.1, the interaction energy W is equal to F/R multiplied by a factor of 2π. This shows that the parameter $F(h)/R$ is an indicator of the energy that draws the foulant molecule to the membrane surface.

The net interaction energy between two surfaces is a sum of the contributions of van der Waals attraction and the electrostatic double layer repulsion.

$$W(h) = W_A(h) + W_R(h) \tag{3.2}$$

where $W_A(h)$ is the attractive van der Waals interaction energy per unit area, and $W_R(h)$ is the electrostatic repulsion energy per unit area. The van der Waals attraction scales with h^{-2}, whereas repulsive forces are proportional to $e^{-h/\kappa^{-1}}$, where κ^{-1} is a characteristic distance indicating the range of these repulsive forces, termed the decay length. For charged surfaces, κ^{-1} is strongly dependent on the composition and ionic strength of the electrolyte separating the two surfaces [175].

Similarly, the adhesion force measured during the retraction of the colloid probe, normalized by the radius of the particle, F_{ad}/R, is proportional to the energy per unit area required to separate the particle and the flat surface by an infinite distance, $W(\infty)$:

$$\frac{F_{ad}}{R} = 2\pi W(\infty) \tag{3.3}$$

F_{ad}/R can, therefore, be viewed as a measure of the strength of foulant adhesion to the membrane surface.

3.3. Results and Discussion

3.3.1. Membrane characterization

In manufacturing the composite membranes, a control coater was used to achieve a uniform and reproducible PVDF-g-POEM coating thickness on the PVDF UF membrane substrates from concentrated DMF solution. Contact angle studies on PVDF-g-POEM coated membranes reported previously demonstrate that these coatings exhibit spontaneous wetting by water [12].

Typical SEM micrographs of the base and coated membranes used in this study are shown in Figure 3.4. As seen in Figure 3.4a, the Sepro PVDF400 base membrane exhibits a surface morphology of sparse, ~0.05 μm circular pores characteristic of PVDF membranes fabricated by immersion precipitation [46]. The relatively high permeability of this membrane (pure water permeability of 2700 L/m^{2}hMPa) can be attributed to large macrovoids seen in cross section (Figure 3.4b). This membrane, with a high permeability, was selected to ensure that the base membrane has a smaller contribution to the hydraulic resistance of the TFC membrane. After coating, surface pores of the UF membrane are no longer observable, and nodular features appear (Figure 3.4c). From SEM cross-sections, the coating layer is approximately 2 μm thick (Figure 3.4d).
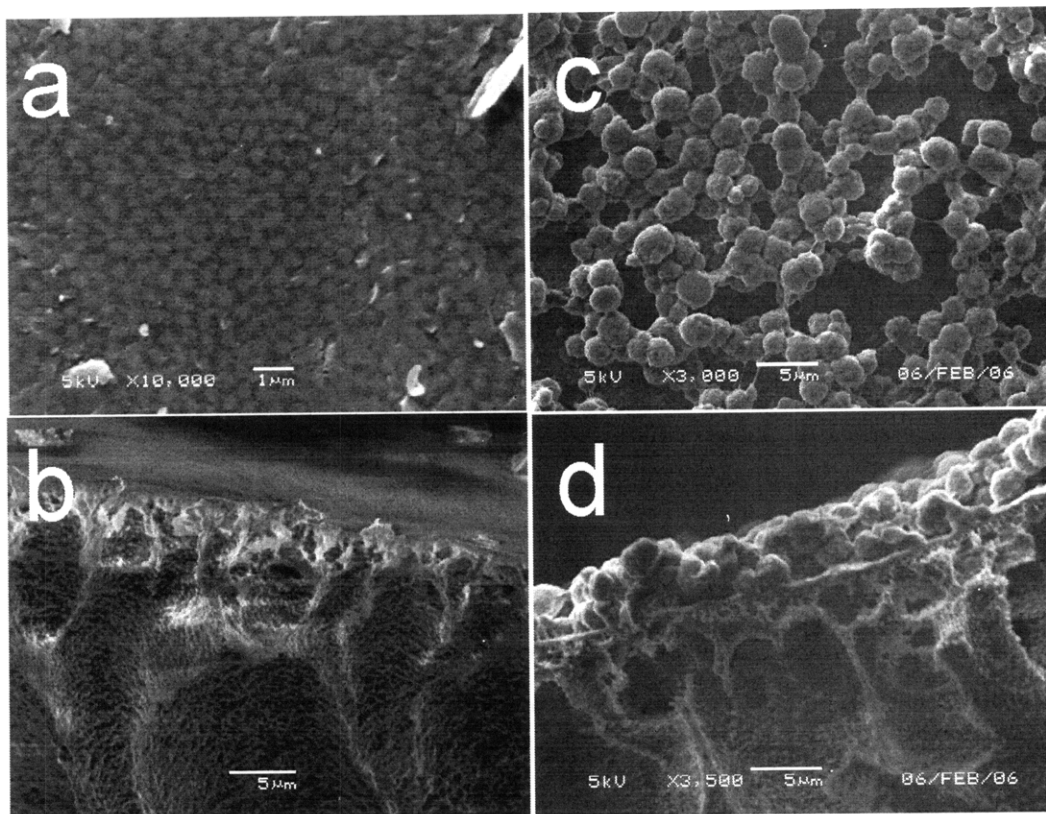
Figure 3.4. SEM micrographs of the PVDF400 UF base (a, surface, and b, cross-section) and PVDF-g-POEM-coated (c, surface, and d, cross-section) membranes.

Pure water permeability (PWP) values for the PVDF-g-POEM TFC NF membranes ranged between 10-56 L/m²hMPa, mostly dependent on the thickness of the PVDF-g-POEM coating layer. These values were consistent with those reported by Akthakul et al. [12], and are in a range on the higher end of common commercial NF membranes [34]. The PWP of these TFC membranes could be significantly improved by developing better coating methods. To achieve good separation, the coating layer of a TFC membrane needs to be only a couple hundred nanometers, provided it is defect-free. This is an order of magnitude thinner than the coatings prepared here, produced using bench-scale processes. However, fabrication of sub-micron scale coatings are a common process in the membrane industry, widely performed in large scale using methods such as dip coating or spray coating [1].

3.3.2. Fouling resistance: Model organic foulants

Previous studies on PVDF-*g*-POEM-coated membranes demonstrated complete resistance to fouling by a 1000 mg/L oleic acid/triethanolamine/water microemulsion over a 1.5 h filtration period, along with complete (>99.9%) retention of oleic acid [12]. Long-term fouling behavior, however, has much greater relevance in industrial applications. Membrane replacement is performed in much less frequent intervals in practice, and as infrequently as possible. Furthermore, more fouling mechanisms can be taken into account in longer term studies [39, 66, 176]. Therefore, 10-day dead-end filtration studies were performed with the PVDF-g-POEM coated NF membranes, using foulants representative of proteins, polysaccharides, and NOM, along with filtration studies of shorter duration (16-24 hours) with the PVDF400 UF base membrane control. The foulants were chosen to represent the most common culprits of fouling in NF operation [35, 66, 153, 155, 164]. They are also known to be major contributors to biofouling in a range of processes [59, 147], including membrane bioreactors (MBRs) [37, 67, 69, 153, 177]. In each case, Milli-Q water was passed through the membrane until the flux stabilized. The flux decline during this initial period is due to membrane compaction. With the application of pressure the base membrane is compressed, resulting in partial blocking of pores. In the data to follow, this effect is less notable for the NF membranes because the flux is largely determined by the non-porous coating layer, which does not deform substantially under pressure.

The experimental setup included a small filtration cell (15 mL liquid capacity) connected to a large tank (3.5 L capacity) by a narrow tube. Therefore, during the filtration studies, diffusion from the cell to the tank was negligible. Since the coated NF membranes were observed to retain essentially all of the foulant, a constant build-up of foulant concentration occurred in the filtration cell, which could be estimated by a simple material balance around the cell. This aspect allowed characterization of the fouling resistance of the described membranes to very high foulant concentrations as well as the 10-day fouling potential in a single experiment. The continuous build up of foulant in these experiments further provides a close parallel to MBR operation, where high molecular weight substances can accumulate in the reactor over time [29, 30, 69, 178].

Figure 3.5a shows the 10-day dead-end filtration results from a TFC NF membrane for a 1000 mg/L solution of BSA in PBS, performed at 0.21 MPa (30 psi), and plotted as a function of normalized flux (flux/initial flux) vs. time [17]. The error bars in this figure (as well as in Figures 3.6 and 3.7) arise from the limitations of the experimental setup, and not from collapsed data of repeated experiments: The permeate flow comes one droplet at a time, and the measured volume at each data point can vary by the amount of a single droplet, approximately 0.05-0.1 mL, indicated by the error bars. For many data points, the error bars lie within the symbol area. The flux shows a slow decline over the course of the filtration (~13% after 10 days), which is fully recovered when the cell is rinsed and the foulant solution is replaced with deionized water. No irreversible flux loss was observed. Also shown in this figure is the calculated BSA concentration in the filtration cell, based on the measured BSA retention of >99.9% for this membrane (Table 3.1). The complete retention of BSA by the NF membrane is consistent with the reported globular dimensions of this protein (a heart-shaped molecule with 8 nm sides and 3 nm width [179]), relative to the width of the hydrophilic nanochannels of PVDF-g-POEM observed by TEM (~2 nm) [6, 12]. At the end of 10 days, the cell concentration had reached 65,000 mg/L. The modest flux loss observed at such high concentrations suggests these membranes could be suitable in filtration operations involving highly concentrated feed streams.

Table 3.1. Foulant retention values of PVDF-g-POEM coated NF membrane and PVDF base membrane. Retentions measured after 1 hour of foulant filtration.

Membrane	BSA retention (%)	Humic acid retention (%)	Sodium alginate retention (%)	Total COD retention (%)
PVDF-g-POEM coated NF	>99.9	99	92	99.5
Sepro PVDF400 base	69	37	60	98
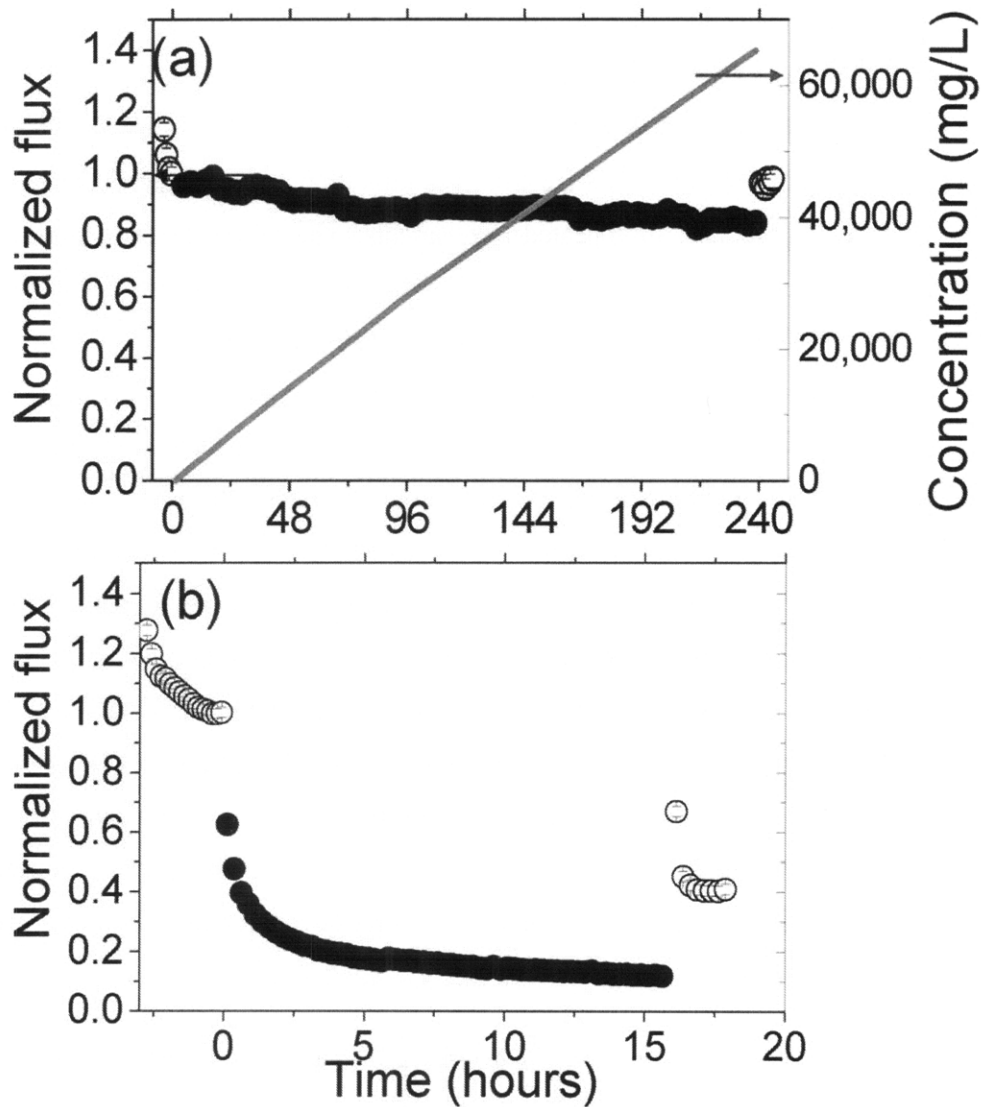
Figure 3.5. Dead-end filtration of model protein solution with a) PVDF-g-POEM-coated NF membrane (average pure water permeability 39±10 L/m²hMPa); b) PVDF base membrane (average pure water permeability 2700±660 L/m²hMPa). ○: Milli-Q water, ●: 1000 mg/L BSA in PBS, —: Calculated concentration in the filtration cell (top graph only). Tests performed at 30 psi (a) and 10 psi (b).

Figure 3.5b shows the normalized flux data for the Sepro PVDF400 UF base membrane for filtration of a 1000 mg/L BSA solution at 0.07 MPa (10 psi) over a period of 16 h. Despite the shorter run time, the irreversible flux loss for the UF membrane was around 60%. BSA retention for the UF base membrane after 1 h filtration was 69%, compared to complete retention (within instrument resolution) for the coated membrane (Table 3.1). The retention of the protein by the UF membrane is expected to increase in time due to internal pore fouling, as indicated by the large decline in flux. The results further illustrate the potential of these NF membranes to significantly enhance effluent quality.

Similar results were obtained upon filtering 1000 mg/L sodium alginate through the coated and uncoated membranes (Figure 3.6) [17]. In this case, the observed flux decline for both membranes was more dramatic. The TFC NF membrane showed approximately 71% loss relative to the pure water flux after 10 days of filtration at 0.21 MPa (30 psi). The coated membrane had an alginate retention of 92% after 1 hour of filtration, suggesting that low molecular weight portions of the foulant could pass through the membrane. The 92% figure can be considered a minimum retention for sodium alginate, since the substantial flux decline over the 10-day filtration was likely accompanied by increased retention. Assuming the retention remained constant throughout the 10-day experiment, Figure 3.6a plots the calculated foulant concentration in the filtration cell as a function of time. By this conservative estimate, the sodium alginate concentration reached 12,000 mg/L by the end of the 10 day period. The flux decline observed in Figure 3.6a can thus be attributed to the substantial rise in osmotic pressure due to alginate accumulation. However, the initial pure water flux could again be fully recovered for the NF membrane upon rinsing the cell and switching the feed to DI water. By contrast, a flux loss of 96% was observed for the UF base membrane after only 24 h filtration at 0.07 MPa (10 psi), with 41% irreversible flux loss (Figure 3.6b). Alginate retention was also substantially lower (60%) for the uncoated membrane (Table 3.1).
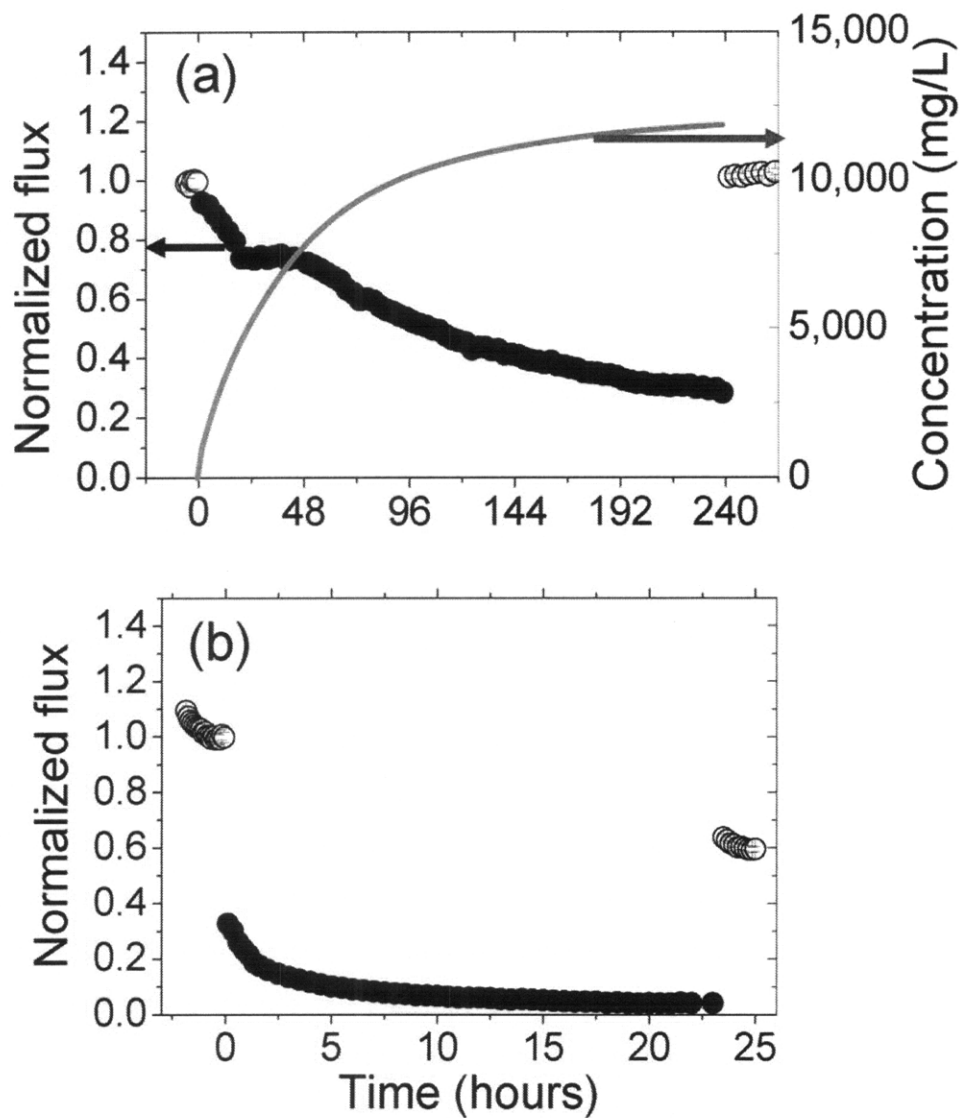
Figure 3.6. Dead-end filtration of model polysaccharide solution with a) PVDF-g-POEM-coated NF membrane; b) PVDF base membrane. ○: Milli-Q water, ●: 1000 mg/L sodium alginate in Milli-Q water, —: Calculated concentration in the filtration cell (top graph only). Tests performed at 30 psi (a) and 10 psi (b).

Membrane susceptibility to fouling by natural organic matter (NOM), represented by its major component humic acid (HA) [160], was also investigated. After 10 days of filtration of 1000 mg/L HA solution at 0.21 MPa (30 psi), the TFC NF membrane showed no decrease in flux (Figure 3.7a) [17]. At the end of this period, the concentration was

calculated to be 24,000 mg/L, based on a measured HA retention of 99%. However during the filtration, humic acid was observed to precipitate from solution, aided by the high concentration of Ca^{2+} in the feed [167]. Thus the calculated concentration values in Figure 3.7 indicate the extent of HA retention, rather than the dissolved concentration of humic acid in the cell. Upon opening the cell at the end of the fouling period, no cake layer was observed on the membrane. The remarkable constant flux demonstrated for the NF membrane stands in marked contrast to the results for filtration of the same HA solution through the UF base membrane. After 24 h filtration through the base membrane at 0.07 MPa (10 psi), an irreversible flux loss of 43% was found (Figure 3.7b), with an HA retention of 37% (Table 3.1).
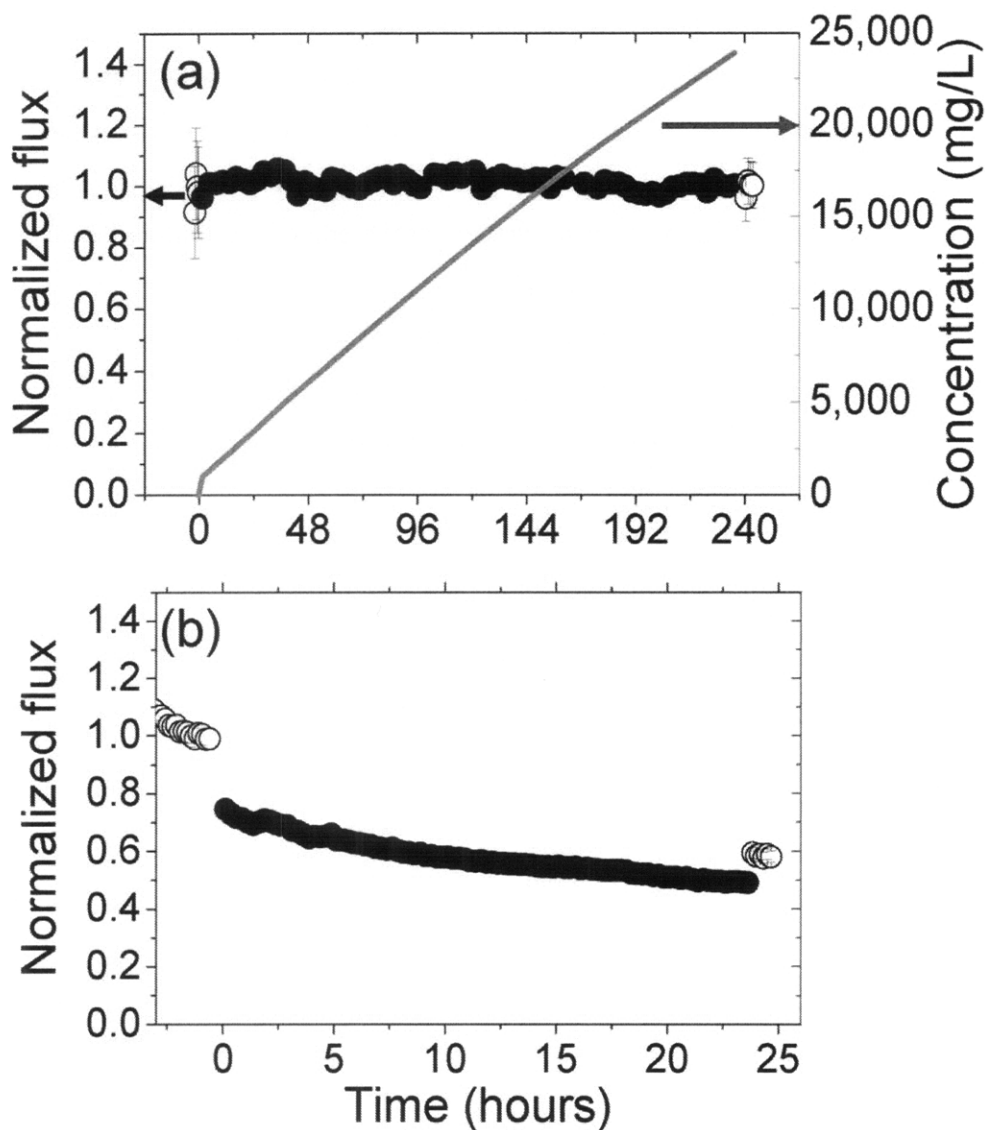
Figure 3.7. Dead-end filtration of model NOM solution with a) PVDF-g-POEM-coated NF membrane; b) PVDF base membrane. ○: Milli-Q water, ●: 1000 mg/L humic acid in 10 mM CaCl₂, ▬: Calculated concentration in the filtration cell (top graph only). Tests performed at 30 psi (a) and 10 psi (b).

3.3.3. Membrane fouling: Membrane bioreactor experiments

The results from the combined studies above suggest that the PVDF-g-POEM TFC NF membranes should exhibit lower fouling and produce higher quality effluents in MBR

operations compared with UF membranes conventionally employed. To further explore this application, dead-end filtration experiments were performed on uncoated and coated membranes using activated sludge taken from an aerobic bioreactor. These tests were performed by Adrienne Menniti in the Morgenroth lab at University of Illinois at Urbana-Champaign. Figure 3.8 compares the normalized flux data for the TFC NF membrane and the PVDF400 base membrane. For the NF membrane (run at 0.28 MPa) no flux decline was observed through the experiment, i.e., no reversible or irreversible fouling occurred over the 16 h run period (Figure 3.8a). The slight increase in flux throughout the experiment was most likely caused by a temperature increase and a corresponding decrease of the water viscosity. (Because of the low inherent flux, heat generated by the stir plate can raise the temperature in the filtration cell by 2 or 3 °C over 16 hours.) The lack of fouling by the activated sludge was confirmed with a second NF membrane sample. By contrast, the PVDF400 base membrane (run at 0.07 MPa) showed extensive fouling (Figure 3.8b). A flux loss of 84% was reached after 4 h of activated sludge filtration, with 57% irreversible flux loss. The NF membrane also exhibited better total COD retention: 99.5% compared with 98% for the base membrane (Table 3.1).
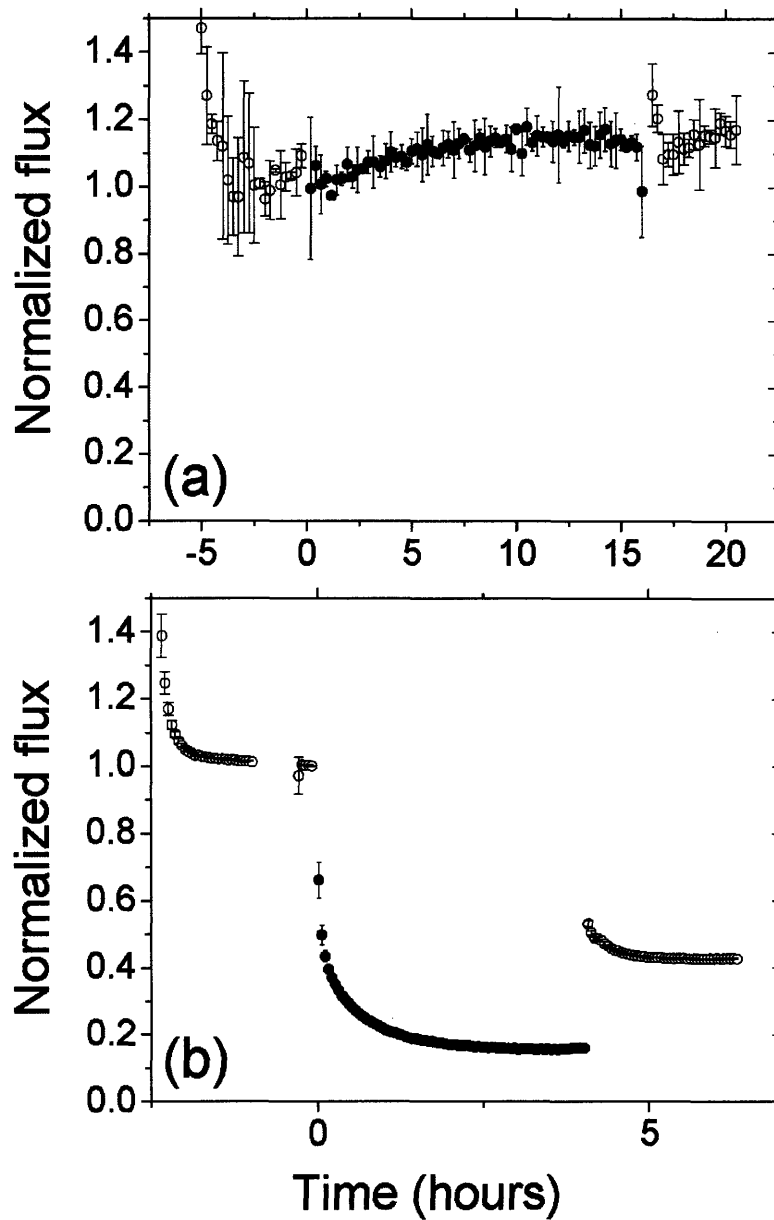
Figure 3.8. Dead-end filtration of MBR activated sludge with a) PVDF-g-POEM coated NF membrane (1745 mg/L VSS); b) PVDF base membrane (1855 mg/L VSS). o: NANOpure water, •: Activated sludge. Tests performed at 40 psi (a) and 10 psi (b). Data and error bars represent averages and standard deviations of five consecutive flux measurements. Tests performed by Adrienne Menniti in the Morgenroth lab at U.I.U.C.

3.3.4. Interaction forces and fouling resistance mechanism

A versatile method of quantifying the fouling potential of a membrane involves the measurement of the interaction forces between the membrane surface and an AFM probe modified to simulate a foulant molecule. This experimental protocol, reported by Li and Elimelech [166], involves attaching a colloid functionalized with carboxylic acid groups (a surrogate for organic foulants) to the tip of an AFM cantilever, and measuring the forces involved as the colloid probe approaches and retracts from the membrane surface. Both approach (extending) and adhesion (retracting) force profiles are analyzed. The approach curves provide information on the type and the range of interaction forces between the foulant and the membrane, while the retracting (pull-off) curves provide information on the strength of foulant adhesion to the membrane surface. Previous research indicates that the magnitude of the adhesion force correlates well with the fouling propensity of membranes in the presence of organic foulants [166, 174].

In this study, interaction forces between the carboxylate-modified latex particle probe and the membrane were determined at a range of ionic strengths (1 to 100 mM NaCl) as well as in the presence of 0.5 mM Ca^{2+} at a fixed ionic strength of 10 mM.

The interaction force profiles for the approach of the colloid probe to the PVDF-g-POEM NF membrane surface showed little variation with ionic strength and composition, with a decay length much greater than that predicted for electrostatic interaction (Figure 3.9). For instance, in 100 mM solution, the Debye screening length, a characteristic length of electrostatic interactions, is about 1 nm whereas the measured decay length for the PVDF-g-POEM membrane was 13 nm. These observations suggest the presence of repulsive steric forces which prevent the adsorption of organic foulants to the membrane surface, consistent with the absence of irreversible fouling seen in dead-end filtration of the model organic foulants and activated sludge from the MBR.
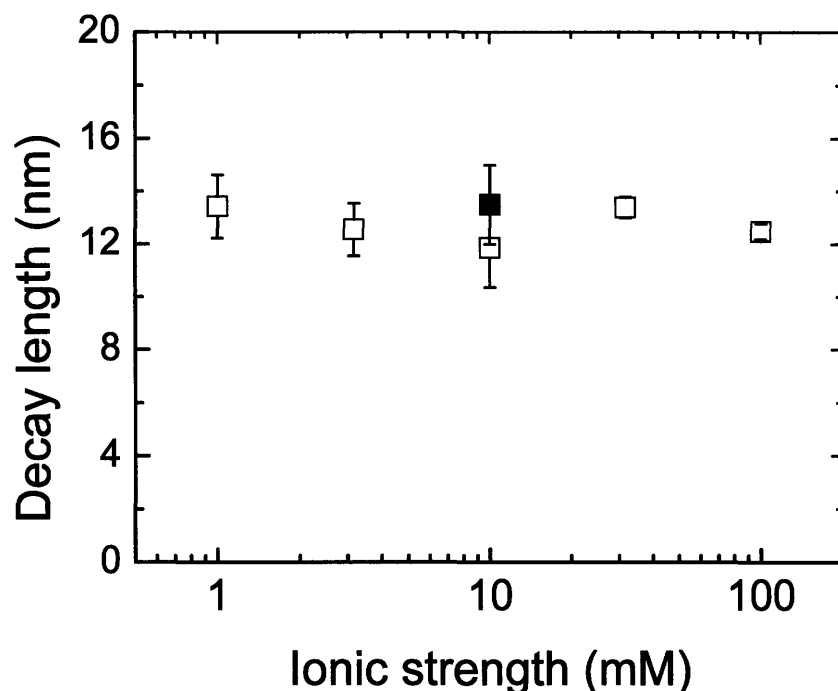
Figure 3.9. Decay lengths of the interaction forces between the AFM particle probe and the PVDF-g-POEM membrane as a function of ionic strength and composition. The error bars indicate standard deviations. Measurements were carried out at room temperature (23°C). NaCl (□) NaCl + CaCl₂ (■) Experiments were conducted by Dr. Seoktae Kang in the Elimelech Group at Yale University.

The adhesion forces, determined from the retraction (pull-off) curves, also support our fouling behavior data. Figure 3.10a shows the pull-off curves of a commercial PVDF membrane in NaCl solutions of different ionic strengths. A deep energy minimum is observed during the retraction of the colloid probe, indicating adhesion forces between the foulant and the membrane surface. This adhesive force becomes stronger at lower ionic strengths. The pull-off curves for the PVDF-*g*-POEM TFC NF membranes, shown in Figure 3.10b, exhibit no energy minima, indicating no adhesive forces between the foulant molecule and the membrane. On the contrary, repulsive forces were observed

near the surface of the membrane, as indicated by the *F/R* measurements reaching positive values.
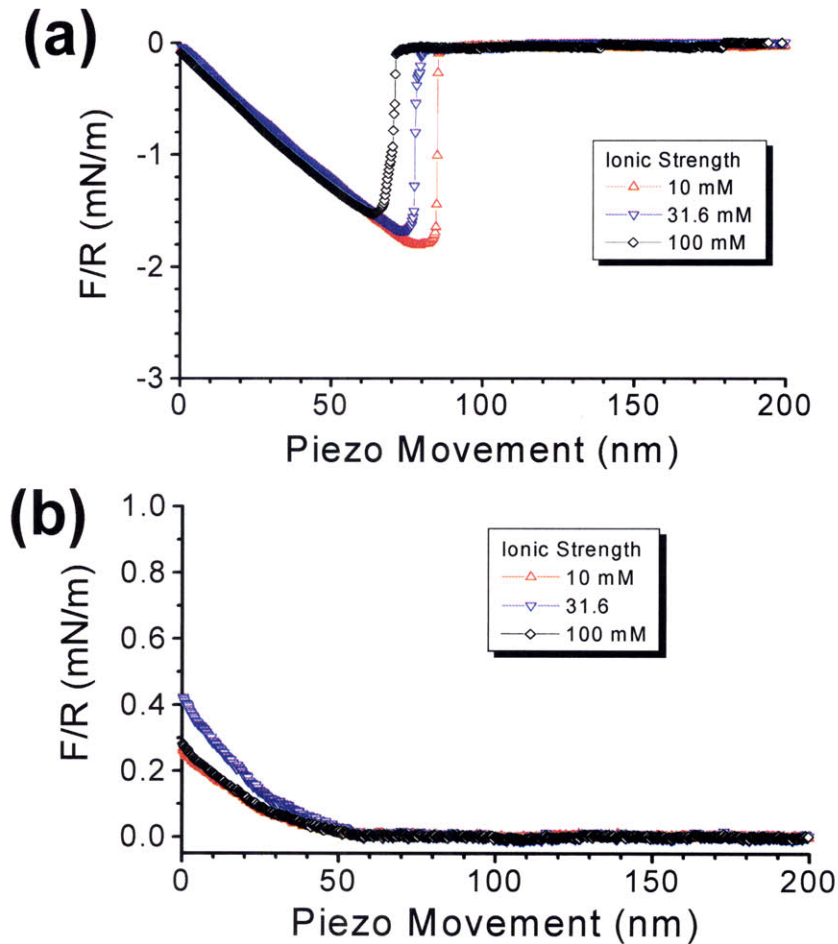
Figure 3.10. Interaction forces during retraction (pull-off) between the colloid probe and the surface of (a) PVDF UF base membrane and (b) PVDF-g-POEM TFC NF membrane. Experiments were conducted by Dr. Seoktae Kang in the Elimelech Group at Yale University.

The magnitude of the adhesion forces for the PVDF UF base membrane and the novel PVDF-g-POEM NF membrane are presented in Figure 3.11 for various solution ionic compositions. For the PVDF base membrane control, strong adhesion forces are detected

as indicated by the large negative values of the measured adhesion force (*F*) normalized by the CML particle radius (*R*). Such strong adhesion forces correlate quite well with the severe organic fouling observed with this membrane. In contrast, no adhesion was detected with the PVDF-*g*-POEM-coated membrane (no negative values of *F*/*R*), even in the presence of divalent calcium ions. This remarkable observation agrees well with the lack of irreversible fouling observed for these membranes, even at high feed concentrations of organic foulants.
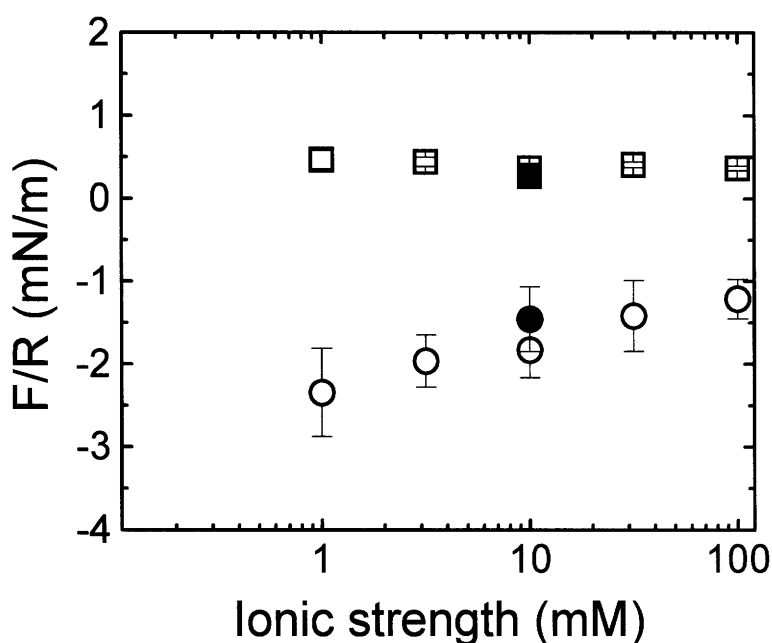
Figure 3.11. Variation of the adhesion force normalized with the AFM particle probe radius as a function of solution ionic composition for the PVDF base UF membrane and the PVDF-g-POEM NF membrane. The experiments with divalent calcium ions were carried out with 0.5 mM CaCl2 plus 8.5 mM NaCl so that the total ionic strength was fixed at 10 mM. The error bars indicate standard deviations. Measurements were carried out at room temperature (23°C). PVDF-g-POEM: NaCl (□); CaCl₂ + NaCl (■). PVDF base: NaCl (○); CaCl₂ + NaCl (●). Experiments were conducted by Dr. Seoktae Kang in the Elimelech Group at Yale University.

3.3.5. Responsive pore size properties

PVDF-*g*-POEM TFC NF membranes were also investigated for their ability to change their permeability and selectivity according to process parameters, enabling the fine-tuning of their effective pore size depending on the separation desired. The responsive qualities of the membrane arise from the dependence of the effective pore size on the conformation of PEO chains within the hydrophilic nanochannels. PEO chains highly swollen in a good solvent create steric hindrance to molecular transport through the channels, reducing the effective channel width. In a poor solvent, the chains collapse toward the walls of the adjacent PVDF domains, allowing relatively larger molecules through. The transition is gradual, as the radius of gyration of polymer chains varies gradually with solvent quality, giving a means to tune the selectivity within a certain range.

3.3.5.1. Effect of ethanol content of the feed

To demonstrate this approach, water at room temperature was employed as a good solvent for PEO [134, 136, 137], to which varying amounts of ethanol were added. PEO solvency is decreased by adding ethanol into water, as shown in previous calorimetric and rheological studies [128]. Therefore, the permeation of a retained solute of size comparable to the channel width through a PVDF-*g*-POEM membrane is expected to increase when ethanol is added to the feed.

Figure 3.12 shows the percentage of Brilliant Blue R (BB) passing through the membrane versus ethanol content in the feed solution. It can be seen that when the feed is water alone, all of the BB was retained (within instrument sensitivity). Thus the effective pore diameter in water is less than the molecular diameter of BB, calculated to be 11.1 Å. As ethanol content in the feed rose, the amount of BB passing through the membrane increased, indicating a widening of the nanochannels due to partial collapse of the PEO chains. For feed compositions beyond 40 volume percent ethanol, additional ethanol did not increase the permeation any further. The maximum percentage of dye passing through the membrane was approximately 45%. This reduction in the dye concentration

69

in the permeate vs. the feed suggests that the diffusion of dye molecules through the membrane selective layer is hindered compared with accompanying water molecules.
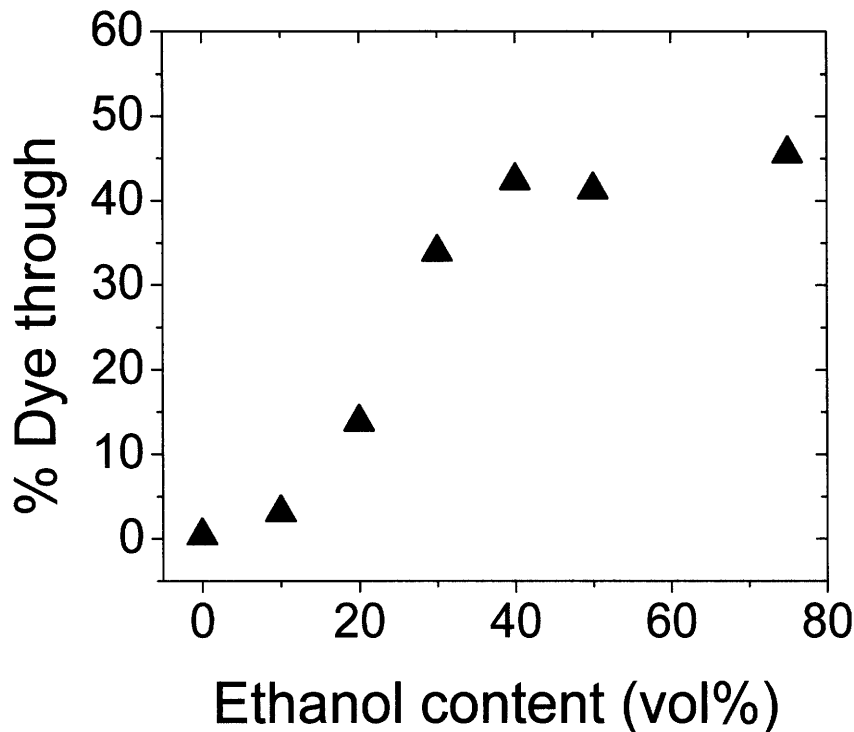
Figure 3.12. Percentage of Brilliant Blue R dye passing through PVDF-g-POEM TFC NF membrane versus ethanol content of the feed. Experiment performed at room temperature and 50 psi. Initial dye concentration: 100 mg/L. Percent dye through is defined as the ratio of the concentration of dye in the permeate to that in the feed.

3.3.5.2. Effect of temperature, pressure and ionic strength

PEO-water systems have been studied extensively in the literature, both due to their applications in biotechnology and water treatment, and because of the interesting and unusual properties of PEO in water when compared with other polyethers [126-135, 137, 139, 140]. PEO-water mixtures exhibit a lower critical solution temperature (LCST), indicating that as a solution of PEO in water is heated, a temperature exists where the polymer's precipitation is thermodynamically favored. The LCST for PEO-water mixtures has been measured to be 99°C for high molecular weight PEO (1020 kg/mol).

As molecular weight decreases, the LCST shifts to higher temperatures, and was measured to be 175.6°C for PEO of 2.27 kg/mol molecular weight [139]. Below the LCST, the solvent quality of water for PEO increases as temperature decreases, causing an expansion of the coils [128, 129, 133-135].

This property implies that the permeability of PVDF-*g*-POEM TFC NF membranes should increase with increasing feed temperature, as PEO side chains contract within the nanochannels. This can be observed in Figure 3.13a, where the permeability of DI water through the membrane is shown at room temperature (triangles) and at 70°C (squares) for different pressures. At each pressure, the permeability of the membrane increased substantially when the temperature was raised to 70°C. At 50 psi pressure, the increase was almost 4.5-fold.

At higher pressures, the increase in permeability with temperature was even more dramatic—up to 5.5-fold at 200 psi. This finding is related to the fact that the LCST of PEO in water is depressed by high pressures [126-128, 130]. The effect of pressure on PEO solvency is relatively small at room temperature, which is quite far from the LCST. This is consistent with the data in Figure 3.13a, which show that the permeability is essentially unaffected by pressure at room temperature. However at temperatures closer to the LCST, the pressure effect becomes more significant. In Figure 3.13a, the permeability of the membrane at 70°C increases by 60% when the pressure is increased from 50 psi to 200 psi.
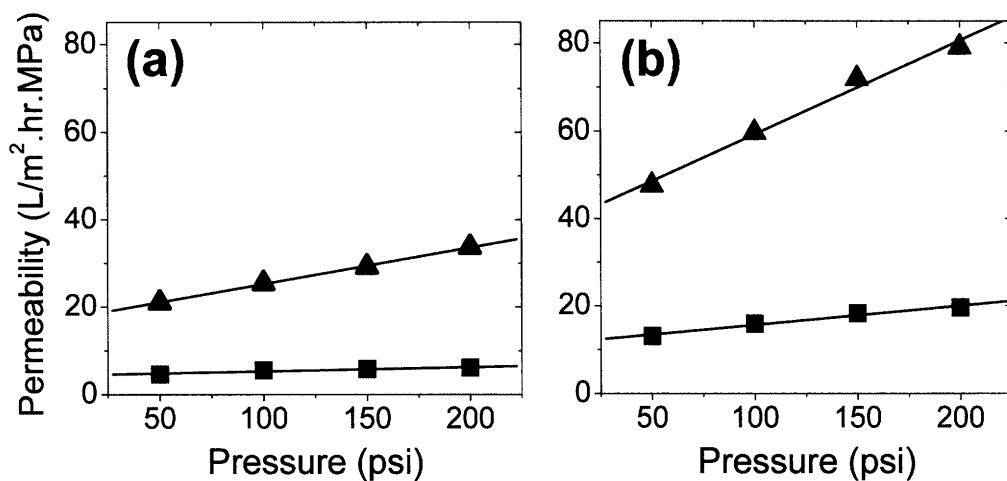
Figure 3.13. Permeability of PVDF-g-POEM TFC NF membrane with a feed of (a) DI water and (b) 0.2 M NaCl, at room temperature (■) and at 70°C (▲) at varying pressures.

Similar effects were observed when the permeation of Reactive Red 120 (RR) was investigated (Figure 3.14a). At room temperature, 5% of RR permeated through the membrane at 50 psi. This increased to 7.5% when the pressure was increased to 200 psi. At 70°C, 9.6% of RR passed through the membrane at 50 psi, significantly higher than the values at room temperature. Increasing the pressure to 200 psi caused the dye permeation to double, reaching 19%.
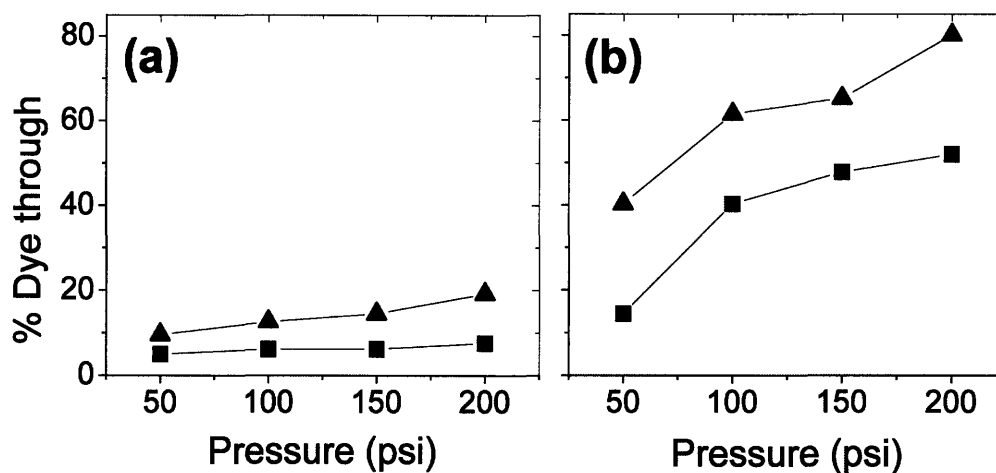
Figure 3.14. Percentage of Reactive Red 120 dye passing through PVDF-g-POEM TFC NF membrane with the dye dissolved in (a) DI water and (b) 0.2 M NaCl, at room temperature (■) and at 70°C (▲) at varying pressures. Initial dye concentration: 100 mg/L. Percent dye through is defined as the ratio of the concentration of dye in the permeate to that in the feed.

Another important parameter in PEO-water solution behavior is the ionic strength of the solution. PEO exhibits salting-out behavior—increasing the ionic strength of a PEO-water solution causes a significant depression in its LCST and a marked decrease in solvent quality [127-129, 140]. The effect is especially strong when the PEO component is of low molecular weight [140]. The addition of salt to a PEO-water system also results in a decrease in its lower critical solution pressure (LCSP), the pressure at which PEO falls out of solution [127-129]. Therefore, high ionic strengths should increase the permeability of the PVDF-g-POEM TFC NF membranes and amplify the effects of high temperature and pressure on coil size.

Figure 3.13b shows the permeability of the PVDF-g-POEM TFC NF membrane at different temperatures and pressures with a feed of 0.2 M NaCl. At room temperature and 50 psi, the permeability of the membrane increased 2.8 times upon the introduction of salt to the feed. At room temperature, the change in permeability with pressure was much

more pronounced compared to the DI water feed. Increasing the pressure from 50 psi to 200 psi caused a permeability increase of 50%. When the temperature was increased to 70°C at 50 psi, the permeability increased from 13 L/m^2 h MPa to 48 L/m^2 h MPa. At this elevated temperature, the pressure effect was even more notable. The permeability of the membrane increased by 66%, up to 79 L/m^2 h MPa, at 200 psi.

Similar trends could be observed in the filtration of Reactive Red 120 when the feed contained 0.2 M NaCl (Figure 3.14b). At room temperature and 50 psi, the addition of salt caused the permeation of RR to increase to 15% from 5.0%. The effect of pressure was very evident even at room temperature, and 40% of the dye passed through the membrane when the pressure was increased to 200 psi. Increasing the pressure at 70°C caused the dye permeation to rise even further, up to 80% at 200 psi. This demonstrates the potential to alter the selectivity of the PVDF-g-POEM TFC membrane quite significantly by changing the operational temperature and pressure.

3.3.5.3. Effect of temperature and ionic strength on the swelling of PVDF-g-POEM

As mentioned in the chapter introduction, there are two main approaches employed in the design of responsive membranes [108]. The first one exploits changes in the coil size of polymer chains lining the pores to alter performance: as the coils expand, permeation is reduced due to steric effects. This is the most common strategy described for responsive UF and MF membranes [7, 111, 112, 115, 118, 120]. Conversely, in the second approach, polymer swelling leads to an increase in membrane permeability. In these systems, the polymer is held together by physical or chemical cross-links to regulate permeation. This is the strategy adopted for most responsive NF membranes [114, 122-125].

To verify that the PVDF-g-POEM membranes operate under the first mechanism and not the second, the swelling of a sample of PVDF-g-POEM was measured at a series of temperatures, in DI water and in 0.2 M NaCl (Figure 3.15). In this figure, swelling ratio is defined as the weight of the swollen polymer to its dry weight.
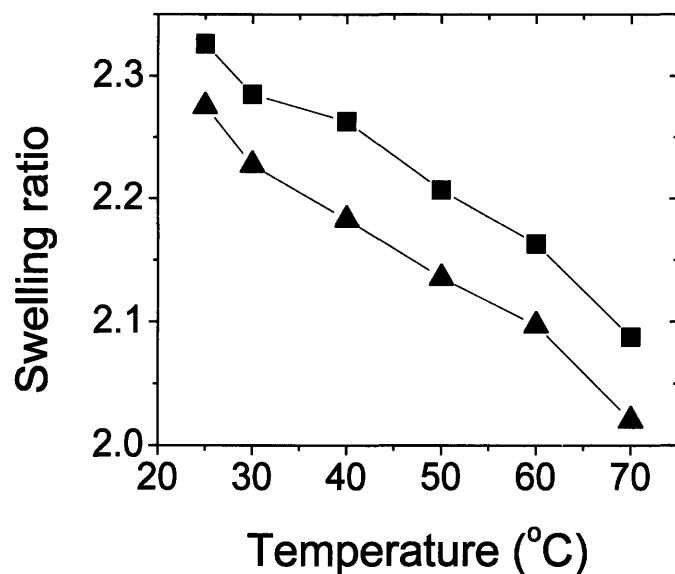
Figure 3.15. Change in swelling ratio of PVDF-g-POEM with temperature in DI water (▲) and 0.2 M NaCl (■)

The swelling of the polymer in DI water decreased gradually as temperature increased. This is consistent with the change in the solvent quality of water for PEO with temperature. Considering the strong hydrophobicity and crystallinity of PVDF, PEO should be the only component that swells in water. A similar effect was observed when the polymer was swollen in 0.2 M NaCl solution. The degree of swelling of PVDF-g-POEM in salt solution was always lower than that in DI water, as expected based on the reduced solubility of PEO in salt solutions. Swelling once again decreased as the temperature was increased.

If the permeability change were caused by increased swelling of the copolymer, then the permeability of the membrane would be expected to decrease with increasing temperature and ionic strength. The fact that the permeability and effective pore size both increase with decreasing swelling is consistent with the first mechanism: the selectivity and permeability of the membrane is altered due to the change in conformation of the PEO chains lining the nanochannels.

3.4. Conclusions and Future Directions

This chapter aimed to provide a better characterization of PVDF-*g*-POEM TFC NF membranes first developed by Akthakul in the Mayes group. The membrane coating method was improved, using a control coater and a base membrane with higher permeability, to obtain higher fluxes and better reproducibility. Better coating techniques, such as dip coating as practiced in the industry, should improve the PWP of these membranes even further.

The exceptional fouling resistance of these membranes was demonstrated with a range of foulants relevant to NF processes, as well as a real-life application, MBR treatment of wastewater. In each of these cases, the membranes showed complete resistance to irreversible fouling due to adsorption. AFM experiments using colloid probes showed that there is a long range steric repulsive force between the membrane surface and the foulant that prevents adsorption. This is believed to be the cause of the exceptional fouling resistance of such membranes.

One of the most important advantages of PVDF-*g*-POEM TFC NF membranes is their ability to perform size-based separations in the small molecule range. This is not possible using commercial NF membranes. Furthermore, this study showed that the effective pore size of these membranes can be tuned to the desired separation by adjusting process parameters such as temperature, pressure, and ionic strength of the feed.

In short, PVDF-*g*-POEM TFC NF membranes have four highly desirable properties: high pure water permeability, exceptional fouling resistance, size-based separation ability on the molecular scale, and a pore size that can be fine-tuned to the application at hand. This combination would be especially promising for the pharmaceutical and food industries, which often perform highly specific separations and involve feeds with high fouling potential. PVDF-*g*-POEM TFC NF membranes would also be useful in other high-fouling applications where it is desirable to retain small molecules but not salts, such as domestic and industrial wastewater treatment, and MBRs.

PVDF-*g*-POEM TFC NF membranes have been studied in detail at the laboratory scale. Further improvements, however, are necessary for commercialization. Better coating methods, such as dip coating or spray coating, can form more uniform and thinner defect-free membranes. This could lead to even higher pure water permeabilities. In addition, the synthesis of PVDF-*g*-POEM needs further study. The ATRP-based synthesis can be unpredictable, since the resultant POEM content is dependent on reaction time and the age of some reactants such as CuCl. Alternative materials with more facile synthesis routes that can form similar membranes would be promising. This is investigated in the next chapter, which focuses on NF membranes based on amphiphilic comb copolymers with polyacrylonitrile backbones.

Chapter 4:

PAN-*g*-PEO as selective layer for TFC NF membranes

4.1. Introduction

As described in the last chapter, the use of poly(vinylidene fluoride)-*graft*-poly(oxyethylene methacrylate), PVDF-*g*-POEM, comb copolymers for the manufacture of thin film composite (TFC) nanofiltration (NF) membranes is very promising [11, 12, 17]. However, certain issues make the production of such membranes in large scale challenging. The main problem lies in the synthesis of this copolymer: The mechanism of the PVDF-*g*-POEM grafting reaction is based on atom transfer radical polymerization (ATRP) [5]. ATRP involves the use of copper complexes as the catalyst [180], which are often very difficult to remove, requiring the use of ion-exchange resins and/or adsorbent columns [181, 182]. These processes are difficult to scale up and hinder the use of ATRP in large-scale commercial production. The purification of PVDF-*g*-POEM suffers from similar difficulties, further amplified by the high viscosity of PVDF-*g*-POEM solutions and the limited choice of solvents for this polymer.

Another obstacle in the synthesis of PVDF-*g*-POEM is limited control: The reaction employs PVDF as a macroinitiator, and the degree of grafting is determined by the extent of reaction. However, the reaction rate is highly dependent on the purity and age of the copper (I) chloride catalyst, making it very difficult to control and estimate the resultant copolymer composition.

Therefore, an alternative amphiphilic comb copolymer would be useful in making the large-scale application of these TFC NF membranes more feasible. Such a polymer would still share the basic properties of PVDF-*g*-POEM: It must have a backbone of a

hydrophobic polymer, either glassy or crystalline, and side-chains of poly(ethylene oxide) (PEO). The two components must microphase separate in a bicontinuous morphology to form an interconnected network of nanochannels for water passage. Finally, the membranes cast using this material must show selectivity and fouling properties comparable to PVDF-g-POEM TFC NF membranes. However, the synthesis of the new copolymer should be simpler and more controlled, and the purification of the polymer must be simpler and more scalable.

A copolymer based on polyacrylonitrile (PAN) would be very promising in these respects. PAN is a glassy hydrophobic polymer that is widely used in the manufacture of ultrafiltration (UF) and microfiltration (MF) membranes [33]. Its monomer, acrylonitrile, can be polymerized easily by free-radical polymerization. It is also possible to form copolymers of acrylonitrile with acrylates and methcarylates. Hence, a graft copolymer with a PAN backbone and PEO side-chains, PAN-g-PEO, made by free radical copolymerization of AN with PEO-acrylate macromonomers, would have the potential to form fouling resistant, size-selective NF membranes similar to those based on PVDF-g-POEM, while eliminating difficulties associated with ATRP.

This chapter focuses on size-selective TFC NF membranes based on PAN-g-PEO. The synthesis of PAN-g-PEO is described, as well as the characterization of its microphase separation properties. The formation of NF membranes prepared by coating a UF membrane with PAN-g-PEO is illustrated. The most significant advantages of these membranes, namely their high pure water permeability, size-based selectivity, and fouling resistance, are demonstrated.

4.2. Experimental Methods

4.2.1. Materials

Acrylonitrile, poly(ethylene glycol) methyl ether acrylate (PEGA, $M_n \sim 454$ g/mol), azobisisobutyronitrile (AIBN) and the dyes used in size cut-off determination were purchased from Sigma-Aldrich (St. Louis, MO). Dimethyl formamide (DMF), toluene, deuterated dimethyl sulfoxide (DMSO), ethanol, isopropanol, bovine serum albumin

(BSA, 66.5 kDa), and hexane were purchased from VWR (West Chester, PA). All chemicals and solvents were reagent grade, and were used as received. PAN400 ultrafiltration membranes, purchased from Sepro Membranes, Inc. (Oceanside, CA), were used as the base membrane for the coating process, as well as a control. Deionized water was produced from a Millipore Milli-Q unit.

4.2.2. Synthesis of PAN-g-PEO

Polyacrylonitrile-*graft*-poly(ethylene oxide) (PAN-*g*-PEO) was synthesized by free radical polymerization. The reaction scheme is shown in Figure 4.1. Five grams each of acrylonitrile and PEGA were charged to a round-bottomed flask. The solvent (25 mL) and AIBN (0.01 g) were added. The flask was sealed with a rubber septum, purged with nitrogen gas for 20 minutes, and placed in an oil bath at 90°C with stirring. Either DMF or toluene could be used as the solvent. The reaction mixture remained homogeneous throughout the reaction when DMF was used as the solvent. During reaction in toluene, after approximately 20 minutes, precipitated polymer was observed in the flask. After 20 hours the flask was removed from the oil bath. The reaction mixture was diluted with approximately 50 mL of DMF to dissolve the precipitated polymer, and precipitated in a 3:1 mixture of ethanol and hexane. The recovered product was filtered and remaining solvent and monomer were extracted by stirring the polymer in an ethanol bath overnight. The polymer was then dried in a vacuum oven overnight.

The data reported in this chapter were obtained from membranes prepared using PAN-*g*-PEO synthesized in toluene. Comparable membranes were also prepared using PAN-*g*-PEO synthesized in DMF.
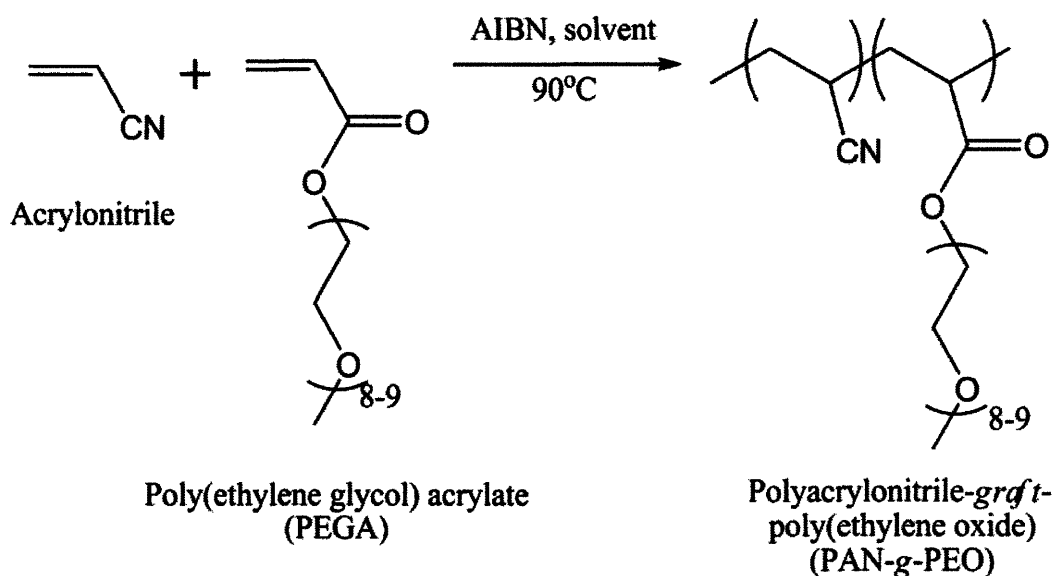
Figure 4.1. Synthesis scheme of PAN-g-PEO

4.2.3. Polymer characterization

4.2.3.1. Nuclear Magnetic Resonance (NMR) Spectroscopy

PEO content of the copolymer was determined by ^{1}H NMR spectroscopy in DMSO-d_6 using a Bruker DPX 400 spectrometer (Appendix B). Four peaks were assigned to the polymer protons (see Figure 4.2). The peak corresponding to the protons on the polymer backbone created two peaks: a broad peak at 1.7-2.2 ppm (A), and a narrower, smaller peak at 3.1 (B) that corresponds to the proton bound to the carbon attached to the nitrile group [86]. The protons of the first CH_2 group attached to the ester bond in PEGA (C) resulted in a peak at 4.3 ppm. The CH_2 and CH_3 protons on the PEO side-chain (D) created a broad peak at 3.5-3.7 ppm. The composition of the copolymer was calculated by comparing the integrations under the peaks corresponding to protons labeled A and C.

81
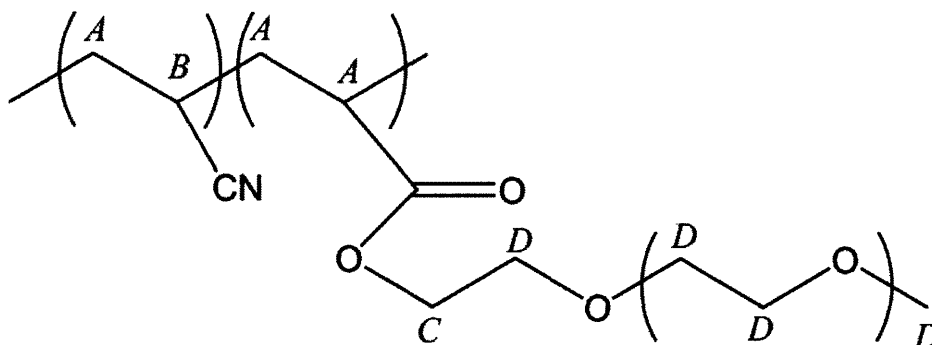
Figure 4.2. The chemical structure of PAN-g-PEO and types of protons studied in ^1H-NMR analysis.

4.2.3.2. Gel Permeation Chromatography (GPC)

The molecular weight distributions of polymers were determined by gel permeation chromatography in DMF at a flow rate of 1 mL/min, using a Waters 510 HPLC pump, Waters Styragel columns, and a Waters 410 differential refractometer (Millipore Corp., Bedford, MA).

4.2.3.3. Modulated Differential Scanning Calorimetry (MDSC)

MDSC was performed with a Q100 TA Instruments differential scanning calorimeter (DSC). The sample was prepared by placing approximately 11.5 mg of PAN-g-PEO in a hermetic aluminum pan. A regular heat-cool-heat cycle was run before the MDSC to equilibrate the polymer. The scan rate for MDSC was 2°C per minute, with modulations of 1.25°C every 60 seconds. Reversible heat flow rate was calculated from this data using TA Universal Analysis software to eliminate kinetic effects on the curve and isolate glass transition temperatures.

4.2.3.4. Transmission Electron Microscopy (TEM)

Microstructural characterization was carried out using a JEOL 2010 CX transmission electron microscope (TEM) in bright field mode at 200 keV by Elsa Olivetti in the Mayes group. Films of PAN-g-PEO cast from a 20% (w/v) DMF solution were mounted onto posts with epoxy and ultra-thin ~15 nm sections were cryomicrotomed using a diamond

knife (Diatome) and placed on copper grids (400 mesh, Ted Pella). PEO domains were preferentially stained with RuO_4 to enhance contrast. The samples were stained by placing grids onto a glass slide and loading them, for one hour, into a chamber containing RuO_4-vapor freshly added from ampoules (EMS Acquisition Corp.). The grids were then coated with 10 nm of carbon through thermal evaporation. Fast Fourier Transform (FFT) analysis was performed on the obtained TEM images using commercial image analysis software (ImageJ).

4.2.4. Fabrication of TFC membranes

The polymer solution was prepared by dissolving 1 g of PAN-*g*-PEO copolymer in 4 mL DMF at approximately 50°C. This solution was passed through a 1-µm syringe filter (Whatman) and degassed in an oven at approximately 90°C for approximately one hour, until no air bubbles could be seen. Membranes were coated using a control coater (Testing Machines Inc., Ronkonkoma, NY). The PAN400 base membrane was fixed onto the coater, and the coating blade adjusted to a nominal film thickness of 40 µm was inserted. The coating solution was poured onto the base membrane to form a thin line about 0.5 cm from the blade, and the coater was used to move the blade at a constant reproducible speed (speed level 4 on the instrument). After 5 minutes, the membrane was immersed in a bath of isopropanol for 30 minutes, then moved into a water bath. The membranes were kept wet at all times due to the poor drying resistance of PAN [33].

4.2.5. Characterization of TFC membranes: Scanning Electron Microscopy (SEM)

Membrane morphology was characterized using a JEOL 5910 Scanning Electron Microscope (SEM) operating at 5 kV. The membranes were fractured in liquid nitrogen for cross-sectional observation, and sputter coated with gold-palladium for SEM imaging.

4.2.6. Filtration Experiments

Circular pieces were cut from coated membranes, keeping them moist at all times. The experiments to determine the size cut-off of the membrane were performed using an Amicon 8050 stirred, dead-end filtration cell (Millipore) with a cell volume of 50 mL and an effective filtration area of 13.4 cm^2. The cell was stirred at 500 rpm using a stir plate

to minimize concentration polarization, and a pressure of 30 psi. The membrane was first allowed to compact by passing DI water through for at least one hour until the flux was stabilized. The pure water permeability (PWP) of the membrane was measured by collecting and weighing the permeate over a five minute interval. Then the cell was filled with a 100 mg/L solution of a dye of known size. The pressure was set to 30 psi, and a sample was collected after at least an hour, after the color of the filtrate was observed to be stable. The solution level in the cell was not allowed to reach less than 60% of the initial level; dye solution was added if necessary. At the end of this period, the cell was rinsed with DI water, and DI water was filtered through the membrane for at least an hour until the filtrate was clear. The above procedure was repeated for each dye.

Dye permeation values were obtained by measuring the dye concentration in this sample by UV-visible spectroscopy using a Cary 500i UV-Vis-NIR dual-beam spectrophotometer. The molecular size of each dye was calculated using Molecular Modeling software by ChemSW (Fairfield, CA). The molecular model of the dye was uploaded and the molecular volume was calculated using the software. Then the molecule was assumed to be a sphere of equivalent volume, and its diameter was reported as the size. The dye molecules used, along with their chemical structures, molecular weights, and molecular sizes, are given in Table 4.1.

Fouling experiments were performed following the procedure described in Section 3.2.4. However, the time period during which the foulant solution was filtered through the membrane was 24 hours for the experiments described in this chapter.

Table 4.1. Chemical structures, molecular weights, and sizes of dyes used in size cut-off determination

Name	Chemical structure	Molecular weight (g/mol)	Molecular size (Å)
Brilliant blue R		712.9	11.1
Congo red		532.2	10.1
Acid blue 45		311.1	8.4
Ethyl orange		292.0	8.23

4.3. Results and Discussion

4.3.1. Synthesis of PAN-g-PEO

The synthesis of PAN-g-PEO was performed using a free-radical copolymerization method, employing a macromonomer approach. PEO content of the resultant copolymers was within ±10% of the intended composition, as is usually observed in random copolymerizations [183]. Two different solvents were used in the synthesis of PAN-g-PEO. DMF solubilizes the resultant polymer, and when this solvent was used, the reaction mixture was homogeneous throughout the reaction. Toluene, on the other hand, is miscible with the monomers but it is not a good solvent for polyacrylonitrile. During the reaction, precipitation of the polymer from toluene was observed within 20 minutes of the start of the reaction, and most of the reaction continued in a heterogeneous medium. The molecular weight distributions of these polymers were determined by GPC in DMF. Figure 4.3 (a) and (b) show typical GPC traces of PAN-g-PEO samples synthesized in DMF and toluene, respectively. The molecular weights and polydispersities of these samples are tabulated in Table 4.2.
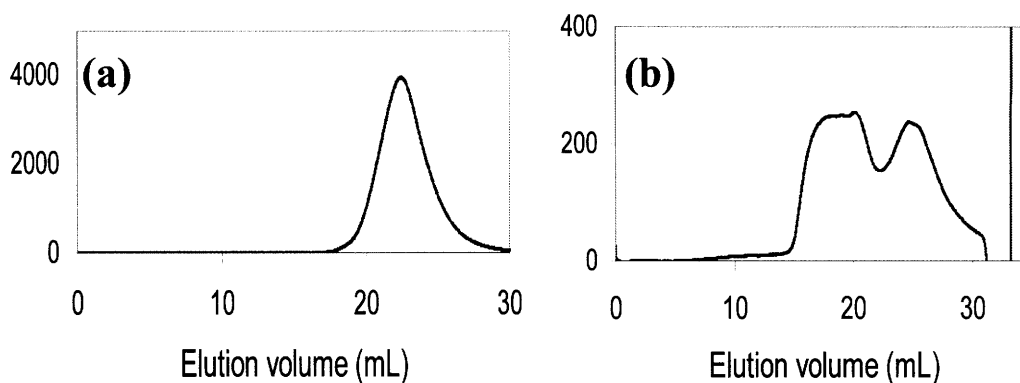
Figure 4.3. GPC traces of PAN-g-PEO samples synthesized in (a) DMF and (b) in toluene

Table 4.2. Molecular weights and polydispersities of PAN-g-PEO samples synthesized in different solvents, based on polystyrene standards

Solvent	Number average molecular weight, M_n (kg/mol)	Weight average molecular weight, M_w (kg/mol)	Z-average molecular weight, M_z (kg/mol)	Polydispersity index, PDI
DMF	135	286	503	2.12
Toluene	92.5	1221	2465	13.2

The molecular weight distribution of the PAN-g-PEO sample prepared in DMF was observed to be monomodal with a polydispersity index (PDI) of 2.12, typical of a free radical polymerization performed in solution. The sample synthesized in toluene, by contrast, had a very broad and multimodal molecular weight distribution, probably due to the gradual precipitation during the polymerization reaction.

4.3.2. Polymer phase separation

For a graft copolymer to be used in the manufacture of NF membranes described in this study, it needs to satisfy one important condition: The two components of the copolymer must undergo microphase separation and form a bicontinuous network structure of each phase, creating the effective "nanochannels" for water passage. To verify that microphase separation occurs in PAN-g-PEO, MDSC was performed. Figure 4.4 shows the reversible heat flow versus temperature plot for a sample of PAN-g-PEO obtained by MDSC analysis. The reversible heat flow was chosen to minimize the observation of kinetic effects, which are especially significant in systems with very small scale phase separation. Three transitions were observed. A large glass transition was observed at approximately -49°C. This value is consistent with the glass transition temperature of low molecular weight, non-crystalline PEO [184], and indicates the presence of a separate PEO phase. A second transition is observed at approximately 70°C. This value corresponds to the second amorphous relaxation observed for PAN cast from DMF [185], indicating the

presence of a separate PAN phase. Finally, a third transition is observed at 153°C, which corresponds to backbone rotation in PAN [185]. The presence of separate transition temperatures for PEO and PAN verify that microphase separation occurs in PAN-g-PEO, and suggests the promise of this copolymer for the preparation of TFC NF membranes.
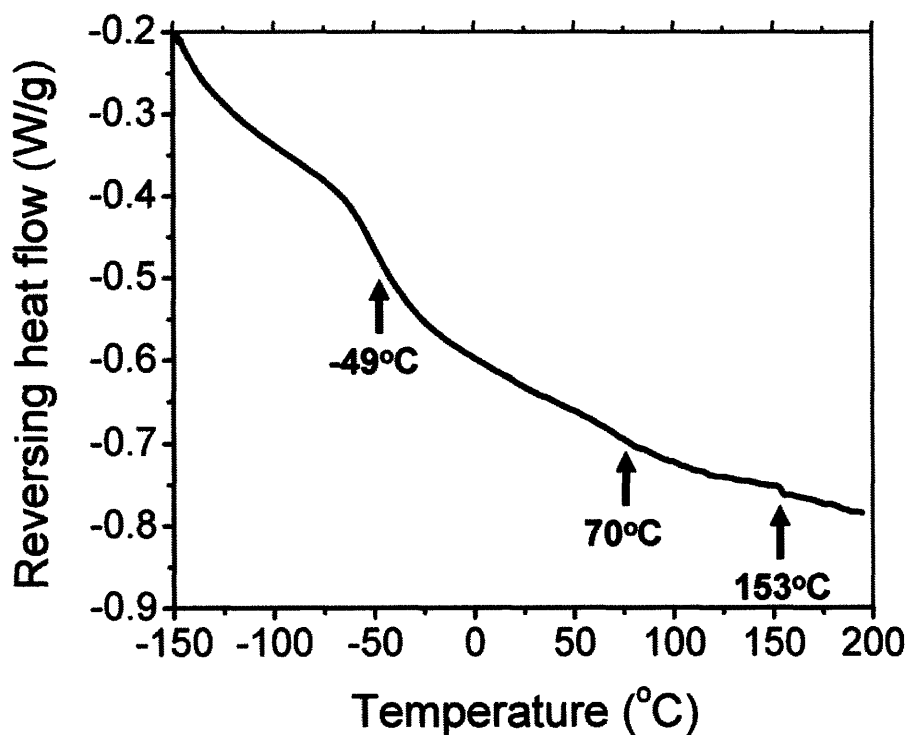
Figure 4.4. MDSC trace of PAN-g-PEO plotted as reversible heat flow vs. temperature.

To determine the microphase-separated morphology, TEM was performed by Elsa Olivetti in the Mayes group. Figure 4.5 presents a typical micrograph negative in which the PEO domains appear as light regions. Both PAN (dark) and PEO domains were observed to form continuous networks, as needed for this application. The PEO-rich nanochannels appear to be around 1-2 nm in width—comparable to those observed for PVDF-g-POEM [5, 12], which showed selectivity in the NF range. This domain periodicity is confirmed by the inset FFT image, which shows a scattering peak (light circle) corresponding to a characteristic length scale of the PAN-g-PEO morphology of ~1.4 nm.
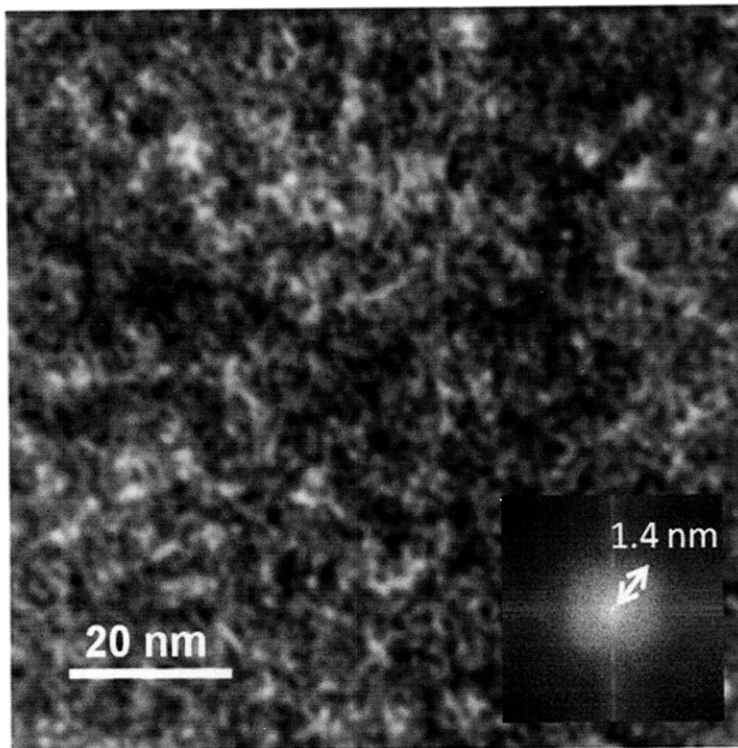
Figure 4.5. TEM micrograph of PAN-g-PEO phase separation. TEM was conducted by Elsa Olivetti in the Mayes group at MIT.

4.3.3. TFC membrane characterization

The membranes were prepared following a method similar to that used for PVDF-*g*-POEM TFC NF membranes (see Chapter 3). A commercial PAN UF base membrane was coated by a thin layer of polymer solution using a control coater, followed by immersion into a non-solvent to precipitate out the polymer. The non-solvent, isopropanol, was selected due to its low diffusivity with DMF, to prevent the formation of a porous coating [1]. Cross-sectional SEM micrographs of the base UF membrane and the coated thin film composite (TFC) NF membrane are given in Figure 4.6. The coating layer was observed to be approximately 2 μm in thickness, and non-porous.
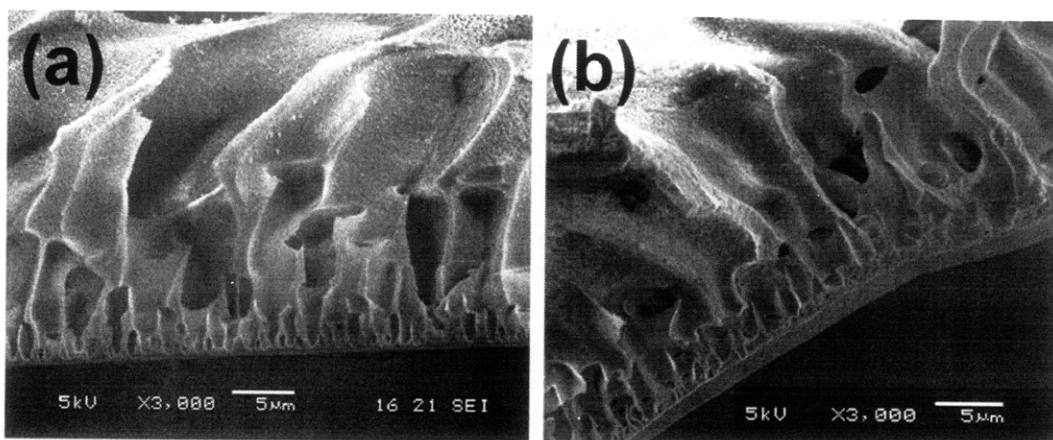
Figure 4.6. Cross-sectional SEM micrograph of (a) PAN UF base membrane before coating, and (b) PAN-g-PEO TFC NF membrane.

PAN-*g*-PEO TFC NF membranes also showed high pure water permeabilities (PWPs). The average PWP of PAN-*g*-PEO TFC NF membranes was 85 ± 25 L/m^2 h MPa, averaged over five samples. This value was compared with the measured PWPs of two commercial NF membranes by GE Osmonics, selected for exhibiting the highest nominal flux among the NF membranes offered by the manufacturer. PAN-*g*-PEO TFC NF membranes exhibited an average PWP over four times that measured for GE Osmonics DS-5-DL (19 ± 3 L/m^2 h MPa, averaged over five samples), and approximately 16 times that measured for Osmonics DS-5-HL (5.1 L/m^2 h MPa, only one test performed). The average PWP of PAN-*g*-PEO TFC NF membranes was also twice that of the TFC NF membranes based on PVDF-*g*-POEM graft copolymers investigated in Chapter 3 (39 ± 19 L/m^2 h MPa) [17]. Optimization of the coating process should allow for membranes with thinner selective layer coatings and even higher pure-water permeabilities.

4.3.4. Subnanometer Size Selectivity

Common commercial NF membranes generally have some negative surface charge, resulting in separation characteristics that are based on a combination of sieving and electrostatics. TFC NF membranes with a neutral-charge microphase-separated graft copolymer as the selective layer offer a different kind of separation. The selectivity is based on size, and the sieving that occurs through the hydrophilic phase, as first demonstrated in our group's studies on PVDF-*g*-POEM based NF membranes [11, 12].

To determine the permeate size cut-off of the PAN-*g*-PEO TFC NF membranes prepared in this study, rigid dyes were used as probes. Characteristics of the dyes that were used are listed in Table 4.1. The percentage of each dye that passed through the PAN-*g*-PEO TFC NF membrane is shown in Figure 4.7. It was observed that the two larger dye molecules, Brilliant Blue R (11.1 Å) and Congo Red (10.1 Å), were retained completely by the membrane, indicating the size cut-off is smaller than one nanometer. 81% of Ethyl Orange, a molecule 8.2 Å in size, permeated through the membrane. This effective pore size, around 1 nm, is consistent with observations from the TEM micrograph in Figure 4.5.
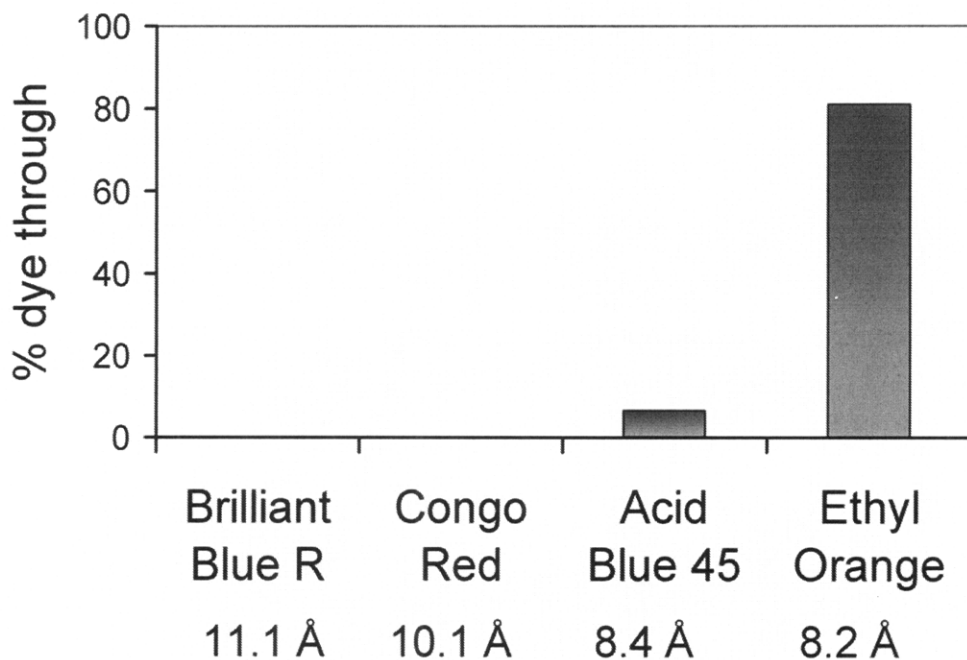
Figure 4.7. Percentage of dyes of different sizes that pass through the PAN-g-PEO TFC NF membrane.

The relatively sharp size cut-off derived from the microphase-separated morphology can be used to fractionate two molecules of like charge and similar dimension. As a demonstration of the diafiltration ability of the PAN-*g*-PEO TFC NF membrane, a solution containing 100 mg/L each of Congo Red and Ethyl Orange, both negatively charged, was filtered. In Figure 4.8, the UV- visible spectrum of the filtrate (solid line) is

compared with the spectra of the two components of the feed, Ethyl Orange (dashed line) and Congo Red (dotted line). All solutions were diluted to one-fifth of their initial concentration to avoid non-linear behavior at high concentrations. It can be seen that the filtrate spectrum follows that of Ethyl Orange, at a slightly lower concentration, calculated to be 82% of the initial concentration. The characteristic peaks of Congo Red, at approximately 344 and 500 nm, are not observed in the filtrate, indicating that the dye was retained completely. The dye retention properties of these membranes, combined with their high permeability, could find use in the treatment of textile wastewater [186] enabling fractionation and recovery of dye constituents. More generally, the capability of the PAN-g-PEO NF membranes to separate small molecules by size could open numerous applications in the biotechnology [24] and food industries [107].
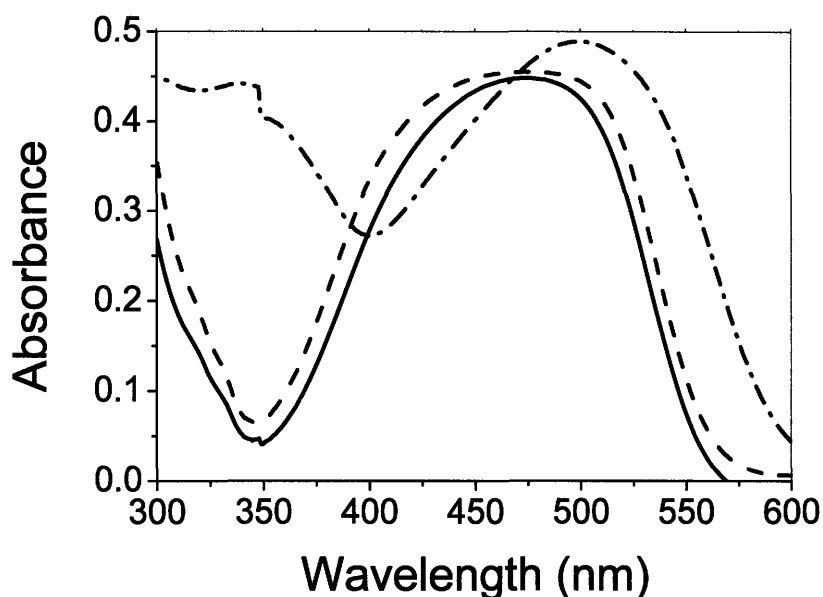
Figure 4.8. UV-visible spectra of permeate in the diafiltration experiment (solid line; feed: 100 mg/L each of Congo Red and Ethyl Orange) compared with the spectra of Ethyl Orange (dashed) and Congo Red (dash-dot). All samples were diluted to 1/5 their initial concentration to avoid high-concentration non-linearities in absorption.

4.3.5. Fouling resistance

Previous research on PVDF-g-POEM TFC NF membranes demonstrated the exceptional fouling resistance of NF systems based on amphiphilic comb copolymers with PEO side chains (chapter 3) [12, 17]. These membranes were shown to completely resist fouling by oily water mixtures [12], protein, humic acid and polysaccharide solutions, and activated sludge from a membrane bioreactor [17]. The similar structure and nanochannel chemistry of PAN-g-PEO TFC NF membranes might be expected to yield equivalently high fouling resistance.

Figure 4.9 shows the 24-hour dead-end filtration results from a PAN-g-PEO NF membrane (filled symbols) for a 1000 mg/L solution of BSA in PBS, performed at 30 psi (0.21 MPa), and plotted as a function of normalized flux (flux/initial flux) vs. time. There is only a small decline in flux over the course of the filtration (~15% after 24 hours). This loss is fully recovered when the cell is rinsed and the foulant solution is replaced with deionized water. This small flux loss, as well as its complete reversibility, makes these membranes promising for feeds with large fouling potential. BSA was completely retained by the PAN-g-PEO membrane. This is consistent with the reported globular dimensions of this protein (a heart-shaped molecule with 8 nm sides and 3 nm width [179]), relative to the pore size data obtained using the dye filtrations and the size scale of microphase separation observed by TEM.
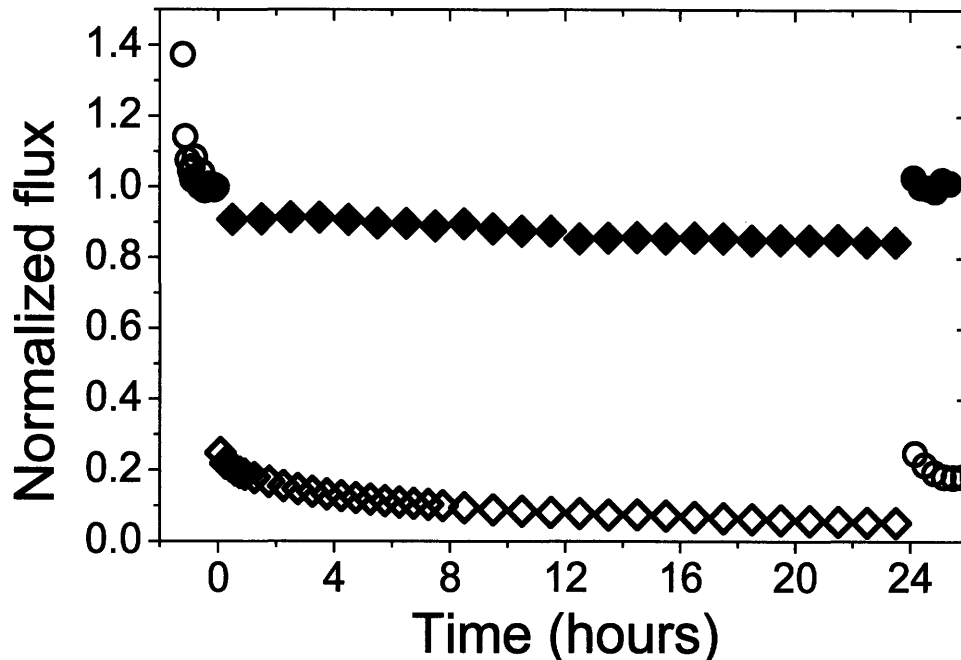
Figure 4.9. Dead-end filtration of model protein solution with PAN-g-PEO TFC NF membrane (filled symbols) and Sepro PAN400 (empty symbols). o,●: *Milli-Q water,* ◆,◊: *1000 mg/L BSA in PBS. Tests performed at 30 psi (0.21 MPa) and 10 psi (0.07 MPa) for the NF and UF membranes, respectively.*

As a control, a similar filtration experiment was conducted using the Sepro PAN-400 base UF membrane, at an operating pressure of 10 psi (0.07 MPa); the results are also shown in Figure 4.9 (open symbols). The base UF membrane lost 81% of its flux irreversibly during the same 24 hour time period. BSA retention for the UF base membrane after 1 h filtration was 73%.

4.4. Conclusions and Future Directions

This chapter focused on novel NF TFC membranes based on the microphase separation of the backbone and side chains of a PAN-g-PEO comb copolymer. These membranes were shown to exhibit high pure water permeability, an ability to fractionate small molecules by size, and complete resistance to fouling by a BSA solution. This membrane system appears very promising for separations in the pharmaceutical, biochemical and

food industries, where the use of membranes for molecular fractionations is currently limited by severe fouling due to the high organic content of the feed, and the limited size selectivity of commercial NF membranes. They also show potential for wastewater treatment applications, for example in membrane bioreactors, due to their fouling resistance and high permeability coupled with their ability to retain smaller contaminants [17, 37, 142]. Furthermore, the scalable synthesis of PAN-*g*-PEO, as well as the simplicity of the TFC manufacturing process, offer easy scale-up of the production of these highly versatile membranes.

Chapter 5

UF Membranes with Complete Resistance to Irreversible Fouling

5.1. Introduction

This chapter focuses on the development of novel ultrafiltration (UF) membranes through the use of amphiphilic comb copolymers. Fouling is an especially important problem in UF membranes, which are used in some of the most demanding processes. Wastewater treatment, membrane bioreactors, food, dairy and biotechnology industries all involve problematic feeds with high concentrations of colloids and biomolecules (see Section 2.5). Of the operating costs of a typical UF plant, 30-50% is spent on membrane replacement, 10-30% on membrane cleaning, and 20-30% on energy [187]. Membranes that resist fouling, therefore, are one of the most important solutions leading to more feasible UF membrane processes, and more affordable clean water.

The greatest potential impact of designing new membranes is in preventing adsorptive fouling, which is irreversible by physical methods and highly dependent on membrane surface chemistry [32]. Altering the surface chemistry of hydrophobic membranes is a common strategy to achieve a hydrophilic, fouling resistant surface without sacrificing the mechanical resistance of the hydrophobic base material. (see Section 2.5.3). To achieve such surfaces, several researchers have focused on amphiphilic copolymer additives in the manufacture of membranes by phase inversion. Hancock and coworkers first prepared membranes from a blend of polysulfone (PSf) and PSf-b-PEO, and reported lower contact angles and platelet adhesion. However, no filtration data were reported [188, 189]. Hester et al. employed a water-insoluble, comb-type graft copolymer of poly(methyl methacrylate) and PEO, PMMA-g-PEO, as a surface segregating additive in the phase inversion casting of PVDF UF membranes. They reported order-of-magnitude

flux enhancements in filtration studies with bovine serum albumin (BSA) solution, derived from reduced fouling and increased porosity in the selective layer [4]. Later research in the Mayes group led to the development of PVDF-g-POEM and PSf-g-PEO comb copolymers and demonstrated their ability to reduce biomolecule adsorption on PVDF [4-6] and PSf [8] membranes, respectively. Similarly, Jiang and coworkers employed commercial macromolecular surfactants (Pluronics) as membrane casting additives [87-89, 190, 191]. These ABA triblock copolymers.of PEO and poly(propylene oxide) (PPO) gave improved pure water permeability and decreased irreversible fouling when added to the casting solution of polyethersulfone (PES) membranes. Wang et $al.$ synthesized an ABA triblock copolymer, POEM-b-PSf-b-POEM for membrane modification, and demonstrated decreased adsorption of BSA on PSf membranes [192]. Rana et $al.$ cast membranes from a blend of poly(ether sulfone) (PES) and PEO-b-polyurethane-b-PEO, but reported no fouling resistance data [193]. Random copolymers that contain hydrophilic groups such as sulfonate [86] or poly(N-vinyl-2-pyrrolidone) [194] were also shown to increase flux and fouling resistance when used as additives.

A recent study comparing different amphiphilic additives suggests that the comb architecture gives superior surface segregation and higher resistance to protein adsorption [87]. Surface segregation of amphiphilic comb copolymers during the phase inversion casting, illustrated in Figure 5.1, is favored due to both hydrogen bonding interactions between the hydrophilic side-chains and water molecules in the bath, and entropic driving forces for side chain ends to localize at the surface [195-197]. The hydrophobic backbone anchors the side-chains. If there is sufficient copolymer, this process results in a brush of hydrophilic polymer lining the membrane surface, as well as the internal pores [3-6, 8]. Combs with PEO side chains have primarily been investigated [3-6, 8, 87, 198-202] due to its well known resistance to protein adsorption [203], but other side-chain chemistries that resist cell adsorption, such as zwitterionic groups [204], phospholipid derivatives [205, 206], and glucose-carrying polymers [207] have also been studied. These studies indicate that comb copolymer additives lead to UF membranes with higher permeability, lower contact angles, and improved resistance to irreversible fouling. However, none of these studies demonstrated complete resistance to irreversible flux loss.
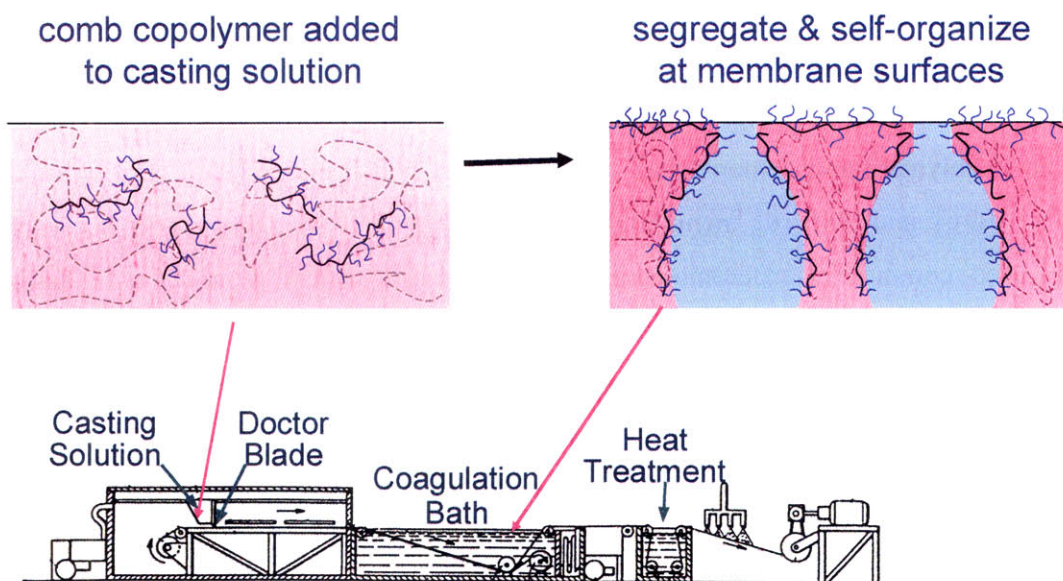
Figure 5.1. Schematic description of immersion precipitation membrane casting in the presence of an amphiphilic comb copolymer additive.

This thesis extends the investigation of comb copolymer-modified UF membranes to polyacrylonitrile (PAN)-based systems [13, 15, 16]. UF membranes incorporating PAN-*g*-PEO as an additive during casting were prepared and tested. The amount of comb copolymer additive and the copolymer composition needed to achieve fouling resistance was investigated using dead-end protein fouling experiments. The performance of the membrane was tested with different representative foulants in dead-end mode. Cross-flow protein fouling experiments were also performed to obtain a better understanding of the mechanism of permeability decline. Finally, atomic force microscopy (AFM) was used to better understand the mechanism of the exceptional fouling resistance exhibited by these novel membranes.

5.2. Experimental Methods

5.2.1. Materials

Materials used were identical to those described in Section 4.2.1. PAN400 ultrafiltration membranes, purchased from Sepro Membranes, Inc. (Oceanside, CA), were used as a

control in dead-end filtration experiments. Another commercial PAN UF membrane, denoted MW (formerly MX50) by the manufacturer (Osmonics, Minnetonka, MN), was used as the control in cross-flow experiments.

5.2.2. Synthesis of PAN-g-PEO

Polyacrylonitrile-*graft*-poly(ethylene oxide) (PAN-*g*-PEO) was synthesized and characterized following the procedure described in Section 4.2.2. DMF was used as the reaction solvent. Three different graft copolymers were synthesized, varying monomer ratios. The synthesis conditions, PEO content and number-averaged molecular weight of each material based on polystyrene standards are given in Table 5.1 [13].

Table 5.1: Properties of PAN-*g*-PEO comb copolymers synthesized

Polymer	Wt% PEGA used in reaction	Wt% PEGA in resultant polymer	Wt% PEO in resultant polymer	Number average molecular weight (kg/mol)	Polydispersity index
P50	50	46	39	169	2.85
P25	25	35	29	157	3.14
P15	15	14	12	224	2.23

5.2.3. Fabrication of UF membranes

Solutions of PAN and PAN-*g*-PEO in DMF were prepared in separate vials by adding 1.2 g polymer to 8.8 mL DMF and heating to approximately 50°C while stirring. After both polymers had dissolved completely, the solutions containing PAN and PAN-*g*-PEO were mixed to obtain the desired blend composition. The resulting solution was passed through a 1-μm syringe filter (Whatman) and degassed by heating to ~90°C in capped heat-resistant vials for at least one hour until no gas bubbles were visible. Solvent loss by evaporation was negligible due to the high boiling point of DMF (153°C). The solution was cast on a first surface optical mirror using a doctor blade (Universal blade applicator, Paul N. Gardner Company, Pompano Beach, FL) set at a gate size of 200 μm. The mirror was immersed in a bath of deionized water at room temperature. The membrane was left

in the coagulation bath for ~ 20 minutes, and then moved to a fresh bath of DI water at least overnight. Subsequently, membranes were annealed in a water bath adjusted to 90°C for 6 hours to enhance the surface coverage of the graft copolymer additive [4-6, 8]. The different membranes prepared for this study are listed in Table 5.2, along with the graft copolymer component and blend composition. In addition to the membranes listed, another membrane was cast from 100% PAN-g-PEO (P50) for contact angle studies.

Table 5.2: Membrane compositions and performance characteristics

Membrane	Comb additive (Table 5.1)	PAN-g-PEO: PAN mass ratio
PAN	-	0:100
P50-5	P50	5:95
P50-10	P50	10:90
P50-20	P50	20:80
P25-20	P25	20:80
P15-20	P15	20:80

5.2.4. Scanning electron microscopy (SEM)

Membrane morphology was characterized using a JEOL 5910 Scanning Electron Microscope (SEM) operating at 5 kV. The membranes were fractured in liquid nitrogen for cross-sectional observation, and sputter coated with gold-palladium for SEM imaging.

5.2.5. Contact angle and wettability tests

Contact angle measurements were performed on the cast membranes using an Advanced Surface Technologies Inc. VCA2000 video contact angle system. The membranes were fixed flat on a glass slide using double-sided tape and dried for 2 hours in air and 2 hours in a vacuum oven before the measurements. Five measurements were taken for the static contact angle, immediately after the droplet was placed on the membrane. The dynamic contact angle of the films was measured as four continuous advancing angles with

deionized water. Membrane wettability was studied by placing 1 μL of deionized water on the membrane surface and observing on the video contact angle system the time required for the water to absorb completely into the membrane. The values reported are averages of 5 measurements.

5.2.6. X-ray photoelectron spectroscopy (XPS)

XPS analysis was used to determine the fraction of PAN-*g*-PEO in the near surface region of the membrane. Rectangular pieces, about 2 cm by 4 cm, were cut from each membrane and dried, first in air and then in a vacuum oven. Experiments were performed on a Kratos Axis Ultra (Kratos Analytical, Manchester, U.K.) X-ray photoelectron spectrometer employing a monochromatic Al K_α source (1486.7 eV) and an electron takeoff angle of 90° relative to the sample plane. A survey scan (0-1100 eV binding energy range, 160 eV pass energy) and a high-resolution scan of the C 1s peak (10 eV pass energy) were run for each sample. To calculate the relative amounts of elements, the default relative surface factor (RSF) values of 0.278, 0.780 and 0.477 were used for C 1s, O 1s and N 1s peaks, respectively. The C 1s peak obtained was fitted with 4 peaks, as shown in Figure 5.2. The first peak, labeled (a) in the figure, was centered at 288.8 ± 0.2 eV, corresponding to carbons in the carboxyl groups of PEGA. The second (b), centered at 286.5 ± 0.2 eV, contained the CH and CN carbons of PAN as well as the $O-CH_2$ and $O-CH_3$ carbons of PEO. The third peak, labeled (c), at 285.5 ± 0.2 eV, contained the CH_2 carbons of PAN and backbone carbons of PEGA [208]. Finally, a peak was observed at 285 eV (d), corresponding to hydrocarbon contamination [209]. The percentage of PEO at the surface was calculated using the peaks at 288.8 and 285.5 eV to obtain the concentration of carboxyl groups at the surface. Each of these groups was assumed to be connected to PEO chains of 8 repeat units, deduced from the molecular weight of PEGA. C 1s peaks acquired for each sample is given in Appendix C. To qualitatively confirm the results, the N/C and O/C ratios from survey scans, tabulated in Appendix C, were also compared.
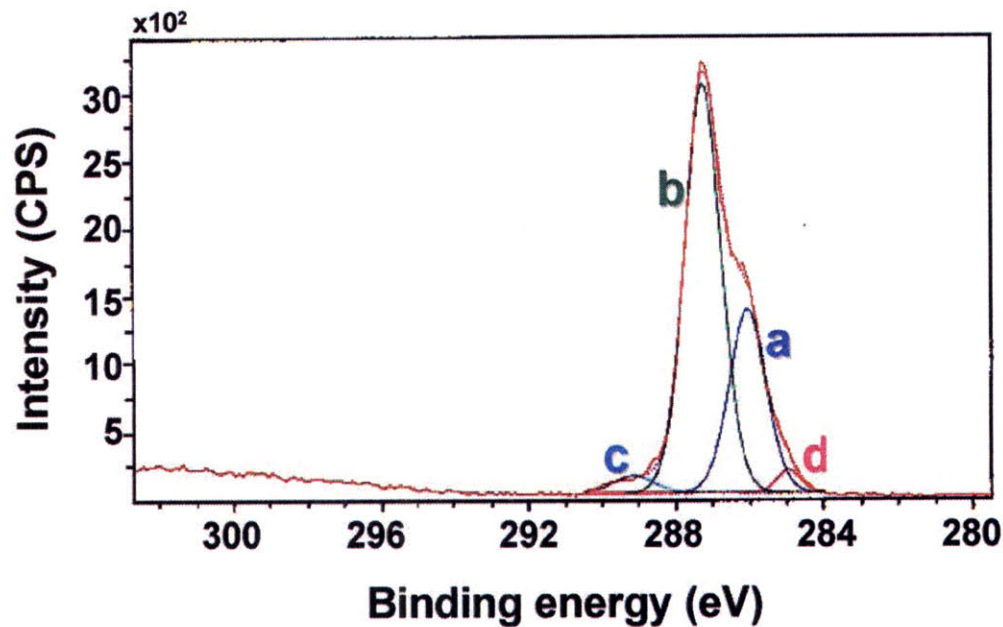
Figure 5.2. XPS high-resolution C 1s spectrum of the membrane P50-20 selective layer surface, and a representative fit.

5.2.7. Dead-end filtration experiments

Circular pieces were cut from the cast membranes while still wet. Membranes allowed to dry became unacceptably brittle, a common problem with PAN membranes [33]. Fouling experiments were performed following the procedure described in Section 3.2.4, except the choice of fouling time, which was 24 hours in UF experiments, and filtration pressure, which was selected to be 10 psi (0.07 MPa).

5.2.8. Cross-flow filtration experiments

Cross-flow experiments were performed by Dr. Seoktae Kang in the Elimelech labs at Yale University. Experiments were conducted on PAN/PAN-*g*-PEO blend membranes of P50-20 composition (see Table 5.2), and MW commercial PAN membrane as a control. A cross-flow membrane filtration (CMF) unit was constructed from acrylic [210]. The cross-flow channel within the flow cell was 1 mm in height, 32 mm in width, and 83 mm in length. The test membrane was placed between the top and bottom plate and was held

tightly by double o-rings. The feed solution was contained in a stainless steel vessel, pressurized to 200 kPa. The entire system was operated in a closed loop, so that the pressure on the feed side was extremely stable during the experiment, as indicated in our previous work [210]. A gear pump (Cole-Parmer, Vernon Hills, IL) was used to circulate the feed solution through the CMF unit. The permeate flux was kept constant during the fouling runs by an 8-roller digital peristaltic pump (Masterflex, Cole-Parmer, Vernon Hills, IL) mounted on the permeate line. Both pumps were calibrated across their entire range of flow. A differential pressure transmitter (Omega, Stamford, CT) recorded the corresponding trans-membrane pressure (TMP) between feed and permeate at all times during the experiments. The transducers were connected to a digital data logger (Vernier Instruments, Springfield, IL), and the TMP was downloaded to a laboratory PC in real time.

The experimental protocol for fouling runs and fouling reversibility tests was adopted from previous research [173]. The membrane was first compacted at a permeation velocity of 40 μm/s (TMP of about 90 kPa) with DI water for 30 minutes until the TMP became stable at a fixed cross-flow velocity of 10 cm/s. Next, the initial baseline performance was obtained at a permeation velocity of 30 μm/s for 15 minutes. The membrane was then equilibrated for an additional 15 minutes with a foulant-free electrolyte solution that had a solution chemistry identical to that used for the subsequent fouling run. An appropriate amount of BSA stock solution (2 g/L) was then added to the feed tank to achieve a 100 mg/L feed BSA concentration. The fouling experiments were carried out for 6 hrs with a sampling of 15 ml permeate being collected every hour in order to analyze BSA retention. Fouling runs were carried out at a total ionic strength of 10 mM by varying the NaCl concentration (i.e., the test solution without Ca^{2+} contained 10 mM NaCl and the test solution with 0.5 mM Ca^{2+} contained 8.5 mM NaCl) at an ambient (unadjusted) pH of 5.9±0.3 and a temperature of 22°C.

At the conclusion of the fouling runs, the foulant solution in the feed tank was disposed of, and the fouled membrane was cleaned in order to investigate the reversibility of fouling. Physical cleaning with foulant-free electrolyte (10 mM NaCl) solution was performed by operating the membrane test unit at a cross-flow velocity of 50 cm/s for 30

minutes. At the end of the physical cleaning stage, the electrolyte solution was emptied, followed by a rinsing of the entire system with foulant-free electrolyte solution. The cleaned membrane was then subjected to the baseline performance conditions (i.e. a permeation velocity of 30 μm/s and a cross-flow velocity of 10 cm/s) with foulant-free electrolyte solution for 15 minutes to determine the TMP after physical cleaning. Chemical cleaning was done by adding sodium hydroxide to a final concentration of 1 mM (pH 11) at a cross-flow velocity of 50 cm/s for 30 minutes. After chemical cleaning, the TMP was determined under baseline performance conditions as described above. Cleaning efficiency was calculated as the percent recovery of the initial TMP from the TMP at the end of the fouling runs. All fouling and post-cleaning runs were performed employing the same feed solution chemistry (i.e., an ambient pH of 5.9±0.3, 0.5 mM calcium, and 10 mM total ionic strength adjusted by varying NaCl concentration) and operating conditions (i.e., permeation velocity of 30 μm/s, cross-flow velocity of 10 cm/s, and temperature of 22°C). To confirm the reproducibility of fouling and post-cleaning runs, all experiments were performed at least twice.

5.2.9. Interaction force measurements

These measurements were performed by Dr. Seoktae Kang in the Elimelech labs at Yale University, following the procedure described in Section 3.2.6. A Nanoscope III Multimode atomic force microscope (AFM) (Digital Instruments, Santa Barbara, CA) was used to quantify the interaction forces between foulant and membrane surfaces.

The AFM was operated in force mode, with an approach/retraction speed of 1 μm/s and 1 μm of piezo-movement. Force measurements were performed at four different locations on the membrane surface, with 15 measurements at each location to minimize inherent variability in the force data. The force data can also be affected by local membrane surface heterogeneity. The solution chemistries of the test solutions in the liquid cell were the same as those used in the fouling experiments.

5.3. Results and Discussion

5.3.1. Synthesis of PAN-g-PEO

The synthesis of PAN-g-PEO was described and discussed in detail previously in section 4.3.1. In this study, copolymers with a range of PEO contents were used to determine the amount of PEO needed in the copolymer to obtain the desired fouling resistance in the membranes prepared (see Table 5.1). This is an important parameter for the practical large scale application of such membranes. Many properties of the copolymer, especially mechanical properties and solubility, are affected by its composition, as well as its production cost.

A good correlation was observed between the amount of monomers charged into the reaction flask and the final composition of the copolymer (see Table 5.1), consistent with the practical range expected from free radical random copolymerization. PAN-g-PEO copolymer composition can be controlled using this reaction, simply by adjusting the ratio of monomers used.

5.3.2. Surface segregation of PAN-g-PEO

Two main parameters were studied as part of this investigation, in determining the best conditions to prepare fouling resistant membranes [13]. The first one of these, as explained in Section 5.3.1, was the PEO content of the copolymer. The second one was the amount of PAN-g-PEO that needed to be added to the blend with PAN during casting. It is important to know the minimum amount of copolymer needed in the blend to obtain fouling resistance for two reasons. First is the economics of the process: No matter how straightforward the synthesis, PAN-g-PEO will be more expensive than the commodity polymer PAN, produced widely in large amounts, and therefore less additive would mean a lower membrane cost. The second reason is that the mechanical strength of PAN-g-PEO is inferior to PAN, and therefore too much PAN-g-PEO could decrease the strength and durability of the membranes. Table 5.2 lists the membrane compositions investigated.

105

To verify the surface segregation of PAN-g-PEO during the casting of blend membranes, XPS analysis was used to analyze the surface chemistry of the membranes. Figure 5.3a shows XPS results for near-surface weight percentage of PEO, calculated from the high-resolution C 1s scans, as a function of P50 comb content in P50/PAN blend membranes. With increasing bulk comb copolymer content, the PEO surface fraction first increases rapidly then asymptotes. This behavior is characteristic of an interfacial adsorption process, expected in this system.
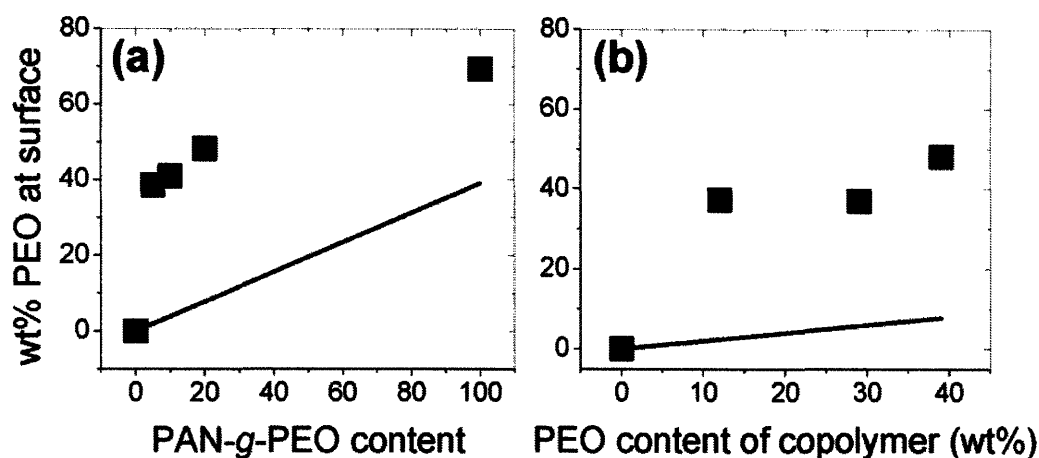
Figure 5.3. PEO content at the surface of the membranes (■) and in bulk (—), as a function of (a) PAN-g-PEO content of P50/PAN blends and (b) PEO content of the PAN-g-PEO copolymer for 20 wt% blends. The values were determined from high-resolution C 1s scans by XPS.

The composition of the comb additive also affects the PEO near-surface composition. Figure 5.3b shows PEO near-surface content versus PEO content in the PAN-g-PEO additive, for blend membranes containing 20 wt% additive. In all cases, a large surface excess of PEO is observed. The membrane incorporating P50 (39 wt% PEO, Table 5.1) gave the highest PEO surface fraction. PAN-g-PEO synthesized with higher comb copolymer contents (60 wt% PEO) exhibited water solubility, and were thus excluded from further investigation.

The PEO content of a PAN/PAN-g-PEO blend can also be calculated assuming homogeneous distribution of these side-chains in bulk (gray line in Figure 5.3). In all

cases, the surface concentration of PEO was found to be much greater than the bulk concentration, again confirming the surface segregation of the copolymer.

Similar trends were found when comparing the surface elemental compositions from XPS survey scans (Figure 5.4). Due to the lack of sample-specific RSF values to convert the peak areas to elemental compositions, default values were used. This prevented the calculation of exact elemental ratios but made it possible to observe trends, as the samples were similar chemically. The atomic ratio of N/C decreased, indicating fewer acrylonitrile segments at the surface, with either higher concentrations of PAN-g-PEO in the blend (Figure 5.4a) or the use of an additive with higher PEO content (Figure 5.4b). The atomic ratio of O/C, indicative of PEGA segments at the surface, increased under both conditions. Taken together, the XPS survey and high resolution data provide definitive evidence for surface segregation of the comb additive.
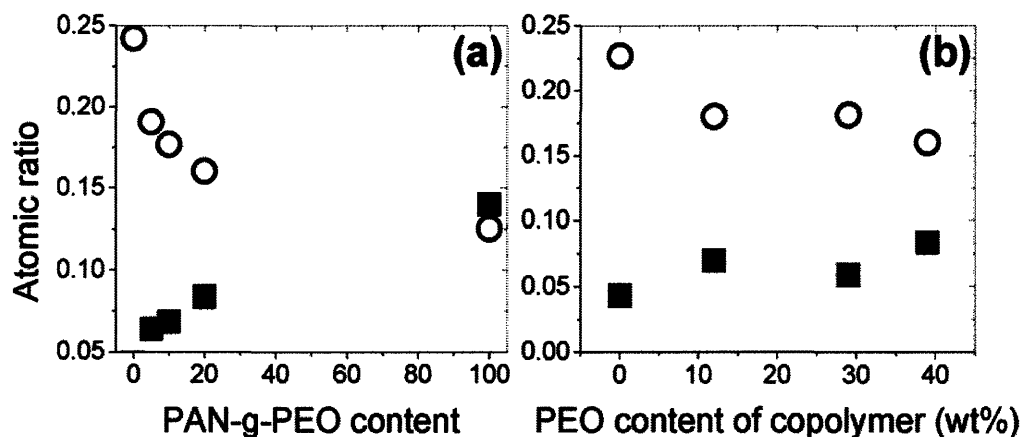
Figure 5.4. O/C (■) and N/C (o) atomic ratios at the near surface of the membranes as a function of (a) PAN-g-PEO content of P50/PAN blends and (b) PEO content of PAN-g-PEO copolymers for 20 wt% blends. The values were obtained from XPS survey scans.

Contact angle measurements are widely used for characterizing the surface hydrophilicity of polymeric surfaces [211], including polymeric membranes [212]. In several studies, a decrease in contact angle was observed in UF membranes treated with hydrophilic polymers to improve fouling resistance [72, 77, 213-215]. The results obtained with this

method were consistent with wetting data on the two membrane series. Figure 5.5a shows the change in sessile drop and advancing water contact angles with the concentration of PAN-g-PEO (P50) in P50/PAN blends. Contact angle was observed to decrease with increasing PAN-g-PEO content. The membrane cast from pure PAN had a static contact angle of 78° and an advancing contact angle of 87°, whereas the membrane P50-20 had a static contact angle of 40° and an advancing contact angle of 48°. For further comparison, a membrane was prepared from 100% P50 copolymer for contact angle studies. The static and advancing contact angles for this membrane were found to be 38° and 39°, respectively. These values are similar to values reported for PEO brushes in the literature [216-218]. The contact angle results suggest a PEO brush covers the polymer surfaces of the membrane selective layer for membranes incorporating ≥20 wt% P50.
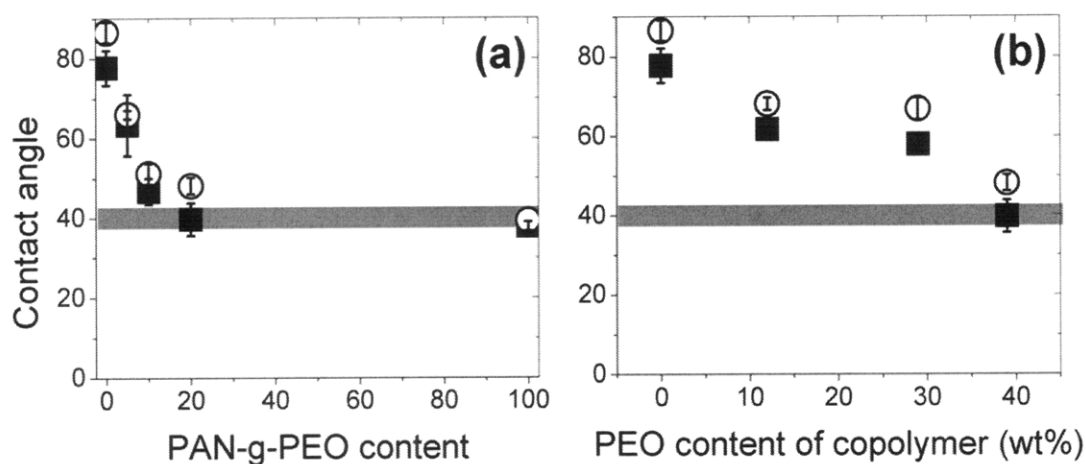
Figure 5.5. Static (■) and advancing (o) contact angles of the membranes as a function of (a) PAN-g-PEO content of P50/PAN blends and (b) PEO content of PAN-g-PEO copolymers for 20 wt% blends. The shaded region indicates contact angle range reported for PEO monolayers [216-218].

The effect of the PEO content of the additive on contact angle is plotted in Figure 5.5b, for blends containing 20 wt% comb copolymer. As the PEO content of the copolymer increased, contact angle decreased. Only for the P50-20 blend did the contact angle reach values reported for PEO brushes [216-218]. The results suggest the formation of a continuous PEO brush on the membrane surface at this copolymer content. For all

membranes containing comb copolymer, the receding contact angle was zero, indicating the membranes are water absorbent.

The addition of PAN-*g*-PEO copolymer was also found to enhance the wettability of the cast membranes. Control membranes cast from 100% PAN solutions absorbed a 1 μL droplet of water in 35.6 ± 4.0 seconds, whereas this time was only 8.4 ± 1.5 seconds for the P50-20 membrane. Both higher PAN-*g*-PEO content in the blend and higher PEO content in the comb led to faster water absorption, as might be expected (Table 5.3).

Table 5.3: Membrane performance characteristics

Membrane	Pure water permeability (L/m^2 h MPa)	BSA retention after 1 hour (%)	Wetting time (s)	Normalized mean adhesion force*, F/R (mN/m)
PAN	193	97	35.6 ± 4.0	-5.04 ± 2.22
P50-5	695	93	24.4 ± 2.7	-1.80 ± 2.57
P50-10	1000	95	16.8 ± 1.3	0.59 ± 0.49
P50-20	1590	89	8.4 ± 1.5	1.42 ± 0.68
P25-20	706	95	13.8 ± 2.2	-0.66 ± 0.48
P15-20	382	94	25.0 ± 4.6	-2.97 ± 1.25
PAN400	4580	73	69.6 ± 2.8	-5.48

* Values represent the mean of measurements made at 4 different locations on the membrane surface (15 measurements per location) using AFM colloidal probe. Error margins represent standard deviations.

5.3.3. Membrane morphology and pure water permeability

In contrast to traditional surface graft polymerization methods used for membrane modification [72, 213, 219, 220], incorporation of a surface-segregating amphiphilic comb copolymer additives during membrane casting has been shown in previous studies [4-6, 8, 87, 200, 201, 204, 207] to increase selective layer porosity and pure water

permeability. For the PAN membranes investigated here, addition of PAN-*g*-PEO was also found to affect selective layer morphology.

Figure 5.6 shows representative SEM micrographs of the selective layer and cross-section of a P50-20 membrane and those of a PAN-only membrane. Both membranes exhibit a selective layer roughly 1 μm thick, supported by a cylindrical pore structure giving way to large tubular macrovoids (Figures 5.6a and 5.6c). Lower magnification micrographs not included here indicated that the overall membrane thickness was approximately 120 μm. The surface of the PAN-only membrane (Figure 5.6d) displays pores in the 0.05-0.1 μm range that appear to be non-spherical, consistent with early stage coarsening of a spinodal morphology [46]. In comparison, the PAN-*g*-PEO-containing membrane exhibited more circular pores of larger maximum diameter (~0.2 μm, Figure 5.6b). Despite the large size of some observed pores, the BSA retention of the membranes ranged between 97 and 89%, appropriate for UF applications and slightly higher than that of the Sepro PAN400 UF membrane used as a control (Table 5.3).
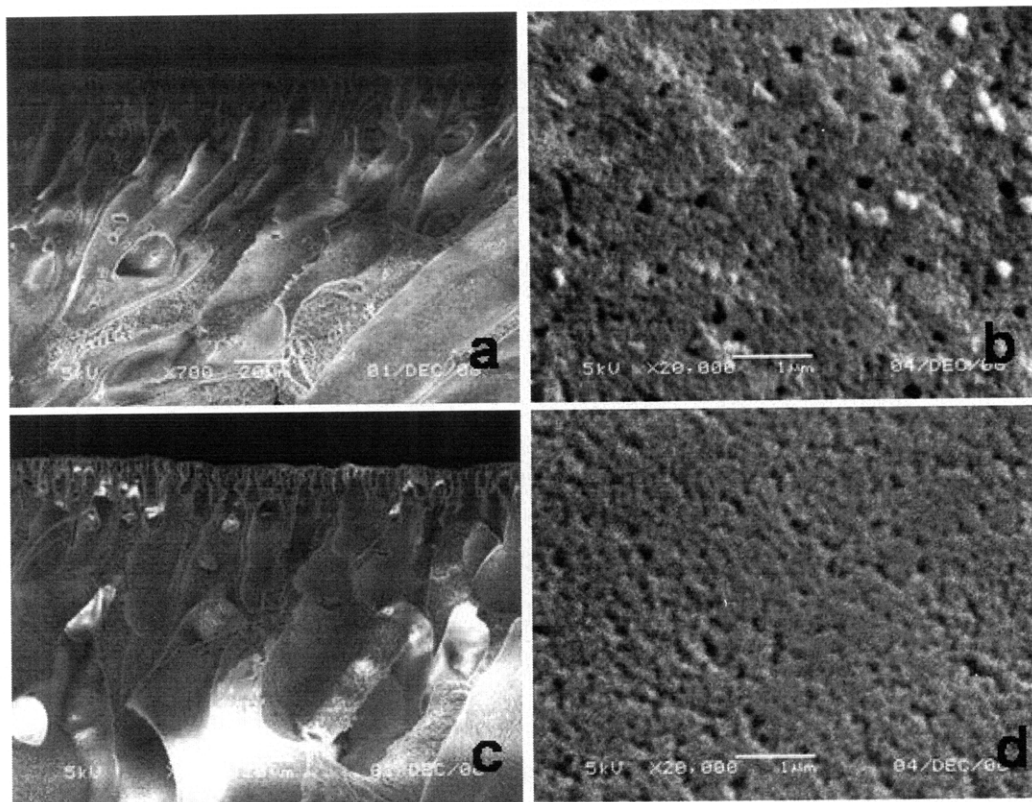
Figure 5.6. SEM micrographs of P50-20 (a, b) and PAN-only (c, d) membranes. (a, c) cross-section, (b, d) surface.

Changes in the selective layer morphology and chemistry with the addition of PAN-*g*-PEO might be expected to influence the pure water flux. The pure water permeability values provided in Table 5.3 show the effect of P50 content on pure water permeability for P50/PAN blend membranes. For the same processing conditions (i.e., total polymer concentration in the casting solution, annealing time, film solution thickness), pure water permeability (PWP) increased linearly with comb content. Addition of only 5 wt% comb to the casting solution caused the permeability to increase to 2.5 times its initial value. For 20 wt% P50, the permeability was observed to increase to over 8 times that of the PAN-only membrane. These results are consistent with those reported previously on comb-modified PVDF membranes, where 10% comb content led to a flux increase of up to 5.2 times [6]. Increasing PEO content in the PAN-*g*-PEO copolymer, also resulted in increased PWP (Table 5.3). It should be noted that an increase in pore size may also

contribute to PWP increase with the addition of PAN-g-PEO (Table 5.3), as indicated by lower BSA retention values.

The increased water flux is a significant potential advantage of these membranes for commercial filtration processes. Common methods of surface modification, especially grafting [72, 213, 219, 220] or adsorption of hydrophilic polymers [221], often lead to decreased flux due to the narrowing and blocking of surface pores. The pure water permeability loss can be up to nearly an order of magnitude, limiting the versatility of the membranes produced as well as the benefits of surface modification [213, 219-221].

5.3.4. Effect of PAN-g-PEO content in blend on fouling resistance

The XPS, wetting, and contact angle results all revealed localization of PAN-g-PEO to the blend membrane surfaces. To determine the effect of the amount of copolymer added to the casting solution on fouling resistance, 24-hour dead-end filtration was performed on the membranes P50-5, P50-10, and P50-20 with a feed solution containing 1000 mg/L BSA in PBS. The results of these filtration runs are shown in Figure 5.7, where membranes with higher P50 content are denoted by darker-shaded symbols. (PAN control is open symbols.) Here, normalized flux is defined as the ratio of the instant flux to the pure water flux at the end of the compaction period. As seen in the data, the behavior of the membranes during protein filtration was quite similar for all PAN-g-PEO contents. After 24 hours of filtration, the flux was reduced to 20-35% of the initial flux for all blend membranes investigated. Higher flux declines were observed for membranes with higher initial flux. This was due to the dead-end set-up used in the experiment, where the rejected BSA built up in the small filtration cell in time, leading to significant concentration polarization effects that got more severe as mole foulant solution was filtered through the membrane.

The most notable differences between different membrane compositions were observed in the recovery step after a pure water rinse. The recoverable flux increased with increasing PAN-g-PEO addition. The membrane with 5 wt% P50 recovered 50% of its initial flux, that with 10 wt% recovered 66%, and that with 20 wt% showed no

irreversible fouling at all, recovering its initial pure water flux completely after a pure water rinse.

Figure 5.7. Dead-end filtration of model protein (BSA) solution through membranes with varying PAN-g-PEO content in blend: P50-20 (black, average pure water permeability 1590±280 L/m² h MPa), P50-10 (dark gray, pure water permeability 1000 L/m² h MPa), P50-5 (light gray, pure water permeability 695 L/m² h MPa), and PAN only (white, pure water permeability 193 L/m² h MPa). ○,●: Milli-Q water, ◆,◇: 1000 mg/L BSA in PBS. Tests performed at 10 psi (0.07 MPa)

Fouling reversibility observed in dead-end BSA filtration was in general agreement with measured adhesion forces in this study. This method was first introduced in Chapter 3, and involves AFM experiments that measure the adhesion forces between the membrane surface and a colloid probe functionalized with carboxyl groups to simulate a foulant molecule. Table 5.3 lists the mean normalized adhesion force, F/R, of membranes with varying P50 content in the P50/PAN blends. The PAN-only and 5 wt% blend (P50-5) membranes exhibited relatively strong adhesion (i.e., large negative values of F/R) to the

probe, thereby explaining the significant irreversible fouling of these membranes. The mean adhesion force for the 10 and 20 wt% blend membranes (P50-10 and P50-20, respectively) was positive (repulsive), indicating no adhesion of the foulant probe to these membranes. Our previous studies correlated a positive mean adhesion force in AFM studies with resistance to irreversible fouling on PVDF-g-POEM coated NF membranes [16, 17] (see Chapter 3). The fact that P50-10 showed some irreversible fouling despite the positive mean adhesion force suggests that further analysis of the adhesion forces is needed to predict the fouling potential of membranes from AFM force studies.

To this end, adhesion force distributions from 60 measurements were analyzed for each of the three membranes containing varying amounts of P50, as presented in Figure 5.8. For the 20 wt% blend membrane (Figure 5.8d), all 60 adhesion force values were positive (i.e., repulsive), consistent with the noted absence of any irreversible fouling. The 10 wt% blend membrane (Figure 5.8c) was found to have a 2.5% incidence of negative (attractive) adhesion force values, probably due to incomplete coverage of the membrane surface with PEO. This suggests that even a small fraction of area left uncovered by the PEO brush is sufficient to cause appreciable irreversible fouling. For the 5 wt% blend membrane (Figure 5.8b), the vast majority of adhesion force values were negative, which correlates well with the low recovery of its initial flux. The PAN only membrane (Figure 5.8a) shows adhesive forces throughout its surface, in corroboration with the low flux recovery observed. The data shown in Figure 5.8 demonstrate that the distribution of adhesion forces can provide additional insights into membrane fouling performance.
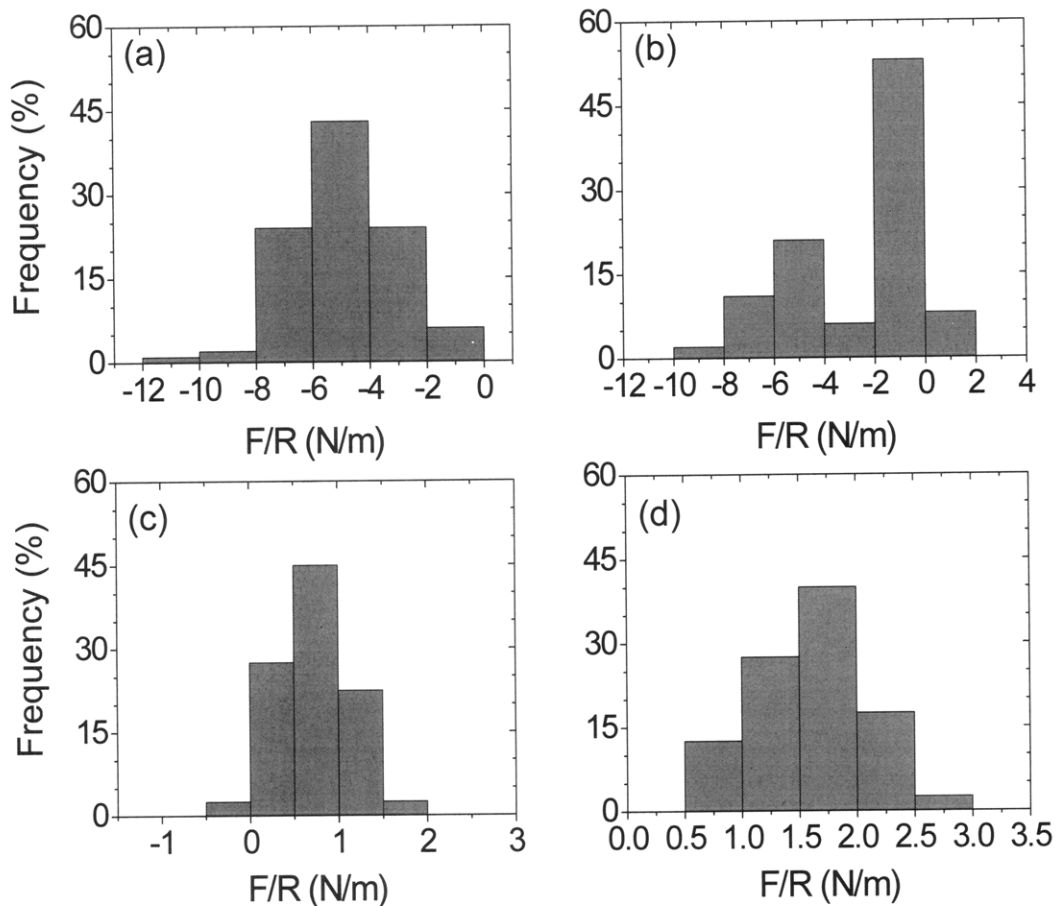
Figure 5.8. Distributions of normalized adhesion forces from 60 measurements between the AFM particle (foulant) probe and membranes P50-5 (a), P50-10 (b), and P50-20 (c) Experiments were conducted by Dr. Seoktae Kang in the Elimelech Group at Yale University.

The complete pure water flux recovery and lack of molecular adhesion forces seen for the P50-20 membrane indicates that the observed flux decline during filtration was not due to BSA adsorption on the membrane surface and pore walls, but instead to concentration polarization. It should be noted that the BSA retention for this series of membranes was comparable, varying between 89 and 97%. Importantly, the findings suggest that PAN membranes incorporating 20 wt% PAN-g-PEO comb additive can be readily cleaned with water alone, obviating the need for aggressive chemical cleaning procedures. Such

membranes might be expected to exhibit substantially longer operational lifetimes, reducing membrane process costs.

5.3.5. Effect of copolymer PEO content on fouling resistance

The effect of comb copolymer PEO content on fouling resistance was also investigated. Filtration data over 24 hours for the membranes P50-20, P25-20, and P15-20 challenged with 1000 mg/L BSA in PBS are given in Figure 5.9. Membranes prepared using PAN-*g*-PEO with higher PEO content are denoted by darker-shaded symbols, while the PAN control is represented by open symbols. As with the previous series, membranes behave comparably, with higher PWP correlating with larger flux decline. The most significant difference was once again observed in the recoverable flux. The membrane containing PAN-*g*-PEO with 12 wt% PEO (P15) recovered only 50% of its flux with a water rinse. The recovery increased to 73% in the membrane prepared with PAN-*g*-PEO containing 29 wt% PEO (P25). Complete recovery of initial flux with water rinse was achieved only in the membrane containing 39 wt% PEO (P50) in the PAN-*g*-PEO additive.
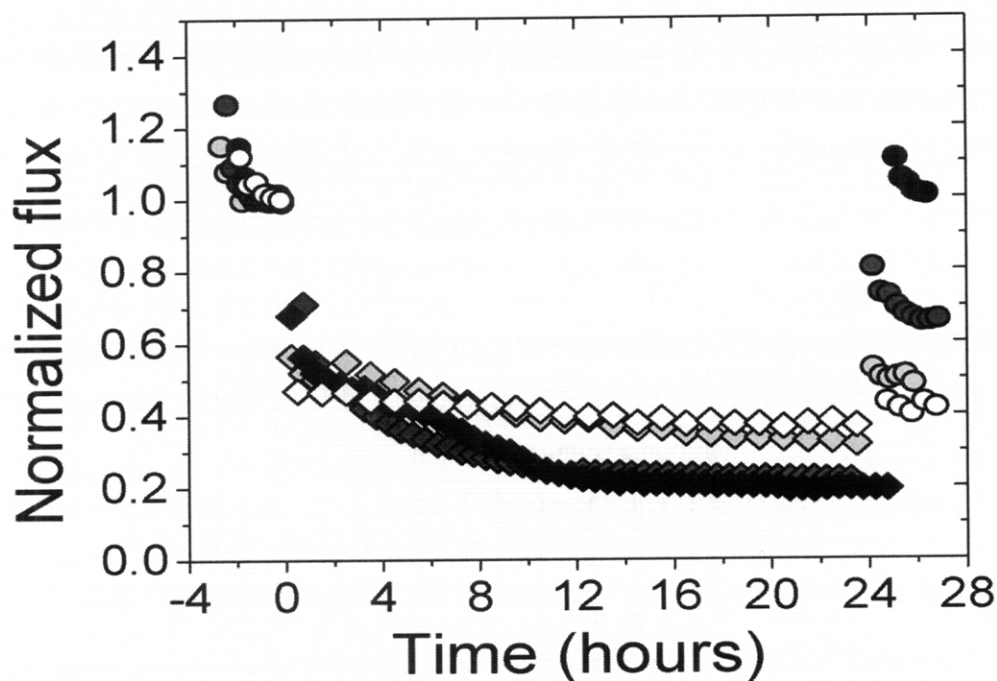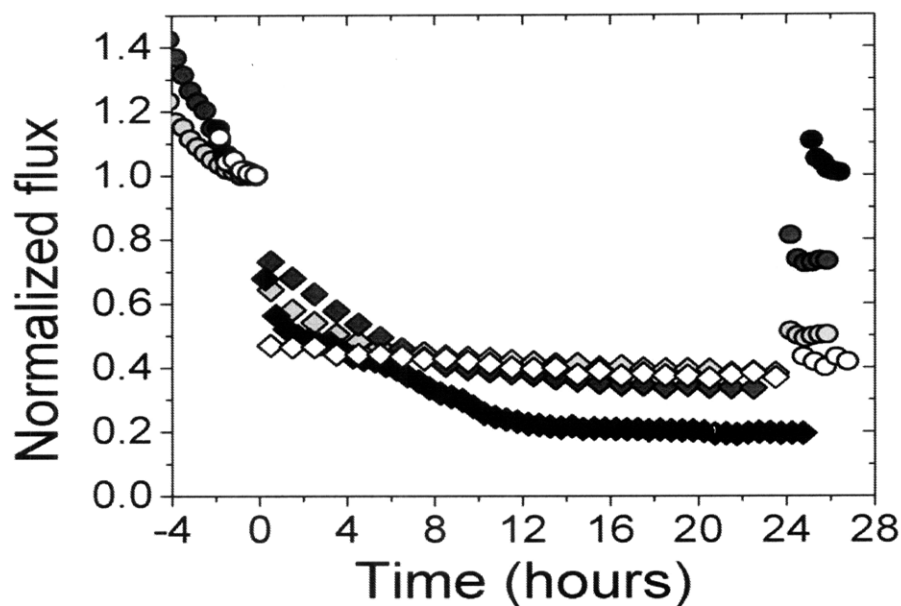
Figure 5.9. Dead-end filtration of model protein solution through membranes with varying PEO content in copolymer: P50-20 (black, average pure water permeability 1590±280 L/m² h MPa), P25-20 (dark grey, pure water permeability 706 L/m² h MPa), P15-20 (light gray, pure water permeability 382 L/m² h MPa), and PAN only (white, pure water permeability 193 L/m² h MPa). ○,●: Milli-Q water, ♦,◊: 1000 mg/L BSA in PBS. Tests performed at 10 psi (0.07 MPa).

These findings were mirrored in the AFM adhesion force measurements provided in the last column of Table 5.3, and in Figure 5.10. P15-20 showed strong adhesion during retraction, with the mean adhesion force having a large negative value. Inspection of the distribution of the normalized adhesion forces for that membrane (Figure 5.10a) also reveals that all the measured adhesion forces are attractive. P25-20 showed relatively weak mean adhesion during retraction, but the majority of the adhesion forces were still negative (Figure 5.10b). As discussed earlier, P50-20 had no adhesion to the particle (foulant) probe, with all 60 adhesion force curves being repulsive (Figure 5.8d). The results further illustrate the utility of this AFM technique in assessing the fouling propensity of membranes [16, 166, 173, 174].
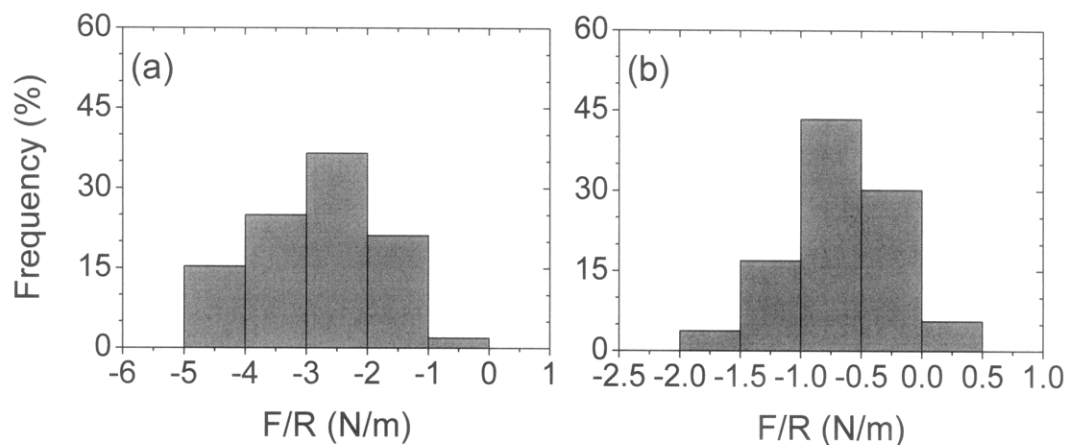
Figure 5.10. Distributions of normalized adhesion forces from 60 measurements between the AFM particle (foulant) probe and membranes P15-20 (a) and P25-20 (b). Experiments were conducted by Dr. Seoktae Kang in the Elimelech Group at Yale University.

5.3.6. Fouling resistance to representative foulants in dead-end filtration

Based on the filtration and adhesion force data above, more extensive fouling studies were performed on the membrane P50-20, which showed the best performance among the membranes studied, and complete resistance to irreversible fouling by BSA. Three foulants were selected as representative foulants in this study: BSA as a representative protein, humic acid in the presence of Ca^{2+} to represent natural organic matter, and sodium alginate as a representative polysaccharide. A commercial PAN UF membrane, the Sepro PAN400, served as a control. These two membranes had comparable retentions for each of the foulants used, as reported in Table 5.4.

Table 5.4: Rejections of model foulants by P50-20 and Sepro PAN400 membranes

Foulant	Retention by P50-20 (%)	Retention by PAN400 (%)
BSA	89	73
Sodium alginate	12	12
Humic acid	84	82

5.3.6.1. Bovine Serum Albumin (BSA)

Figure 5.11 shows the 24-hour dead-end filtration results from P50-20 and Sepro PAN400 membranes for a 1000 mg/L solution of BSA in PBS, performed at 0.07 MPa (10 psi), and plotted as a function of normalized flux (flux/initial flux) vs. time. BSA rejection was found to be 73% and 89% for PAN400 and P50-20, respectively. The flux shows a marked decline in both cases during the filtration of the protein solution, although the decline is less with the PAN-g-PEO-containing membrane, which has a lower initial flux. At the end of the 24-hour time period, the flux loss through the P50-20 membrane is 80%, compared with 95% for the commercial membrane. The most significant difference in performance, however, is the reversibility of flux loss. It was observed that upon a water rinse, the PAN-g-PEO-containing membrane recovered its initial flux completely, indicating no irreversible fouling. After similar treatment, the commercial PAN UF membrane lost 80% of its flux due to irreversible fouling.

119
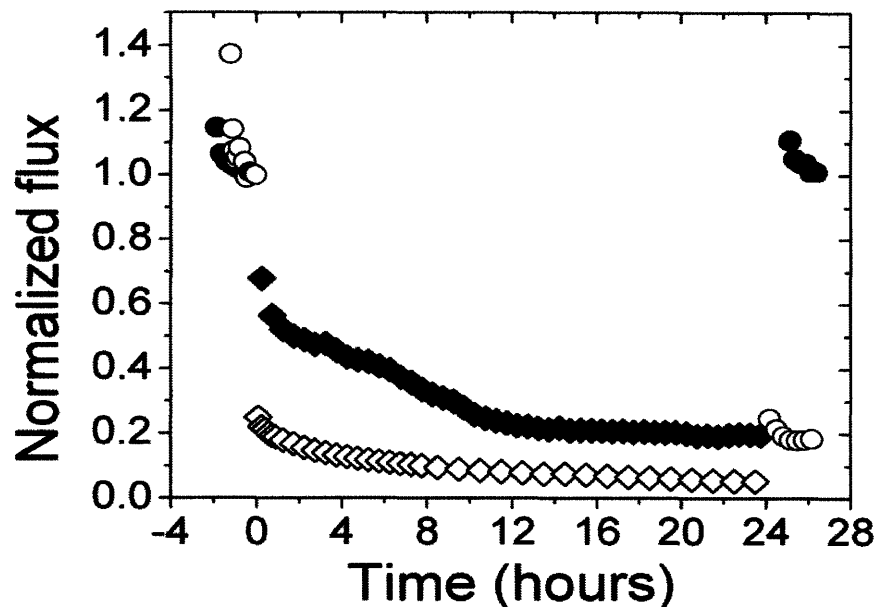
Figure 5.11. Dead-end filtration of model protein solution with P50-20 (filled symbols, average pure water permeability 1590±280 L/m² h MPa) and Sepro PAN400 (empty symbols, average pure water permeability 4580±1210 L/m² h MPa). o,●: Milli-Q water, ♦,◊: 1000 mg/L BSA in PBS. Tests performed at 10 psi (0.07 MPa).

5.3.6.2. Sodium alginate

Sodium alginate was selected as a representative polysaccharide. It was also chosen as it is known to be a component of extracellular polymeric substances (EPS) observed in the presence of microorganisms in the feed [71, 148], and a significant contributor to biofouling [159]. Results obtained upon filtering 1000 mg/L sodium alginate through the P50/PAN blend and commercial membranes were similar to those obtained for BSA (Figure 5.12). The sodium alginate retention was found to be 12% for both the P50-20 and Sepro PAN400 membranes. In this case, the flux decline was more dramatic during the filtration of the foulant: the PAN-g-PEO-containing membrane lost 93% of its flux over 24 hours, while the commercial PAN UF membrane lost 97%. However, upon a pure water rinse, the blend membrane again recovered its flux completely, whereas the commercial membrane showed a 42% irreversible flux loss.

120
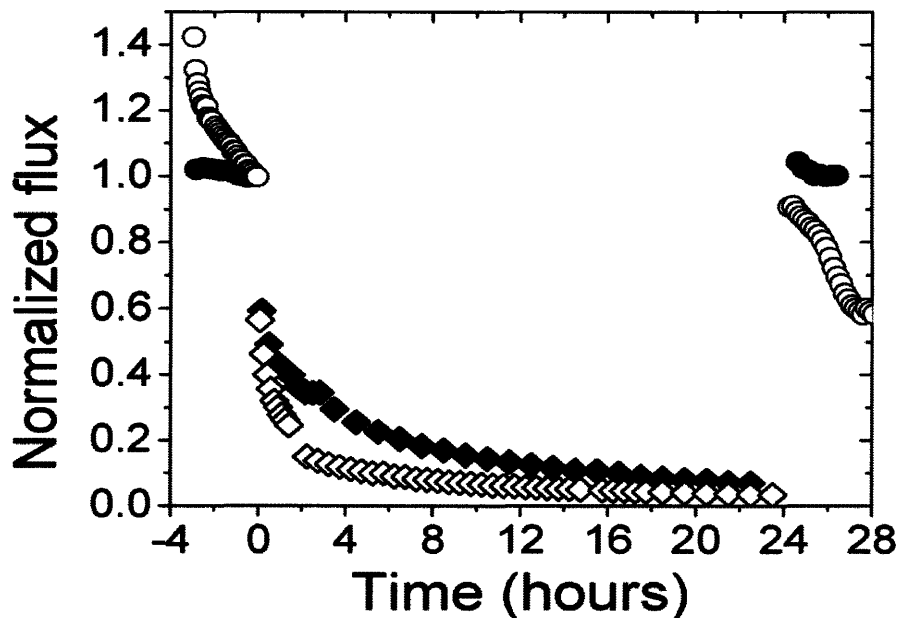
Figure 5.12. Dead-end filtration of model polysaccharide solution with P50-20 (filled symbols) and Sepro PAN400 (empty symbols). ○,●: *Milli-Q water,* ◆,◇: *1000 mg/L sodium alginate in Milli-Q water,* △,▲: *Milli-Q water after simulated backwash. Tests performed at 10 psi (0.07 MPa).*

5.3.6.3. Humic acid

Membrane susceptibility to fouling by humic acid (HA) was also investigated. Humic acid is a major component of natural organic matter (NOM) found in surface and groundwater [222]. It is also a contributor to fouling in wastewater treatment [153], and to biofouling [150]. The fouling characteristics of humic acid are highly dependent on solution chemistry [26, 160, 164, 222, 223]. Membrane fouling by humic acid has been found to increase with the presence of divalent cations, particularly Ca^{2+}. Complexation of Ca^{2+} ions with the carboxyl groups of humic acid leads to intermolecular linkages that result in the formation of a compact cake layer that significantly reduces flux. Hence in these studies, 10 mM $CaCl_2$ was added to the humic acid feed solution.

The two membranes tested had comparable humic acid rejections. After 1 hour of filtration, the Sepro PAN400 rejected 88% of the humic acid, whereas P50-20 rejected 87%. During the filtration of 1000 mg/L humic acid in 10 mM CaCl₂, the commercial PAN UF membrane again showed larger flux decline than the PAN-*g*-PEO-containing membrane (Figure 5.13). At the end of the 24 hour period, the commercial membrane had lost 78% of its flux, compared with 56% for the PAN-*g*-PEO containing membrane. Upon rinsing the cell with water, the commercial membrane showed essentially no recovery in flux, whereas the PAN-*g*-PEO containing membrane recovered 58% of its initial flux.
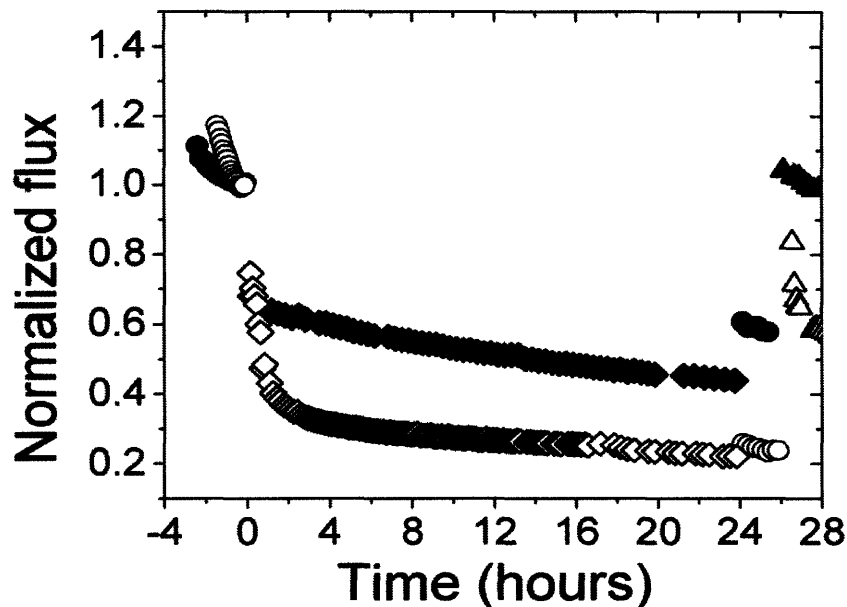
Figure 5.13. Dead-end filtration of model NOM solution with P50-20 (filled symbols) and Sepro PAN400 (empty symbols). ○,●: Milli-Q water, ◆,◇: 1000 mg/L humic acid in 10 mM CaCl₂. Tests performed at 10 psi (0.07 MPa).

For both membranes, at the end of the filtration period, a cake layer of precipitated humic acid was observed on the membrane surface. This layer could not be removed by water rinsing of the cell. Therefore, a simulated backwash was performed on the membranes to attempt to dislodge the precipitate. For this purpose, the membrane was inverted and pure

water was filtered for 30 minutes, and the membrane re-inverted. After this treatment, the commercial PAN UF membrane had recovered only 56% of its flux. Remarkably, the PAN-*g*-PEO containing membrane recovered its flux completely after the same treatment, indicating that the fouling observed was still fully reversible by treatment with water alone.

5.3.7. Protein fouling resistance in cross-flow filtration

Dead-end filtration, used in all of the fouling resistance experiments above, is a good tool for initial characterization of membranes. It is, in a way, a worst-case scenario for fouling, as concentration polarization effects are at their maximum. However, dead-end filtration is rarely used in large scale processes, and cross-flow filtration is the industry standard. Therefore, experiments conducted in cross-flow mode have much more relevance in real life applications. Furthermore, in dead-end filtration, it is very difficult to deconvolute the contributors to flux decline during the filtration of a foulant solution. The only method, as described above, is to consider irreversible flux loss. However, cross-flow experiments give a much better understanding of the process. Finally, dead-end filtration is not a steady-state process. If the membrane retains any of the foulant, the feed concentration increases constantly, complicating the study of retention properties. Cross-flow experiments are especially valuable for such analyses.

For further assessment of the fouling-resistance potential of the novel PAN/PAN-*g*-PEO blend UF membranes, cross-flow fouling experiments were performed by Dr. Seoktae Kang in the Elimelech group at Yale University [16]. In these experiments, a different commercial PAN UF membrane, Osmonics MW, was used as a reference. The experiments were performed using BSA as a model foulant.

The pure water resistance (R_m) of a membrane is defined as

$$R_m = \frac{\Delta P}{\eta J}$$

(5.1)

where ΔP is the applied pressure difference, also termed trans-membrane pressure (TMP), η is the viscosity of water, and J is the pure water flux through the membrane. R_m of the

Osmonics MW membrane was determined to be $(1.87\pm0.05)\times10^{12}$ m^{-1} at a permeation velocity of 20 μm/s (72 L/m^2 h) and $(1.98\pm0.06)\times10^{12}$ m^{-1} at a permeation velocity of 50 μm/s (180 L/m^2 h). The pure water resistance of the PAN-g-PEO/PAN blend membrane increased from $(2.04\pm0.02)\times10^{12}$ m^{-1} at a permeation velocity of 20 μm/s to $(2.45\pm0.04)\times10^{12}$ m^{-1} at a permeation velocity of 50 μm/s. The variation in membrane resistance with permeation velocity arises from the compaction of the membrane. The membrane resistance was recovered when the permeation velocity was decreased from 50 μm/s to 20 μm/s, indicating that the compaction was reversible.

5.3.7.1. Variation of differential pressure with time

In this experiment, the flux through the membrane was kept constant while the pressure was adjusted to maintain this flux, a procedure commonly used in industrial operations. Figure 5.14 shows typical data of the normalized trans-membrane pressure as a function of time during the filtration of 100 mg/L BSA in 10 mM NaCl (denoted as "Na") or 8.5 mM NaCl plus 0.5 mM CaCl$_2$ (denoted as "Ca+Na") solution using the MW control and PAN-g-PEO/PAN blend membranes. The increase in trans-membrane pressure (TMP) for the PAN/PAN-g-PEO blend membrane was fairly slow during the entire fouling run. By contrast, the TMP for the MW membrane rose dramatically, with most of the increase occurring within the first hour. These results demonstrate the superior antifouling properties of the PAN/PAN-g-PEO membrane in comparison to the commercial MW membrane.

Two regimes can be seen in the fouling of the MW membrane: an early regime in which the increase in TMP is very steep, followed by a regime with a much slower rise in TMP. The fouling in the initial regime may be attributed predominantly to BSA adsorption on the membrane surface or pore walls (internal pore plugging), thus causing the rapid increase in TMP [224, 225]. The dominant fouling mechanism in the second regime is considered to be cake layer formation, which would explain the slower and linear TMP increase.
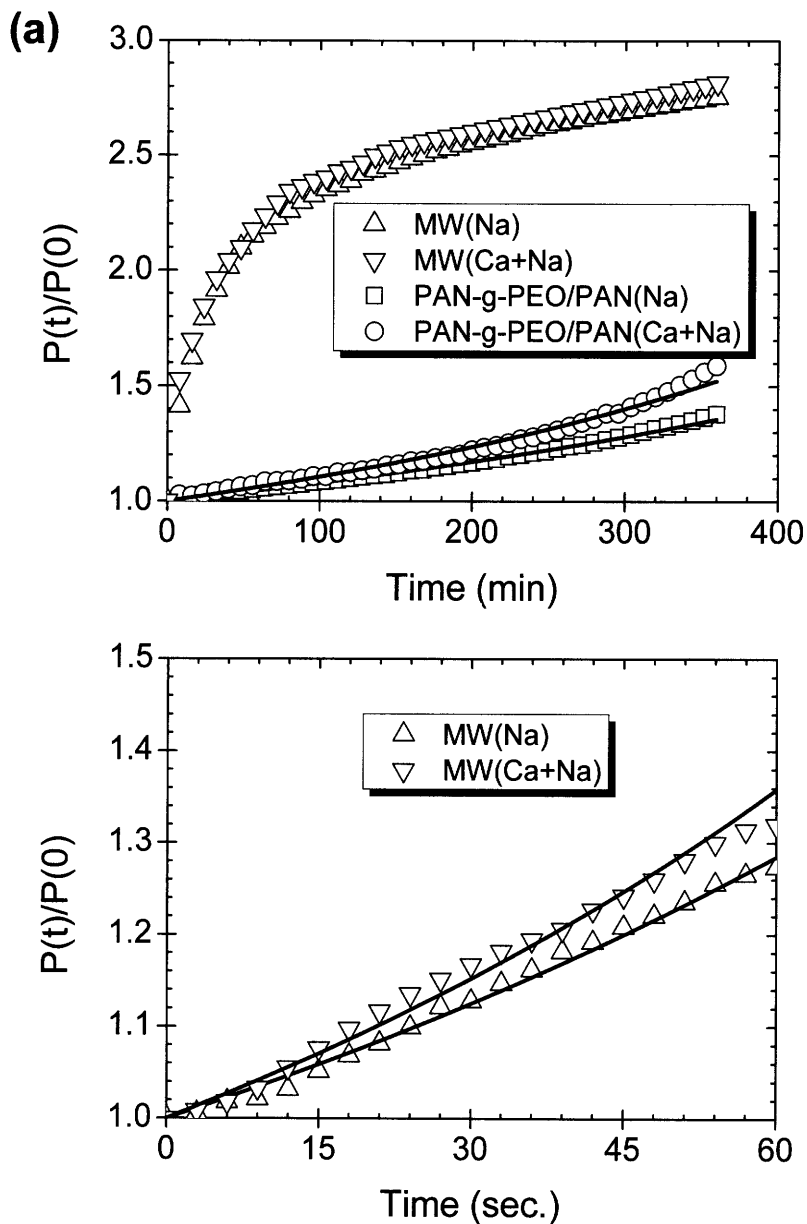
Figure 5.14. BSA fouling behaviors of the PAN/PAN-g-PEO and MW membranes at various ionic compositions: (a) comparison over the entire fouling run of 6 hours, and (b) the MW membrane at the very initial stage (1 min). Experimental conditions: 100 mg/L BSA, pH 5.9±0.3, and ionic composition of 10 mM NaCl, denoted as (Na), or 8.5 mM NaCl plus 0.5 mM CaCl$_2$, denoted as (Ca+Na). Solid lines denote fits with the complete blocking model [224, 225]. Experiments were conducted by Dr. Seoktae Kang in the Elimelech Group at Yale University.

The fouling was higher for the cases where the feed contained Ca^{2+} ions, although the increase is not as dramatic as it is with other macromolecules [166, 173, 174]. This can be due to the screening of the electrostatic repulsion between protein molecules and the membrane surface [226, 227]. In this study, however, the ionic strength was fixed at 10 mM for all experiments, resulting in comparable charge screening (or double layer compaction). Therefore, the higher fouling rate in the presence of divalent calcium ions may be attributed to charge neutralization that occurs due to the complexation of calcium ions with carboxyl groups of BSA, thus leading to a more compact fouling layer [166, 174].

5.3.7.2. BSA retention

The BSA retentions by the blend and control membranes were studied under the same physical (i.e. cross-flow velocity, permeation velocity, and temperature) and chemical (i.e. ionic strength, ionic composition, and pH) conditions. Figure 5.15 shows the retention of BSA during filtration by the PAN/PAN-g-PEO blend and MW membranes at various ionic compositions. For the MW membrane, BSA retention is low initially and increases up to 90% after 300 minutes of filtration. This phenomenon is typical for membrane systems: As foulant molecules adsorb on the membrane, the pores are narrowed, resulting in increased retention [1, 31, 32]. This is not a desirable outcome in many applications, especially in the biotechnology industry, where the objective is to fractionate macromolecules by size.
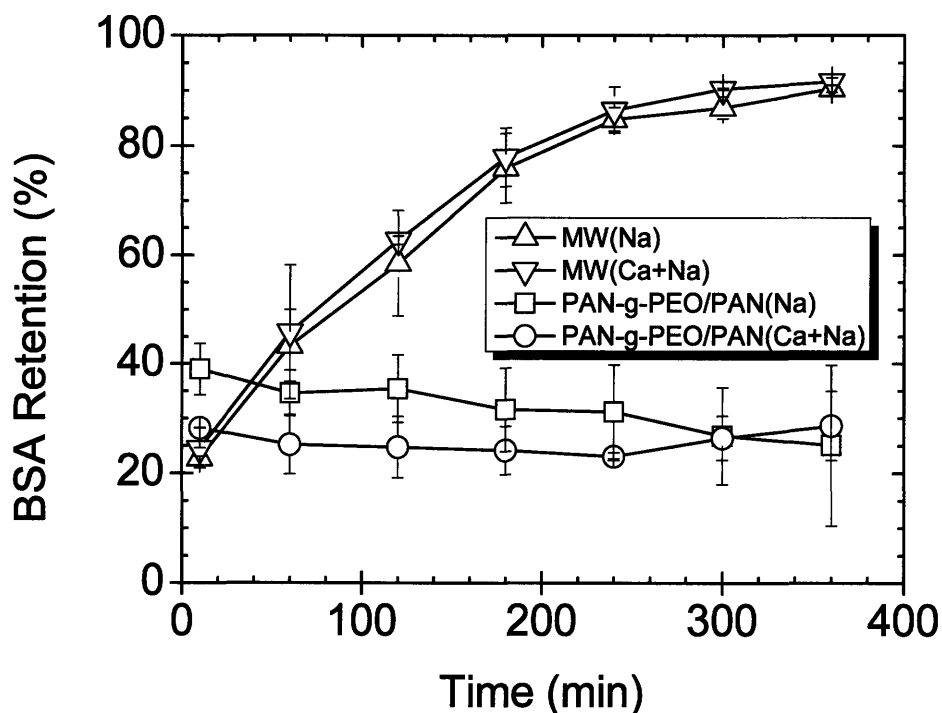
Figure 5.15. BSA retention of PAN/PAN-g-PEO and MW membranes at various ionic compositions. Experimental conditions: 100 mg/L BSA, pH 5.9±0.3, and ionic composition of 10 mM NaCl, denoted as (Na), or 8.5 mM NaCl plus 0.5 mM CaCl₂, denoted as (Ca+Na). All measurements repeated at least three times. Experiments were conducted by Dr. Seoktae Kang in the Elimelech Group at Yale University.

In contrast to the commercial membrane, BSA retention for the PAN/PAN-*g*-PEO blend membrane remains low for the entire filtration run. The constant BSA retention observed for the PAN/PAN-*g*-PEO blend membrane implies that there was negligible pore (standard) blocking and cake formation. The results indicate that the blend membranes may be suitable for the separation of macromolecules based on molecular weight difference without significant fouling and, as importantly, without the shifting of molecular weight cut-off which results when fouling takes place.

Protein retention is affected by the physicochemical characteristics of the protein molecules and the UF membrane, and the resulting interactions that take place during filtration [224]. For the PAN/PAN-g-PEO blend membrane, the constant BSA retention implies a negligible attraction between BSA molecules and the PEO brush layer formed by PAN-g-PEO molecules localized at the blend membrane surface and internal pores [4-6, 8, 13]. Numerous studies have reported the effectiveness of hydrated PEO layers at inhibiting protein adsorption [76, 228, 229].

For the MW membrane, the addition of calcium had little influence on BSA retention, as seen in Figure 5.15. By contrast, the PAN/PAN-g-PEO blend membrane exhibited slightly lower retention in the presence of calcium ions. The data might be explained by a difference in swelling of the PEO brush layer [230], which in turn would influence the effective pore dimensions.

5.3.7.3. Fouling reversibility

In dead-end studies, the PAN/PAN-g-PEO blend membrane showed no irreversible flux loss. This behavior was also tested in a cross-flow system, in comparison with MW membranes. Figure 5.16 shows the cleaning efficiencies of BSA-fouled membranes when subjected to either NaCl or NaOH solution at elevated cross-flow velocity for 30 minutes. For the MW membrane, physical cleaning with saline solution at higher cross-flow velocity (50 cm/s) did not result in TMP recovery, and over 90% of the fouling was irreversible. The initial permeability could only be restored by a chemical cleaning, using a chemical agent such as NaOH. In agreement with the AFM data, the irreversible fouling of the MW membrane is due to the favorable adhesion and deposition of BSA to the membrane surface and inside the pores.
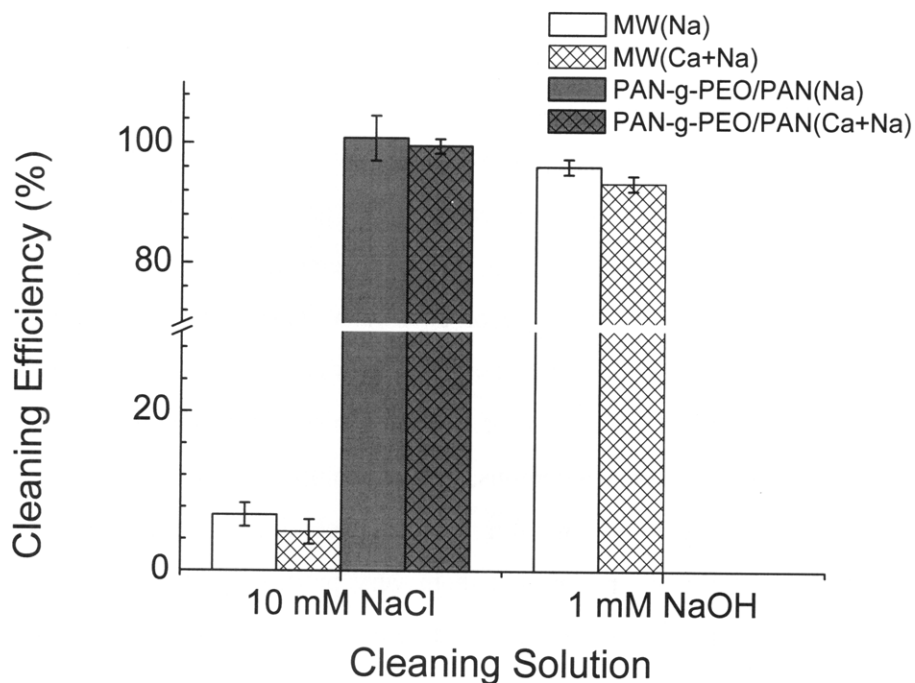
Figure 5.16. Cleaning efficiencies of BSA-fouled membranes with respect to cleaning agents. All cleaning runs were conducted at the cross-flow velocity of 50 cm/s for 30 minutes. Experiments were conducted by Dr. Seoktae Kang in the Elimelech Group at Yale University.

In contrast, the cleaning efficiency (or TMP recovery) of the PAN/PAN-*g*-PEO blend membrane after physical cleaning was close to 100%, irrespective of the presence of calcium ions during BSA filtration. Because any fouling could be reversed by simply increasing the cross-flow rate, there was no need for chemical cleaning. These results clearly demonstrate the superior antifouling performance achieved by the addition of PAN-*g*-PEO comb copolymer to PAN. Irreversible protein adsorption or deposition is inhibited and the initial flux can be readily recovered by simple rinsing.

5.4. Conclusions

UF membranes prepared with amphiphilic comb copolymers as additives in the casting solution show improved fouling resistance, higher pure water flux, and improved wettability, without any added processing steps in production. PAN-*g*-PEO was shown to be very successful as such an additive. Membranes prepared with 20 wt% comb copolymer additive with 40% PEO content resist irreversible fouling completely, and recover their initial flux by a water rinse or backwash. This eliminates the need for chemical cleanings, which are costly, create hazardous waste of spent cleaning solution, and can degrade the membrane material and shorten membrane life. To the author's knowledge, this is the first report of a demonstration of complete resistance to irreversible fouling to biomolecules by a UF membrane. The exceptional fouling resistance of PAN/PAN-*g*-PEO blend membranes makes them very promising for applications with high fouling potential, such as wastewater treatment, membrane bioreactors, food and biotechnology industries.

Chapter 6

Application of PAN-g-PEO Containing UF Membranes in the Treatment of Oily Wastewater

6.1. Introduction

This chapter aims to demonstrate the use of PAN/PAN-g-PEO blend UF membranes described in Chapter 5 to a specific application: the treatment of wastewater streams from the oil industry. The hydrocarbon processing industry, including petroleum refining, petrochemical processing and oil and natural gas production, generates large quantities of wastewaters that have high contents of oil [27]. The largest single wastewater stream of this industry is the saline water brought to the surface during oil and gas production, known as produced water [79, 231]. It often contains salts, heavy metals, oil, and other organics, including polycyclic aromatic hydrocarbons (PAH), phenols, and traces of chemical additives used in drilling [231-234]. Its composition can vary drastically by location and throughout the life of the well [232]. Treatment and disposal of produced water is expensive, and in constant need of improvement as discharge specifications tighten [235]. For on-shore disposal or for reuse as process water, produced water needs to be treated to remove oil, toxic substances, and high salt concentrations [232, 236, 237]. In off-shore oil wells, discharge into the sea is possible without the removal of saline [234, 237], but essentially all oil and grease (O&G) contaminants still need to be removed [235, 237, 238]. Refinery wastewater is another problematic stream of the oil industry, as it contains hydrocarbons that remain even after conventional wastewater treatment due to difficulty in biological degradation [239]. This makes further treatment necessary to meet discharge requirements [240, 241], or for its reuse [239].

The oil in wastewater streams is generally found in three forms: Free oil is in large droplets that coalesce if allowed to settle. Emulsified oil is in the form of small droplets

less than 20 μm in size that are stabilized. Finally, dissolved oil comprises the water-soluble components of oil, including phenol derivatives and organic acids [27, 234]. The removal of a large portion of free oil is possible with conventional methods using hydrocyclones or dissolved air flotation, but the resultant water quality is not sufficient for discharge or reuse [238]. Membrane purification is a strong candidate for this application [27, 233].

Ultrafiltration (UF) membranes can remove essentially all of free and dispersed oil from wastewater, and the permeate is consistently able to meet O&G standards for discharge [231, 233, 235, 239, 241, 242]. The degree of removal for hydrocarbon contaminants is very high [235, 241], but dissolved oils are only partially retained [233, 235, 239, 240]. Moreover, UF membranes do not retain salt. Depending on feed composition and discharge requirements, UF treatment might be sufficient [235], especially in off-shore platforms [234]. Further treatment is generally necessary for on-shore disposal or for reuse of the effluent as process or cooling water, due to more stringent regulations. In these cases, reverse osmosis (RO) membranes are required to remove salts and small molecule contaminants [236, 238, 243]. However, they are limited by severe fouling due to the oil in the feed, especially in the form of free and dispersed oil [27]. The removal of oils by UF largely prevents the fouling of the RO membrane, making the process more feasible [239, 243].

In all of these cases, UF treatment of oily feeds is economically limited by one factor: loss of membrane flux due to severe fouling [231, 233, 235, 240, 242]. Flux is often reduced by one to two orders of magnitude, severely impacting the economic viability of membrane treatment of oil industry wastewaters [231, 235]. Fouling resistant membranes that can remove oil are needed to improve the process economics [231]. In general, membranes with more hydrophilic surfaces have been found to resist fouling [32]. Nevertheless, there is limited literature on developing fouling resistant membranes for this demanding application. Ju *et al.* proposed coatings of cross-linked poly(ethylene glycol) diacrylate (PEGDA) to decrease fouling of polysulfone UF membranes [79]. In cross-flow fouling experiments with oil/water mixtures, cross-linked PEGDA coated membranes showed 4 times higher flux after 24 hours of filtration. Yet, the properties of

real oil industry wastewater are very different from oil/water mixtures prepared in the laboratory due to the presence of a myriad of other chemicals, including salts and additives. Therefore, testing with industrial samples is crucial in evaluating the value of a novel membrane system for oily wastewater applications.

6.2. Experimental Methods

6.2.1. PAN/PAN-g-PEO blend UF membranes

The comb copolymer PAN-g-PEO was synthesized following the procedure described in Section 5.2.2, following the synthesis protocol for P50. The UF membranes were prepared following the procedure described in Section 5.2.3, according to the formulation for P50-20.

6.2.2. Analysis of water samples

The wastewater samples and the filtrates were characterized by three methods: UV-visible spectroscopy was performed at five wavelengths: 250, 350, 450, 550 and 650 nm, on a Thermo Scientific UV/Visible Scanning Spectrometer. Conductivity was measured by a VWR Expanded Range Conductivity Meter, and also converted to units of total dissolved solids (TDS). Chemical oxygen demand (COD) was measured using commercial test kits (WTW). Samples whose TDS was above 2000 ppm were diluted to 1/10 of their initial concentration for COD analysis to avoid errors due to the presence of chlorine ions. To determine the total suspended solids (TSS) values for wastewater samples, a glass fiber filter (Whatman, 1 μm pore size) was dried at 105°C in vacuum, and weighed. Twenty milliliters of the wastewater sample were filtered through, and the filter was again dried until its weight stabilized. The TSS value was determined using the change in the weight of the filter. The COD of the filtrate was determined and listed as "<1 μm COD".

6.2.3. Oil industry wastewater samples

In this study, three wastewater samples were studied. The first was a sample of oil well produced water, labeled PW-A, supplied by BJ Services Co.. It was diluted to ¼ its initial

concentration using Milli-Q water to obtain sufficient quantities for 24 hour filtration experiments. The second sample was also a produced water sample, supplied by ConocoPhillips and labeled PW-B. The third sample, labeled RW, was a sample from a refinery wastewater stream, supplied by ConocoPhillips. Some basic properties of these samples, including COD, conductivity, equivalent TDS derived from the conductivity measurement, and TSS values, are listed in Table 6.1.

Table 6.1: Properties of oil industry wastewater samples

Sample name	Sample classification	COD (mg/L)	Conductivity (μSi/cm)	TDS (ppm)	TSS (ppm)	<1μm COD (mg/L)
PW-A	Produced water	14300	2.1×10^4	1.4×10^4	6400	5150
PW-B	Produced water	2310	6.6×10^2	440	170	1770
RW	Refinery wastewater	970	2.5×10^3	1600	52	646

6.2.6. Filtration experiments

Fouling experiments were run following the procedure described in Section 5.2.7. The fouling experiments on PAN/PAN-g-PEO blend membranes and the control were performed simultaneously in duplicate set-ups to minimize aging effects. The wastewater sample was agitated for 60 seconds before dividing it into the foulant reservoirs to minimize heterogeneity effects. In some cases, two backwash steps were necessary to remove the deposit layer.

6.3. Results and Discussion

6.3.1. Membrane permeabilities

The PAN/PAN-g-PEO blend membranes used in this study were investigated in detail in Chapter 5, and were demonstrated to have exceptional resistance to biofoulants [13, 16],

with membranes incorporating 20 wt% PAN-g-PEO exhibiting complete resistance to irreversible fouling by serum albumin, sodium alginate and humic acid at concentrations of 1 g/L. In the present investigation, the optimized blend composition of 80/20 PAN/PAN-g-PEO determined from these previous studies was used for all blend membrane samples. The pure water permeability (PWP) of the blend membrane was 1160 ± 70 L/m^2 h MPa. A commercial PAN UF membrane, the PAN-400 by Sepro Membranes, Inc. was used as the control due to its similar serum albumin retention [13]. The PWP of the control membrane was 3280 ± 580 L/m^2 h MPa.

6.3.2. Ultrafiltration of produced water sample PW-A

PW-A was a produced water sample that was especially high in suspended solids (Table 6.1). It was very high in oil content, as indicated by the high COD. Upon resting for extended periods of time, the oily fraction would collect at the top of the solution, indicating a high free oil content. This is in agreement with the relatively larger fraction, around 65%, of oil that can be removed by the 1 μm membrane (Table 6.1). However, the <1 μm COD value was still high, indicating microfiltration is not a sufficient method for removing the oil from this sample. Another property of PW-A was its very high salinity, equivalent to 14,000 ppm TDS (compare to seawater values of 35,000-50,000 ppm TDS [1]). All these properties make this sample one of the most challenging for reuse, as well as one with great fouling potential.

Dead-end filtration was performed on PW-A using a PAN/PAN-g-PEO blend membrane and the Sepro PAN-400 control. Effluent quality was analyzed to determine the ability of the membrane to remove the contaminants. COD retention was measured to be 96.5% and 96.1% for PAN/PAN-g-PEO blend and control membranes, respectively. This large reduction in COD arises mainly from the removal of free and dispersed oil from the system, as well as the smaller molecules that partition into the oil phase [232].

The retention was also evaluated using the absorbance at different wavelengths (Table 6.2). The performance of the two membranes was comparable, in agreement with the COD removal. Solutes that absorbed visible light were found to be removed completely, within instrument sensitivity. This was corroborated by the fact that the filtrate appeared

135

completely clear (see inset in Figure 6.1). The retention in the lower wavelengths was slightly lower, but still above 84%. The conductivities of the feed and permeates were approximately equal, indicating that all salt ions pass through the UF membranes, as expected. The permeate obtained in this process still has a quite high COD value as well as high salinity. Nevertheless, it is expected to have a much lower oil content, as COD measurements include soluble components such as small molecule acids that do not contribute to the O&G measure, regulated for off-shore disposal [244]. As long as these O&G limitations are met, UF may be a sufficient method for the treatment of this stream. For onshore wells, UF treatment would be a good choice for pre-treatment of this stream before using RO or NF to remove salts and small molecule contaminants.

Table 6.2: Retention of wastewater samples by the PAN/PAN-g-PEO blend and control membranes calculated at different wavelengths

Membrane	Feed sample	Retention (%)				
		250 nm	350 nm	450 nm	550 nm	650 nm
PAN/PAN-g-PEO	PW-A	84	96.9	99.5	99.9	>99.9
Sepro PAN400		84	96.8	99.5	99.9	>99.9
PAN/PAN-g-PEO	PW-B	98.6	99.8	>99.95	>99.95	>99.95
Sepro PAN400		98.7	99.8	>99.95	99.9	99.9
PAN/PAN-g-PEO	RW	23	54	84	90.1	94.0
Sepro PAN400		49	65	85	89	92.2

As described earlier, fouling is the limiting issue in the use of UF membranes for produced water treatment. Hence, 24-hour dead-end fouling tests were conducted using PW-A as the feed. Figure 1 shows the normalized flux versus time data from such experiments for each membrane. During the filtration of the produced water, the

normalized flux of the PAN/PAN-*g*-PEO blend membrane remained much above that of the commercial PAN membrane. After 24 hours of dead-end filtration, the blend membrane lost 68% of its flux, whereas the commercial PAN membrane lost 92%. Furthermore, after a backwash to remove the cake layer, the PAN/PAN-*g*-PEO membrane recovered its initial flux completely, indicating that even with this complex feed, the membrane resisted irreversible fouling. Under similar conditions, the Sepro PAN-400 lost 37% of its flux irreversibly. The ability of PAN/PAN-*g*-PEO blend UF membranes to maintain a larger portion of their initial flux shows the distinct advantage of such membranes over a commercial PAN UF membrane of similar selectivity.
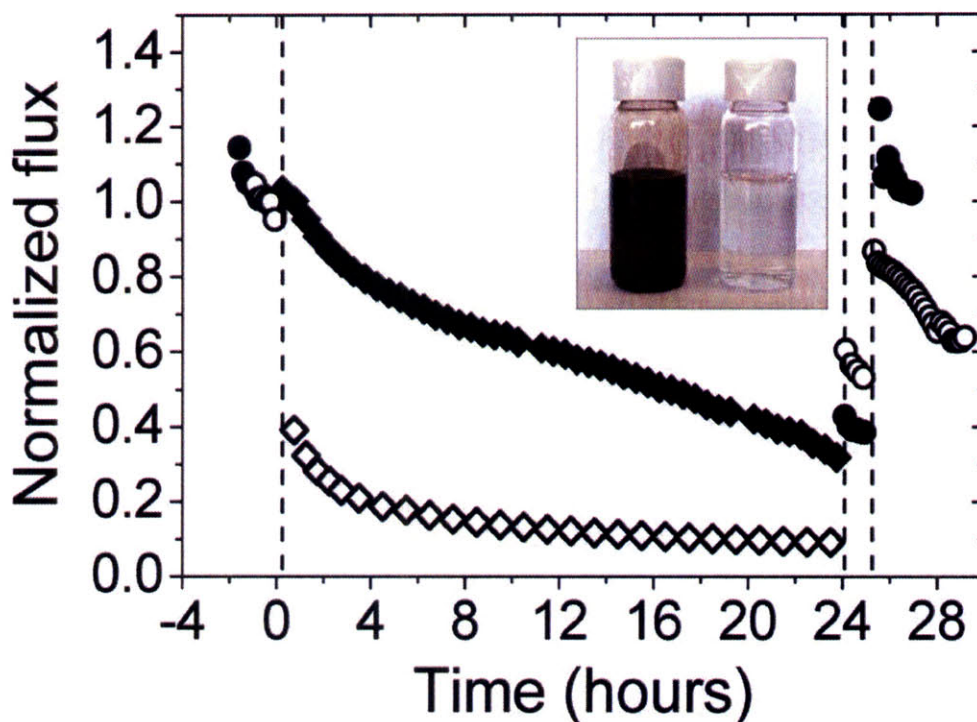
Figure 6.1. Dead-end filtration of PW-A through PAN/PAN-g-PEO blend membrane (filled) and Sepro PAN-400 (open) ○,●: Milli-Q water; ♦, ◊: PW-A. Switches between water and foulant, and backwash steps are marked by dashed lines. Tests performed at 10 psi (0.7 MPa). Inset shows a picture of the feed (left) with typical UF permeate (right).

137

6.3.3. Ultrafiltration of produced water sample PW-B

PW-B was a highly heterogeneous produced water sample, and had a high particulate content. These particles were probably precipitated high molecular weight hydrocarbons, as they were observed to dissolve easily in hexane. The COD of this feed was measured to be 2310 ppm. The conductivity of this sample was much lower than PW-A, equivalent to 440 ppm total dissolved solids (TDS). This is a value acceptable even for drinking water [1], so salt removal would probably not be necessary.

In the filtration of PW-B by the two UF membranes studied, COD retention was measured to be 98.3% and 99.4% for PAN/PAN-g-PEO blend and control membranes, respectively. The retentions based on absorbance at different wavelengths were also comparable for the two membranes (Table 6.2). Solutes that absorbed visible light were found to be removed completely, within instrument sensitivity, as indicated by the fact that the filtrate appeared completely clear (see inset in Figure 2). The retention in the lower wavelengths was slightly lower, but still above 98.6%. The conductivities of the feed and permeates were approximately equal, indicating that the UF membranes do not retain salts, as expected from their pore size.

The UF permeate quality in this case was quite high. The effluent COD value corresponds to a total organic carbon (TOC) between 11-15 ppm for the PAN/PAN-g-PEO blend membrane, and 4-5 ppm for the Sepro PAN-400 membrane [245]. Even if all of this organic carbon were hydrocarbons, the O&G content of the effluent would still fall below the limit of 48 mg/L set by the Environmental Protection Agency (EPA) [237]. The conductivity was high but still in the acceptable range even for drinking water use [1]. Depending on the concentrations of toxic components such as phenols, and the presence of heavy metals in this permeate, it might be possible to discharge this effluent safely. If there are toxic organic molecules such as phenols and BTEX in the permeate, these components can be removed by adsorption methods while preventing the loss of adsorbent activity due to the presence of oil [246]. In short, UF is a very promising treatment method for this sample of produced water, as long as membrane flux can be maintained at a level that justifies it economically.

Figure 6.2 shows the change in normalized flux with time for a 24-hour dead-end filtration using PW-B as the foulant. A large decrease in the flux was observed for both membranes in the presence of the foulant. The PAN/PAN-g-PEO membrane shows slightly lower flux loss for the first 6 hours. Thereafter, the stir assembly in the cell containing the blend membrane became jammed, so concentration polarization and cake fouling in this cell was much more severe. The feed contained a large amount of particulates that formed a cake on both membranes. To investigate the irreversible flux loss, therefore, two simulated backwashes were performed. At the end of these steps, the pure water flux of the blend membrane was recovered completely, indicating that no irreversible fouling had occurred, despite the dramatic loss of flux during operation. By comparison, the control membrane lost 26% of its initial flux irreversibly. The results suggest the PAN/PAN-g-PEO blend UF membranes could be suitable for use in the treatment of similar produced water samples by decreasing membrane cleaning and replacement costs.
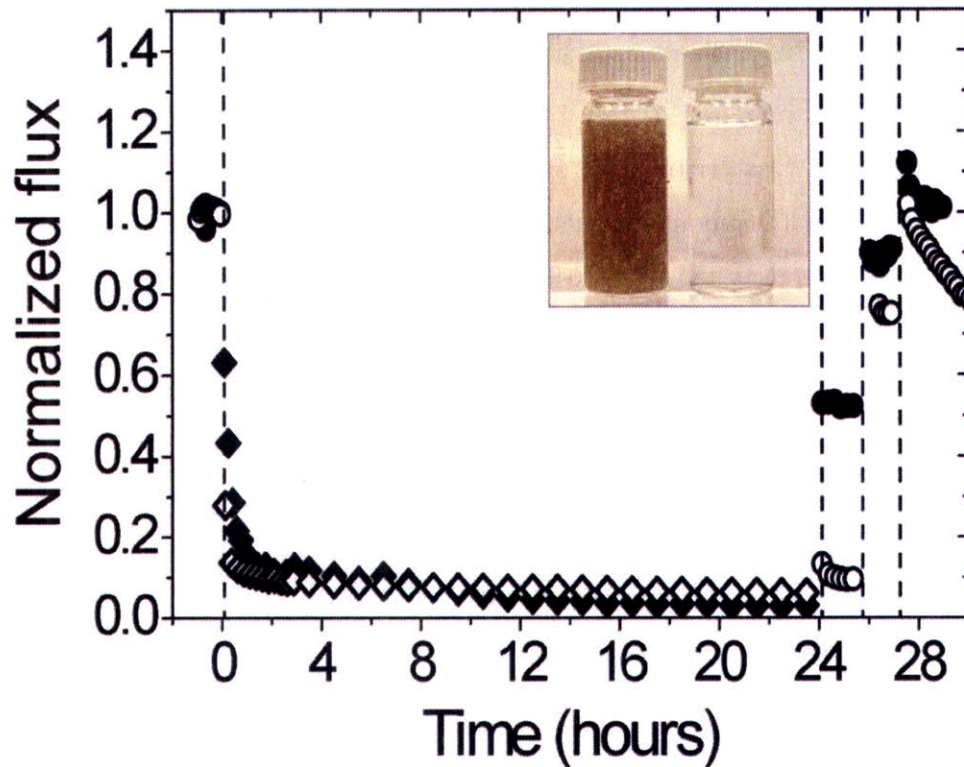
Figure 6.2. Dead-end filtration of PW-B through PAN/PAN-g-PEO blend membrane (filled) and Sepro PAN-400 (open) ○,●: Milli-Q water; ♦, ◊: PW-B. Switches between water and foulant, and backwash steps are marked by dashed lines. Tests performed at 10 psi (0.07 MPa). Inset shows a picture of the feed (left) with typical UF permeate (right).

When the UF treatment of the two produced water samples, PW-A and PW-B, are considered, a few conclusions can be made. UF was found to be a good option in the treatment of these samples. It was successful in removing free and dispersed oils, and can potentially be used to meet O&G discharge regulations, or as a pretreatment step for RO. Both the commercial control and the PAN/PAN-g-PEO blend UF membranes were comparable in this sense, and showed similar performance in effluent quality. However, the most important economic limitation to the use of UF membranes in produced water treatment is fouling [235]. In terms of fouling resistance, the blend membranes showed a significant advantage. They generally retained more of their flux, especially visible in the treatment of PW-A. Furthermore, they recovered their initial flux by a backwash,

whereas the commercial control lost a quarter to a third of its flux irreversibly after 24 hours of operation. The results show the potential of these novel membranes for the economical UF treatment of produced water.

6.3.4. Ultrafiltration of refinery wastewater sample RW

The refinery wastewater sample, denoted RW, was much more homogeneous than the oil well produced water samples. This implies a higher content of dissolved oil, and a lower content of free and emulsified oil. The COD of this sample was the lowest at 970 ppm. The conductivity was 2500 μmho, equivalent to 1600 ppm TDS (see Table 1), considered to be in the brackish water range [1].

COD retention was much lower for this sample, measured to be 44% and 41% for PAN/PAN-g-PEO blend and control membranes, respectively. These values are comparable with values reported in other studies on UF treatment of refinery wastewater samples that found very high O&G removal but much lower decreases in COD [233, 235, 239, 241]. The limited retention was also visible by the yellowish color of the filtrate (see inset in Figure 6.3), and by the retentions calculated using absorbance at different wavelengths, given in Table 6.2. The retentions were higher at higher wavelengths, but still lower than those observed for the produced water samples. Once again, the conductivity of the filtrate was the same as the feed, indicating no salt retention.

The most important reason for the low organics removal is a higher content of soluble small molecule contaminants in the feed. The absence of much free and emulsified oil may also decrease the removal of these components: Many toxic components in oil industry wastewater tend to partition into the oil phase when present [232]. Therefore, together with the free and dispersed oil, UF is able to remove components that partition into the droplets. In the absence of an oil phase, these toxic molecules are dissolved in water and can only be removed by RO or NF membranes, depending on their size.

The retention for the refinery wastewater sample was not sufficient for reuse or discharge, as the final COD value was above the limits set by the EPA [247], which are much more stringent than those set for produced water disposal in off-shore oil wells. However, since

emulsified and free oils are the most significant contributors to fouling in the RO treatment of oily feeds [1, 27], UF may be an effective pretreatment method before using RO to remove salts and low molecular weight contaminants [236, 240, 248].

To be economically feasible, the UF membrane should resist fouling considerably and maintain high fluxes in the presence of oil. Figure 6.3 shows the change in normalized flux with time in the 24-hour dead-end filtration of RW using a PAN/PAN-g-PEO blend UF membrane and a PAN-400 control. The flux decline in the presence of foulant was very severe for the commercial PAN membrane, which lost 90% of its flux within one hour. By contrast, the blend membrane retained 55% of its flux after one hour. After 24 hours, the commercial membrane flux was only 3% of its initial value, whereas the blend membrane retained 23% of its initial flux. Furthermore, the blend membrane regained its initial pure water flux completely after a simulated backwash, demonstrating its resistance to irreversible fouling as seen with the produced water samples, and with various biofoulants in previous studies [13]. In comparison, the commercial PAN membrane lost 45% of its flux irreversibly.
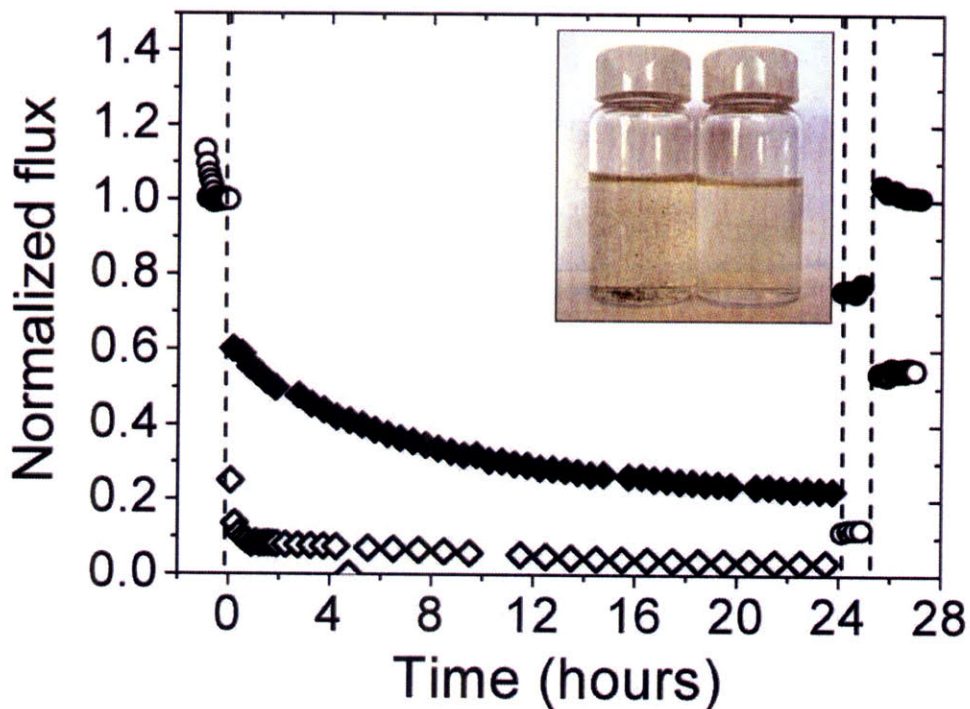
Figure 6.3. Dead-end filtration of RW sample through PAN/PAN-g-PEO blend membrane (black) and Sepro PAN400 (white) ○,●: Milli-Q water,◆, ◊: RW. Backwash step is marked by dashed lines. Tests performed at 10 psi. Inset shows a picture of the feed (left) with typical UF permeate (right).

6.4. Conclusions

This chapter focused on the use of PAN UF membranes incorporating PAN-g-PEO in the treatment of oil industry wastewaters, which pose several challenges due to their high fouling potential. The membranes prepared using the composition optimized in Chapter 5 were shown to exhibit highly improved fouling resistance while showing effluent quality comparable with commercial UF membranes. Due to their ability to resist adsorptive fouling, these membranes can sustain higher fluxes, require less frequent backwashes, eliminate the need for chemical cleanings, and achieve longer membrane lifetimes, translating to reduced energy consumption during operation and better process economics.

Chapter 7:

Summary and Future Outlook

7.1. Thesis Summary

This thesis focused on the design of improved filtration membranes through the use of self-organizing properties of amphiphilic comb copolymers. One focus of this work was to further characterize the properties of thin film composite (TFC) NF membranes made with a selective layer of the comb-shaped graft copolymer poly(vinylidene fluoride)-*graft*-poly(oligooxyethylene methacrylate), PVDF-*g*-POEM. These membranes were first shown by Akthakul *et al.* to filter small molecules by size due to the formation of effective "nanochannels" upon the microphase separation of the comb copolymer backbone and side-chains [11, 12]. That work also showed that the membranes resisted irreversible fouling by emulsified oil/water mixtures [12]. The first objective of this thesis was to better quantify and understand the fouling resistance of these membranes. Fouling experiments with representative foulants as well as activated sludge from a membrane bioreactor (MBR) indicated that these membranes resisted irreversible fouling completely. Atomic force microscopy (AFM) experiments measuring the interaction forces between a model foulant and the membrane surface showed a steric repulsive force between the PVDF-*g*-POEM coating and the probe, which accounts for the exceptional fouling resistance observed [17]. This study indicates that these novel NF membranes are very promising for NF MBR systems [37, 142]. Their high flux and fouling resistance are crucial to achieving good process economy [29, 30]. Their ability to remove small molecules without salt retention could be useful in removing small molecule contaminants such as pharmaceuticals and endocrine disrupting agents (EDAs), without the need for the high pressure differences required in RO systems due to osmotic pressure [29, 37, 142, 143].

Another important property of PVDF-*g*-POEM TFC NF systems, a pore size that can be tuned by feed properties, was also investigated in this thesis. Akthakul *et al.* had observed shifts in effective pore size of these membranes when the feed solvent was changed from water to ethanol or toluene [11]. This thesis showed that other feed properties can also be used to tune the selectivity of these membranes in a controlled and continuous manner. The effective diameter of the nanochannels available for the passage of solutes is determined by the size scale of microphase separation, and the size of the poly(ethylene oxide) (PEO) side-chain coils lining the walls. The swelling of the PEO chains depends on the solvent quality of the feed solution, which is affected by parameters such as temperature, pressure, and ionic strength. The variation in these dimensions is negligible in porous membranes, as the overall chain size is much smaller than the pore size. However, in the PVDF-*g*-POEM TFC NF system, where the selectivity is in the subnanometer range, slight variations were shown to lead to significant changes in effective pore size. This was demonstrated by shifts in water flux and dye passage in agreement with the phase diagrams of PEO/water systems [18]. Membranes with size-based selectivity in the small molecule range, combined with the ability to tune this pore size in operation, are very promising for pharmaceutical applications, where many separations are used at different stages in the production of an active therapeutic chemical. They would also have applications in the food industry for the same reason.

This thesis also presented the development of a new material platform for similar anti-fouling, subnanometer size selective membranes. Polyacrylonitrile-*graft*-poly(ethylene oxide (PAN-*g*-PEO), a copolymer with a PAN backbone and PEO side-chains, was synthesized by free radical copolymerization. This method is more controlled and scalable, bringing the NF technology based on comb copolymers a step closer to industrial realization. The microphase separation of PAN-*g*-PEO, and the size selectivity and fouling resistance of TFC membranes prepared from it, was demonstrated.

The size cut-off displayed in both of these NF systems is essentially a 'missing link' in the currently available spectrum of commercial membranes: The tightest UF membranes have molecular weight cut-off around 10,000 Da, whereas NF membranes retain salts. The novel PAN-*g*-PEO TFC NF membranes, as well as PVDF-*g*-POEM TFC NF

membranes, make it possible to separate and desalt smaller molecules. These types of separations are widely used in pharmaceutical and biotechnology industries, often by chromatographic methods. Introduction of a membrane with this type of ability would be very valuable in cutting process costs in such separations.

Another focus of this thesis was the use of PAN-g-PEO comb copolymers as surface segregating additives in the formation of fouling resistant UF membranes, following the strategy first described by Hester *et al.* [3-7, 249]. The fouling resistance of PAN/PAN-g-PEO blend UF membranes was tested with three representative foulants, and it was demonstrated that membranes of optimal composition recovered their initial water fluxes completely with either a water rinse or a backwash. These results, combined with AFM interaction force measurements, indicate that PAN/PAN-g-PEO blend membranes could resist adsorptive fouling completely. The ability to clean these membranes without the need for aggressive chemicals can lead to much longer membrane life times, higher sustained fluxes, lower energy use, and decreased use of chemicals. Furthermore, the pure water permeability and wettability of the membranes cast with PAN-g-PEO was significantly improved. All of this could decrease the operating cost of the system by 20-50%, making the UF process more economically viable. This is especially significant in industries where fouling is the limiting issue, such as in wastewater treatment, MBRs, the food industry, pharmaceuticals, and the oil industry.

The last portion of the thesis was a demonstration of the advantages of the new PAN/PAN-g-PEO blend UF membranes in a real life application, the treatment of oil industry wastewaters. Oily wastewater, including oil well produced water and refinery wastewater, is very difficult to treat due to its very high fouling potential and poor biodegradability. In this study, three oil industry wastewater samples were filtered through PAN/PAN-g-PEO blend membranes as well as a commercial PAN membrane as a control. The separation properties of the two membranes were comparable, while the PAN/PAN-g-PEO blend membrane retained a higher portion of its flux in these operations. Complete resistance to irreversible fouling was demonstrated by the comb-modified membranes with these challenging feeds as well, confirming the potential of

PAN/PAN-*g*-PEO blend membranes for the more economical treatment of oily wastewaters.

7.2. Future Outlook

The research described in this thesis examines only a small number of the various systems that can be developed using the two approaches studied: surface segregation of comb copolymers for UF surface modification, and their microphase separation to form nanometer-scale channels for NF. As a starting point, these systems need to be developed further, to form commercial membranes optimized for each application. New copolymer chemistries can also be promising for the development of other fouling-resistant membrane systems, porous and non-porous. This would broaden the range of applications and operating conditions that can be accessed. The surface segregation approach can be used to incorporate functional groups on the polymer/water interface of porous membranes in a single step, leading the way for improved membranes for heavy metal removal and affinity filtration. A functionalized copolymer can also be used as a non-porous selective layer, similar to the NF systems, to perform reverse osmosis (RO). Each of these systems are described in further detail in the sections below.

7.2.1. Optimization of the systems developed

The objective of the research described in this thesis was to demonstrate the novel membranes that can be prepared taking advantage of amphiphilic comb copolymers. However, industry uses membranes for a wide range of applications, each demanding different properties. For example, for biotechnology applications, the homogeneity of the membranes over large areas and dependability will be of great importance [24], while for municipal and wastewater applications, cost will be the critical parameter [2]. The pore sizes required for different applications will also vary widely. Commercialization of these membranes will thus require both scale-up and optimization of membrane casting conditions to achieve the desired pore size and pore size distribution, flux, and physical/mechanical properties based on end-use specifications [1, 41].

7.2.2. Comb copolymer chemistry considerations

One potential drawback of the macromonomer chemistry employed in this thesis is the ester bond linkage of the PEO side chain to the comb polymer backbone through the acrylate co-monomer. This functional group is susceptible to hydrolysis in the presence of acidic or basic media, which can severely limit the applications suitable for these membranes to ones that occur near neutral pH. This was investigated briefly during the course of this thesis, in two different time scales.

One experiment aimed to observe the stability of the fouling resistance of these membranes in a short-term treatment, such as a chemical cleaning or sterilization cycle. In this experiment, a 24-hour fouling cycle with bovine serum albumin (BSA) was performed, as described in section 5.2.7. Then, 0.1 M NaOH solution was filtered through the membrane for 10 minutes. After this period, the cell was rinsed several times and another fouling cycle was performed. The results of this test, in normalized flux versus time, are shown in Figure 7.1. The first fouling cycle for both the PAN/PAN-*g*-PEO blend membrane and the control was in agreement with previous experiments (Figure 5.7). The PAN-*g*-PEO-containing membrane recovered its initial flux completely, while the commercial PAN membrane lost a significant portion of its flux irreversibly. After NaOH treatment, the permeability of the control membrane was increased only very slightly, indicating this aggresive cleaning solution was not very effective in countering the fouling. Furthermore, the flux through this membrane was lost irreversibly to an even greater extent after the second fouling cycle, to about one-tenth of its initial value. These results are in agreement with literature reports that indicate chemical cleanings often change the membrane's surface chemistry, making it more susceptible to further fouling [1].

In contrast, the flux through the PAN/PAN-*g*-PEO blend membrane was unchanged by the NaOH treatment. Furthermore, the membrane retained its complete resistance to irreversible fouling after this treatment, indicating the PEO brush is still intact. Therefore, the PAN/PAN-*g*-PEO system is stable to short-term pH rises.
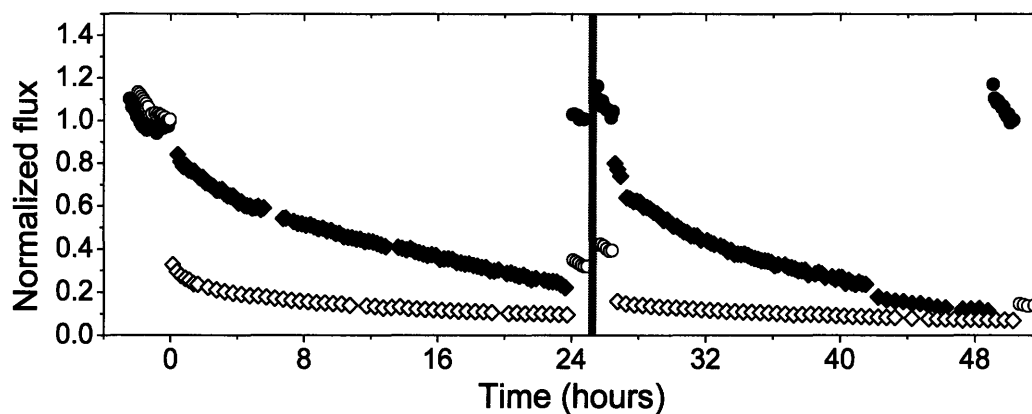
Figure 7.1. Dead-end fouling and simulated "NaOH cleaning" of PAN/PAN-g-PEO blend membrane (filled) and Sepro PAN400 (empty) ●,○: Milli-Q water,◆, ◊: 1 g/L BSA in PBS. The gray line indicates the filtration of 0.1 M NaOH for 30 minutes. Tests performed at 10 psi.

However, the stability of a membrane to a sustained, non-neutral pH is also important. To test this, round pieces of PAN/PAN-g-PEO blend UF membranes 2.5 cm in diameter were cut and stored in Hydrion buffer solutions and PBS for 1 week. Then, a 24-hour BSA fouling cycle was performed, as described in Section 5.2.7. The percentage of initial flux recovered after a backwash for each membrane is shown in Figure 7.2. It can be seen that the membranes are stable when operated between pH 5-8. However, any more acidic or basic systems caused a degradation in fouling resistance in time. This limits the pH range in which these membranes can be used effectively.
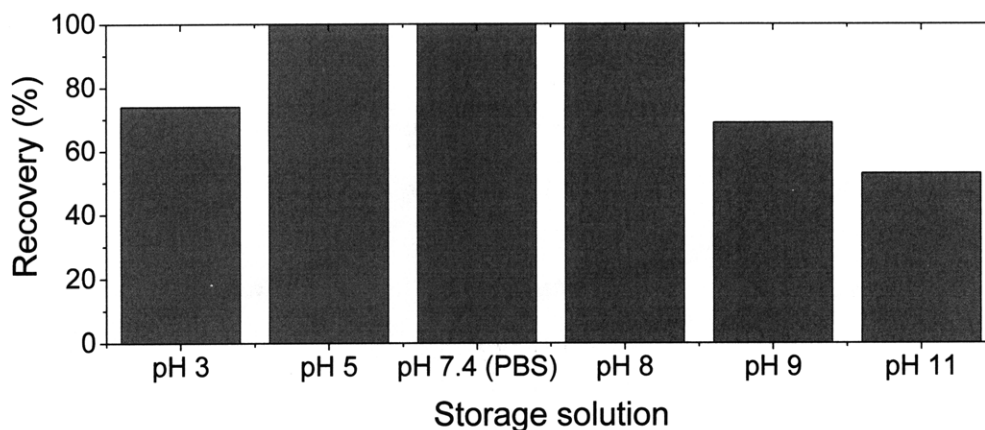
Figure 7.2. Flux recovery of PAN/PAN-g-PEO blend UF membranes stored in buffers of different pH levels, after 24 hour BSA fouling.

The most important way of countering this problem is by designing a PAN-g-PEO comb copolymer with stronger linkages between the side-chains and the backbone. Amide linkages can be stronger than ester groups, yet easy to accomplish by known chemistries. For example, acrylamide and an amine-terminated PEO chain can undergo reaction in the presence of 1-Ethyl-3-[3-dimethylaminopropyl]carbodiimide hydrochloride (EDC or EDAC) to form PEO-terminated with an acrylamide group, which in turn can be copolymerized with acrylonitrile [250]. Similar approaches can be used for other co-monomer chemistries as well.

Finally, side-chain chemistries other than PEO can be considered. Though known as the "gold standard" for protein resistance, PEO brushes have been reported to degrade and lose their resistance to cell attachment when exposed to cells over a time scale measured by days [251, 252]. Having several options of fouling resistant side-chain chemistries may also facilitate the development of membrane systems for a wider range of applications, through the availability of backbone-side-chain linkage chemistries, or sites for further functionalization. Surfaces that strongly resist protein adsorption and cell adhesion, termed "inert" surfaces, have been the focus of much research [229, 251-257]. These studies mainly consider biomaterials applications, but the findings are relevant to the design of membrane materials as well. Research indicates that surfaces that resist

150

protein adsorption share four molecular-level characteristics: They are hydrophilic, they include hydrogen bond acceptors, they do not include hydrogen bond donors, and they are neutral in charge [229, 255]. Some of these chemistries are shown in Figure 7.3.

Poly(N-acroylsarcosine methyl ester)

PEO

R = H, CH$_3$

Mannitol derivatives

Peptidomimetic polymers
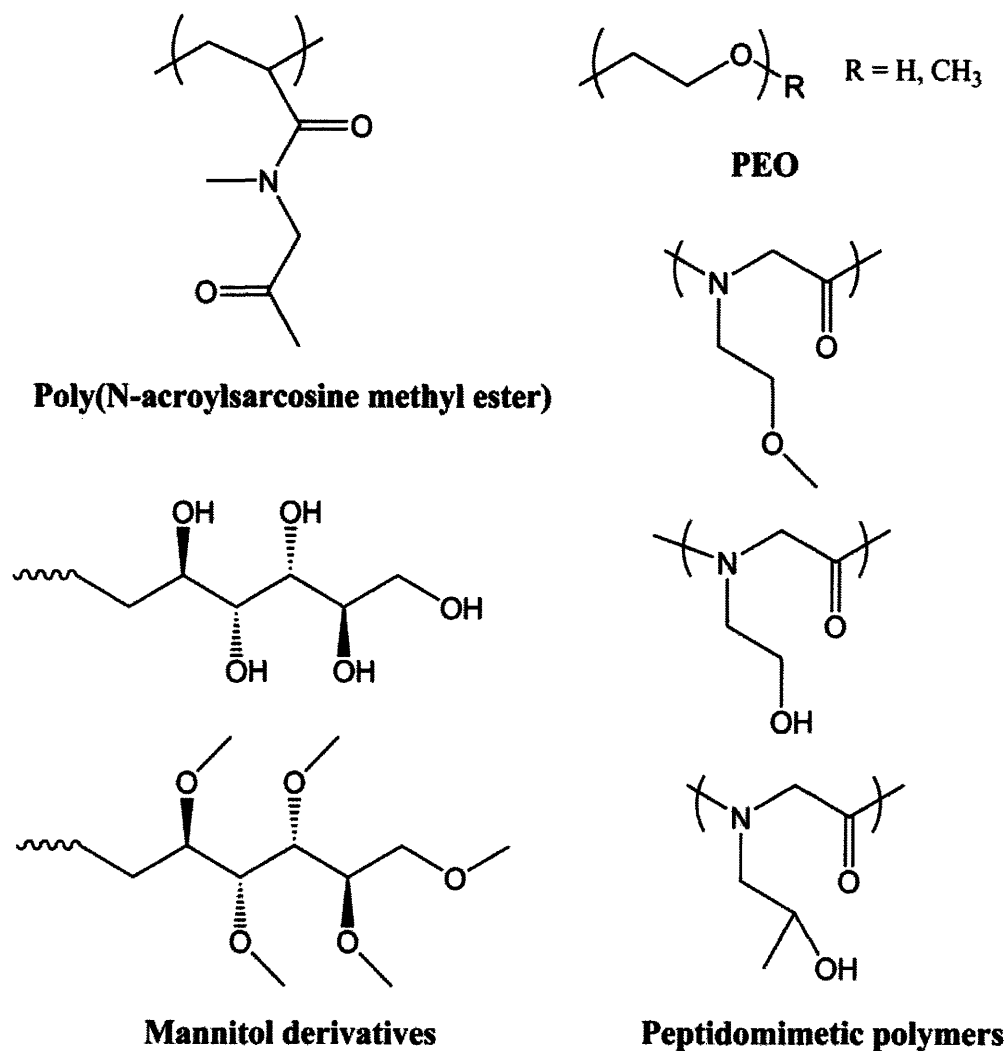
Figure 7.3. Some structures found to create protein resistant surfaces

Whitesides and coworkers reported large surveys of self-assembled monolayers (SAMs) that expose different chemical groups on the surface that obey the above rules [229, 253]. They observed that surfaces that presented derivatives of oligo(sarcosine), N-acetylpiperazine, and permethylated sorbitol groups showed protein resistance close to PEO-modified surfaces. Luk *et al.* have observed that self-assembled monolayers

151

(SAMs) that expose mannitol groups resist the adsorption of proteins and the attachment of cells to a degree comparable to SAMs exposing PEO oligomers [252]. Statz *et al.* obtained similar results with monolayers of some chimeric peptoids – oligomers of peptide structures made of non-natural aminoacids [256, 257]. Each of these chemistries can be considered for membrane applications. Graft copolymers with mannitol groups can be formed by grafting-to reactions using mono-functionalized versions of the chemical. The peptoids are currently prepared by solid-state synthesis, a method too expensive for large-scale application in the membrane industry. However, due to the fact that precise molecular weight and polydispersity control is not necessary for membrane applications, a simpler polymerization method could potentially be designed. Teare *et al.* have reported protein resistant surfaces based on poly(N-acroylsarcosine methyl ester) prepared by pulse plasma deposition [258]. This method might be adapted to form graft copolymers, perhaps by ATRP initiated from the hydrophobic backbone. Having several options for anti-fouling side-chain chemistries would make it possible to design membranes that can be used with a wider variety of feeds.

7.2.3. Functionalized membranes by surface segregation

The surface segregation of the hydrophilic side-chains during the phase inversion casting of porous membranes can also be used to incorporate functionality into the membrane. Functional groups can be attached to the ends of the PEO side-chains [82, 259-261], or incorporated as randomly copolymerized components on the backbone. A potential application involves the selective removal of heavy metal ions from streams that contain many other cations. Metal ions are valuable intermediates in metal extraction, and their recovery from a waste stream could be profitable. Most heavy metal ions are also toxic, and the disposal of waste streams with even low concentrations can be expensive. It would be very desirable to have a membrane system that can remove the heavy metal ions selectively, without interference from cations like Ca^{2+} and Mg^{2+} that are present in much greater concentrations [262, 263]. This could be done by incorporating functional groups that will chelate the metal ions in question on a MF or UF membrane [262-269]. Such membranes could be used to adsorb the metal ions during filtration, and release them during a regeneration step that involves an acidic wash.

Membranes for heavy metal removal are generally created by surface-grafting of chelating polymers from the membrane surface [262-269]. This grafting reaction is initiated by the irradiation of the membrane surface, followed by the immersion of the membrane into a functional monomer like glycidyl methacrylate (GMA) [262, 264-266, 269] or maleic anhydride [267], which is then converted to the chelating group desired. Radiation grafting, however, is an expensive method. The grafting may also be poorly controlled, and heterogeneous across the cross-section of the membrane. The surface segregation of comb copolymers may be an ideal method for the formation of such membranes in a single step, with the chelating groups distributed evenly through the membrane pores. This is facilitated by the fact that most of the chelating groups are hydrophilic. Some possible functional groups that can be considered include iminodiethanol for the recovery of germanium [264], antimony [265, 266, 269] and cadmium [263], amidoxime for uranium [262], and polyaminoacids such as polyaspartic acid and polycysteine for heavy metals such as cadmium, mercury and chromium [263, 268].

Another possible application is membrane chromatography for protein separations. Microporous membranes for chromatography separations have several advantages compared with their packed-bed counterparts: They allow high velocities and very short residence times with low trans-membrane pressures. Diffusional resistance is eliminated, which allows for faster binding kinetics. They also have potential for high binding capacities, and are more easily scalable [270]. One of the most important limitations posed by the membrane systems is the scarcity of functionalizable groups and ligand attachment sites within membrane pores. Another problem is non-specific binding due to the hydrophobicity of the surface [270, 271]. For hydrophobic base materials, radiation-induced grafting is the most common way of introducing ligands to the membrane [270], but such line-of-sight techniques tend to leave the internal surfaces of the membrane unmodified. By contrast, surface segregation leads to coverage of all external and internal membrane surfaces with a PEO brush layer, enabling functionality throughout.

For example, a comb copolymer that includes PEO side-chains that are terminated with OH groups (rather than $-OCH_3$ as in the systems described in this study) can be used to

incorporate resistance to non-specific adsorption while providing –OH groups as functionalization sites. The attachment of ligands to –OH groups can be done by various chemistries, including methods that employ reagents such as carbonyl diimidazole (CDI) [272] or 2-fluoro-1-methyl pyridinium toluene-4-sulphonate (FMP) [270, 273]. The attachment of the ligand to the PEO chain end can also be beneficial, compared to direct surface attachment, as it allows more mobility to the ligand. This can be especially advantageous with small molecule ligands [270, 274].

7.2.4. New comb copolymers for NF membranes

The novel TFC NF membranes investigated in this thesis are based on the microphase separation of amphiphilic comb copolymers having PVDF or PAN backbones. For some applications, backbones of polyethylene (PE) and polypropylene (PP) might also be of considerable interest due to their exceptional heat and chemical resistance. PE copolymerized with monomers containing functional groups like epoxides are available commercially, and can be used in grafting-to reactions to form graft copolymers (Figure 7.4) [275]. Alternatively, chlorinated PE or PP can be used as a macroinitiator to graft side-chains using atom transfer radical polymerization (ATRP) [180, 275]. . Membranes which are stable in a broad range of organic solvents including polar aprotic solvents and display tunable molecular weight cut-off (MWCO) profiles in the molecular weight range 200–1000 g/mol are highly sought in the membrane industry [276-278]. PE and PP backbones are insoluble in most solvents [279], and their comb copolymers may form membranes that can fill in this significant gap, providing a solution for separations in the pharmaceutical, chemical and petrochemical industries [276, 277].

154
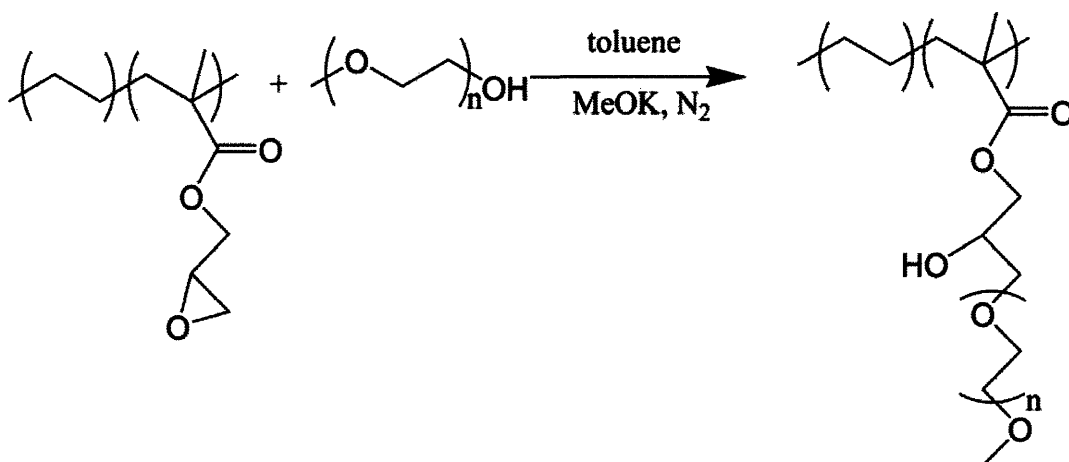
Figure 7.4. Reaction scheme for the synthesis of PE-g-PEO

7.2.5. Charged comb copolymers for desalination

The uncharged graft copolymers employed for size-based NF separations offer very low ion retentions. While this is a desirable quality for the applications described here, there are several applications where the retention of ionic species is necessary. The most significant of these is the desalination of water in reverse osmosis (RO) applications. Water softening, one of the most important applications of NF, also involves the retention of ions such as Ca^{2+} and Mg^{2+}. Therefore, the development of a TFC membrane based on amphiphilic copolymers, where ions are retained together with small molecules while exhibiting high permeability and fouling resistance, is highly desirable.

The separation mechanism of PVDF-*g*-POEM and PAN-*g*-PEO TFC NF membranes is based on sieving abilities of the nanochannels. If charge is incorporated into the nanochannels, however, Donnan exclusion effects can enable the retention of salts. For typical TFC membranes, the amount of charge that needs to be incorporated to exclude ions by the Donnan mechanism is quite high. However, the microphase-separated morphology of amphiphilic copolymers can enhance this effect greatly by concentrating the charges in the hydrophilic phase. The nanochannel geometry will also make the overlap of electrical double-layers easier, enhancing the repulsion of charged species. Hence, amphiphilic comb copolymers incorporating charge would be promising materials in the creation of desalination membranes.

155

The most straight-forward method of achieving this type of structure would be to form a terpolymer that consists of a hydrophobic backbone with two types of side-chains: PEO side-chains for fouling resistance and the formation of nanochannels of desired size, and charged side-chains to achieve Donnan exclusion of ions. As described in Section 7.2.2, inert surfaces need to be of net neutral charge, however. Therefore, having charged groups on the surface of such a membrane may compromise the complete adsorptive fouling resistance. One way of preventing this would be to perform more than one coating step, for example, a first layer of charged polymer coated by a comb copolymer of PEO side-chains. Alternatively, PEO side-chains that are much longer than the charged groups may be able to shield the charges sufficiently. Finally, annealing the membranes in a solution that preferentially exposes PEO in comparison to charged groups may be able to prevent the exposure of charge to foulants on the membrane surface.

Such a structure can be formed by the copolymerization of macromonomers of PEO and the charged polymer, together with the monomer corresponding to the hydrophobic backbone (such as polyacrylonitrile, polystyrene, etc.). A difficulty with this method arises from the fact that terpolymer synthesis is inherently more complicated. Random terpolymerization can be difficult to achieve due to the possibility of unequal monomer reactivities, and it may be more difficult to control the composition of the product.

An alternative is to form a blend of two comb copolymers, one having PEO side-chains and the other with charged side-chains, to create the selective layer of the membrane. As both types of side-chains are hydrophilic, both would segregate into the nanochannels. This method would have the advantage of avoiding issues with monomer reactivity ratios. It would also allow more flexibility in tuning and optimizing the selective layer composition.

One difficulty associated with these methods may be in solubilizing the charged copolymer for the coating step. The hydrophobic backbone polymer and the charged side-chains generally dissolve in different solvents, and finding a solvent that will dissolve both components can be a challenge. It may be necessary to use protected groups that can be converted to charged moieties after casting. For example, side-chains of

poly(t-butyl methacrylate) can be converted to poly(methcarylic acid) groups by the hydrolysis of the ester [7]. Alternatively, side-chains containing amine groups can be converted to querternary amine groups using alkyl halides [280, 281]. Another option is the selection of side-chains that contain aromatic groups, which can in turn be sulfonated [282, 283].

Regardless, these methods hold promise for designing nanostructured, yet easily cast, systems for desalination. The comb copolymer approach allows for many options and opportunities. Proper choice of backbone chemistry can be helpful in designing solvent-resistant membranes, perhaps by incorporating UV cross-linking groups [284]. Side-chain chemistry can enable fouling resistance as well as responsive behavior if desired. Membrane properties can be tuned by changing parameters such as copolymer composition, side-chain length, casting conditions, and feed specifications. In short, this method provides great versatility in designing functional membranes.

Bibliography

[1] R. W. Baker, Membrane technology and applications, J. Wiley, Chichester; New York, 2004

[2] S. P. Nunes and K. V. Peinemann, Membrane technology in the chemical industry, Wiley-VCH, Weinheim; New York, 2001

[3] J. F. Hester, Surface modification of polymer membranes by self-organization, Ph. D. thesis, MIT, Cambridge, MA (2001)

[4] J. F. Hester, P. Banerjee and A. M. Mayes, Preparation of protein-resistant surfaces on poly(vinylidene fluoride) membranes via surface segregation, Macromolecules, 32 (1999) 1643-1650

[5] J. F. Hester, P. Banerjee, Y. Y. Won, A. Akthakul, M. H. Acar and A. M. Mayes, ATRP of amphiphilic graft copolymers based on PVDF and their use as membrane additives, Macromolecules, 35 (2002) 7652-7661

[6] J. F. Hester and A. M. Mayes, Design and performance of foul-resistant poly(vinylidene fluoride) membranes prepared in a single-step by surface segregation, Journal of Membrane Science, 202 (2002) 119-135

[7] J. F. Hester, S. C. Olugebefola and A. M. Mayes, Preparation of pH-responsive polymer membranes by self-organization, Journal of Membrane Science, 208 (2002) 375-388

[8] J. Y. Park, M. H. Acar, A. Akthakul, W. Kuhlman and A. M. Mayes, Polysulfone-graft-poly(ethylene glycol) graft copolymers for surface modification of polysulfone membranes, Biomaterials, 27 (2006) 856-865

[9] J. Y. Park and Massachusetts Institute of Technology. Dept. of Materials Science and Engineering., Synthesis and use of polysulfone-g-poly(ethylene glycol) graft copolymers as modification agents for polysulfone membranes, M.S. thesis, (2003)

[10] A. Akthakul, Design of chemistry and morphology of polymer filtration membranes, Ph.D. thesis, MIT, Cambridge, MA (2003)

[11] A. Akthakul, A. I. Hochbaum, F. Stellacci and A. M. Mayes, Size fractionation of metal nanoparticles by membrane filtration, Advanced Materials, 17 (2005) 532-535

[12] A. Akthakul, R. F. Salinaro and A. M. Mayes, Antifouling polymer membranes with subnanometer size selectivity, Macromolecules, 37 (2004) 7663-7668

[13] A. Asatekin, S. Kang, M. Elimelech and A. M. Mayes, Anti-fouling ultrafiltration membranes containing polyacrylonitrile-graft-poly(ethylene oxide) as an additive, Journal of Membrane Science, 298 (2007) 136-146

[14] A. Asatekin and A. M. Mayes, Oil industry wastewater treatment with fouling resistant membranes containing amphiphilic comb copolymers, Environmental Science & Technology, Submitted

[15] A. Asatekin and A. M. Mayes, Fouling resistant membranes formed with polyacrylonitrile graft copolymers, PCT #60/791,003, filed 04/11/06

[16] S. Kang, A. Asatekin, A. M. Mayes and M. Elimelech, Protein antifouling mechanisms of PAN UF membranes incorporating PAN-g-PEO, Journal of Membrane Science, 296 (2007) 42-50

[17] A. Asatekin, A. Mennitti, S. Kang, M. Elimelech, E. Morgenroth and A. M. Mayes, Antifouling nanofiltration membranes for membrane bioreactors from self-assembling graft copolymers, Journal of Membrane Science, 285 (2006) 81-89

[18] A. Asatekin and A. M. Mayes, Responsive pore size properties of composite NF membranes based on PVDF graft copolymers, Separation Science and Technology, (Submitted)

[19] H. Strathmann, Ullmann's encyclopedia of industrial chemistry, Wiley, New York, http://mrw.interscience.wiley.com.libproxy.mit.edu/emrw/9783527306732/ueic/article/a1 6_187/current/html (2000)

[20] S. Loeb and S. Sourirajan, Sea water demineralization by means of an osmotic membrane, ACS, Washington DC, 1963

[21] J. E. Cadotte, Reverse osmosis membrane, 4,039,440, 1977

[22] Cross-flow market set for solid growth, Membrane Technology, 2006 (2006) 4

[23] Solid growth forecast for filtration membranes, Membrane Technology, 2007 (2007) 3-4

[24] R. van Reis and A. Zydney, Membrane separations in biotechnology, Current Opinion in Biotechnology, 12 (2001) 208-211

[25] A. Vernhet and M. Moutounet, Fouling of organic microfiltration membranes by wine constituents: Importance, relative impact of wine polysaccharides and polyphenols and incidence of membrane properties, Journal of Membrane Science, 201 (2002) 103-122

[26] W. Yuan and A. L. Zydney, Effects of solution environment on humic acid fouling during microfiltration, Desalination, 122 (1999) 63-76

[27] M. Cheryan and N. Rajagopalan, Membrane processing of oily streams. Wastewater treatment and waste reduction, Journal of Membrane Science, 151 (1998) 13-28

[28] M. Kumar, S. S. Adham and W. R. Pearce, Investigation of seawater reverse osmosis fouling and its relationship to pretreatment type, Environmental Science & Technology, 40 (2006) 2037-2044

[29] W. B. Yang, N. Cicek and J. Ilg, State-of-the-art of membrane bioreactors: Worldwide research and commercial applications in North America, Journal of Membrane Science, 270 (2006) 201-211

[30] J. A. Howell, T. C. Arnot and W. Liu, Membrane bioreactors for treating waste streams, Advanced Membrane Technology, 984 (2003) 411-419

[31] M. F. A. Goosen, S. S. Sablani, H. Ai-Hinai, S. Ai-Obeidani, R. Al-Belushi and D. Jackson, Fouling of reverse osmosis and ultrafiltration membranes: A critical review, Separation Science and Technology, 39 (2004) 2261-2297

[32] N. Hilal, O. O. Ogunbiyi, N. J. Miles and R. Nigmatullin, Methods employed for control of fouling in MF and UF membranes: A comprehensive review, Separation Science and Technology, 40 (2005) 1957-2005

[33] N. Scharnagl and H. Buschatz, Polyacrylonitrile (PAN) membranes for ultra- and microfiltration, Desalination, 139 (2001) 191-198

[34] R. J. Petersen, Composite reverse osmosis and nanofiltration membranes, Journal of Membrane Science, 83 (1993) 81-150

[35] N. Hilal, H. Al-Zoubi, N. A. Darwish, A. W. Mohammad and M. Abu Arabi, A comprehensive review of nanofiltration membranes: Treatment, pretreatment, modelling, and atomic force microscopy, Desalination, 170 (2004) 281-308

[36] B. van der Bruggen and C. Vandecasteele, Removal of pollutants from surface water and groundwater by nanofiltration: Overview of possible applications in the drinking water industry, Environmental Pollution, 122 (2003) 435-445

[37] J. H. Choi, S. Dockko, K. Fukushi and K. Yamamoto, A novel application of a submerged nanofiltration membrane bioreactor (NF MBR) for wastewater treatment, Desalination, 146 (2002) 413-420

[38] J. W. Cho, G. Amy, J. Pellegrino and Y. M. Yoon, Characterization of clean and natural organic matter (NOM) fouled NF and UF membranes, and foulants characterization, Desalination, 118 (1998) 101-108

[39] A. I. Schafer, A. G. Fane and T. D. Waite, Nanofiltration of natural organic matter: Removal, fouling and the influence of multivalent ions, Desalination, 118 (1998) 109-122

[40] A. Akthakul, C. E. Scott, A. M. Mayes and A. J. Wagner, Lattice Boltzmann simulation of asymmetric membrane formation by immersion precipitation, Journal of Membrane Science, 249 (2005) 213-226

[41] P. van de Witte, P. J. Dijkstra, J. W. A. van den Berg and J. Feijen, Phase separation processes in polymer solutions in relation to membrane formation, Journal of Membrane Science, 117 (1996) 1-31

[42] L. Yilmaz and A. J. Mchugh, Modeling of asymmetric membrane formation.1. Critique of evaporation models and development of a diffusion equation formalism for the quench period, Journal of Membrane Science, 28 (1986) 287-310

[43] R. M. Boom, I. M. Wienk, T. Vandenboomgaard and C. A. Smolders, Microstructures in phase inversion membranes 2. The role of a polymeric additive, Journal of Membrane Science, 73 (1992) 277-292

[44] C. Stropnik, L. Germic and B. Zerjal, Morphology variety and formation mechanisms of polymeric membranes prepared by wet phase inversion, Journal of Applied Polymer Science, 61 (1996) 1821-1830

[45] M. J. Han and D. Bhattacharyya, Changes in morphology and transport characteristics of polysulfone membranes prepared by different demixing conditions, Journal of Membrane Science, 98 (1995) 191-200

[46] A. Akthakul, W. F. McDonald and A. M. Mayes, Noncircular pores on the surface of asymmetric polymer membranes: Evidence of pore formation via spinodal demixing, Journal of Membrane Science, 208 (2002) 147-155

[47] S. Y. Yang, I. Ryu, H. Y. Kim, J. K. Kim, S. K. Jang and T. P. Russell, Nanoporous membranes with ultrahigh selectivity and flux for the filtration of viruses, Advanced Materials, 18 (2006) 709-712

[48] W. A. Phillip, J. Rzayev, M. A. Hillmyer and E. L. Cussler, Gas and water liquid transport through nanoporous block copolymer membranes, Journal of Membrane Science, 286 (2006) 144-152

[49] M. C. Porter, Handbook of industrial membrane technology, Noyes Publications, Park Ridge, N.J., U.S.A., 1990

[50] I. Pinnau, J. G. Wijmans, I. Blume, T. Kuroda and K. V. Peinemann, Gas permeation through composite membranes, Journal of Membrane Science, 37 (1988) 81-88

[51] K. Scott, Handbook of industrial membranes, Elsevier Advanced Technology, Oxford, 1998

[52] K. Scott and R. Hughes, Industrial membrane separation technology, Blackie Academic & Professional, London, 1996

[53] A. Malek, M. N. A. Hawlader and J. C. Ho, Design and economics of RO seawater desalination, Desalination, 105 (1996) 245-261

[54] S. A. Avlonitis, K. Kouroumbas and N. Vlachakis, Energy consumption and membrane replacement cost for seawater RO desalination plants, Desalination, 157 (2003) 151-158

[55] B. van der Bruggen, J. Q. J. C. Verberk and J. Verhack, Comparison of pressure-driven membrane processes and traditional processes for drinking water production in Europe based on specific impact criteria, Water SA, 30 (2004) 413-419

[56] S. A. Stern and R. D. Noble, Membrane separations technology: Principles and applications, Elsevier, Amsterdam; New York, 1995

[57] P. Mikulasek, Methods to reduce concentration polarization and fouling in membrane filtration, Collection of Czechoslovak Chemical Communications, 59 (1994) 737-755

[58] H. C. Flemming, G. Schaule, T. Griebe, J. Schmitt and A. Tamachkiarowa, Biofouling - the Achilles heel of membrane processes, Desalination, 113 (1997) 215-225

[59] J. S. Baker and L. Y. Dudley, Biofouling in membrane systems - a review, Desalination, 118 (1998) 81-90

[60] I. C. Escobar, E. M. Hoek, C. J. Gabelich, F. A. DiGiano, Y. A. Le Gouellec, P. Berube, K. J. Howe, J. Allen, K. Z. Atasi, M. M. Benjamin, P. J. Brandhuber, J. Brant, Y. J. Chang, M. Chapman, A. Childress, W. J. Conlon, T. H. Cooke, I. A. Crossley, G. F. Crozes, P. M. Huck, S. N. Kommineni, J. G. Jacangelo, A. A. Karimi, J. H. Kim, D. F. Lawler, Q. L. Li, L. C. Schideman, S. Sethi, J. E. Tobiason, T. Tseng, S. Veerapanemi, A. K. Zander and A. M. T. R. Comm, Committee report: Recent advances and research needs in membrane fouling, Journal American Water Works Association, 97 (2005) 79-89

[61] A. D. Marshall, P. A. Munro and G. Tragardh, The effect of protein fouling in microfiltration and ultrafiltration on permeate flux, protein retention and selectivity - a literature-review, Desalination, 91 (1993) 65-108

[62] Y. L. Li and K. L. Tung, The effect of curvature of a spacer-filled channel on fluid flow in spiral-wound membrane modules, Journal of Membrane Science, 319 (2008) 286-297

[63] A. L. Ahmad and K. K. Lau, Impact of different spacer filaments geometries on 2d unsteady hydrodynamics and concentration polarization in spiral wound membrane channel, Journal of Membrane Science, 286 (2006) 77-92

[64] H. Choi, K. Zhang, D. D. Dionysiou, D. B. Oerther and G. A. Sorial, Influence of cross-flow velocity on membrane performance during filtration of biological suspension, Journal of Membrane Science, 248 (2005) 189-199

[65] G. Taylor, J. A. Levesley and M. Hoare, Pilot-scale ultrafiltration of concentrated protein precipitate suspensions - the effect of concentration and fluid-dynamics, Chemical Engineering Communications, 129 (1994) 227-250

[66] M. Manttari, L. Puro, J. Nuortila-Jokinen and M. Nystrom, Fouling effects of polysaccharides and humic acid in nanofiltration, Journal of Membrane Science, 165 (2000) 1-17

[67] G. J. Zhang, S. L. Ji, X. Gao and Z. Z. Liu, Adsorptive fouling of extracellular polymeric substances with polymeric ultrafiltration membranes, Journal of Membrane Science, 309 (2008) 28-35

[68] M. Taniguchi, J. E. Kilduff and G. Belfort, Modes of natural organic matter fouling during ultrafiltration, Environmental Science & Technology, 37 (2003) 1676-1683

[69] I. S. Chang, P. Le Clech, B. Jefferson and S. Judd, Membrane fouling in membrane bioreactors for wastewater treatment, Journal of Environmental Engineering-ASCE, 128 (2002) 1018-1029

[70] P. T. Cardew, M. S. Le and Royal Society of Chemistry (Great Britain) Process Technology Group, Membrane processes: A technology guide, Royal Society of Chemistry, Cambridge, 1998

[71] H. Evenblij and J. H. J. M. van der Graaf, Occurrence of EPS in activated sludge from a membrane bioreactor treating municipal wastewater, Water Science and Technology, 50 (12) (2004) 293-300

[72] M. Ulbricht and G. Belfort, Surface modification of ultrafiltration membranes by low temperature plasma 2. Graft polymerization onto polyacrylonitrile and polysulfone, Journal of Membrane Science, 111 (1996) 193-215

[73] F. Poncin-Epaillard and G. Legeay, Surface engineering of biomaterials with plasma techniques, Journal of Biomaterials Science-Polymer Edition, 14 (2003) 1005-1028

[74] A. Bhattacharya and B. N. Misra, Grafting: A versatile means to modify polymers - techniques, factors and applications, Progress in Polymer Science, 29 (2004) 767-814

[75] B. Gupta, N. Anjum, R. Jain, N. Revagade and H. Singh, Development of membranes by radiation-induced graft polymerization of monomers onto polyethylene films, Journal of Macromolecular Science Part C - Polymer Reviews, C44 (2004) 275-309

[76] P. Wang, K. L. Tan, E. T. Kang and K. G. Neoh, Plasma-induced immobilization of poly(ethylene glycol) onto poly(vinylidene fluoride) microporous membrane, Journal of Membrane Science, 195 (2002) 103-114

[77] F. Q. Nie, Z. K. Xu, Y. Qian, W. Jian and L. S. Wan, Surface modification of poly(acrylonitrile-co-maleic acid) membranes by the immobilization of poly(ethylene glycol), Journal of Membrane Science, 235 (2004) 147-155

164

[78] R. H. Li and T. A. Barbari, Performance of poly(vinyl alcohol) thin-gel composite ultrafiltration membranes, Journal of Membrane Science, 105 (1995) 71-78

[79] H. Ju, B. D. McCloskey, A. C. Sagle, Y. H. Wu, V. A. Kusuma and B. D. Freeman, Crosslinked poly(ethylene oxide) fouling resistant coating materials for oil/water separation, Journal of Membrane Science, 307 (2008) 260-267

[80] Z. G. Wang, L. S. Wan and Z. K. Xu, Surface engineerings of polyacrylonitrile-based asymmetric membranes towards biomedical applications: An overview, Journal of Membrane Science, 304 (2007) 8-23

[81] M. Taniguchi, J. E. Kilduff and G. Belfort, Low fouling synthetic membranes by UV-assisted graft polymerization: Monomer selection to mitigate fouling by natural organic matter, Journal of Membrane Science, 222 (2003) 59-70

[82] D. J. Irvine, A. M. Mayes and L. G. Griffith, Nanoscale clustering of RGD peptides at surfaces using comb polymers. 1. Synthesis and characterization of comb thin films, Biomacromolecules, 2 (2001) 85-94

[83] K. L. Prime and G. M. Whitesides, Adsorption of proteins onto surfaces containing end-attached oligo(ethylene oxide) - a model system using self-assembled monolayers, Journal of the American Chemical Society, 115 (1993) 10714-10721

[84] S. P. Nunes, M. L. Sforca and K. V. Peinemann, Dense hydrophilic composite membranes for ultrafiltration, Journal of Membrane Science, 106 (1995) 49-56

[85] R. H. Li and T. A. Barbari, Characterization and mechanical support of asymmetric hydrogel membranes based on the interfacial cross-linking of poly(vinyl alcohol) with toluene diisocyanate, Journal of Membrane Science, 111 (1996) 115-122

[86] B. Jung, Preparation of hydrophilic polyacrylonitrile blend membranes for ultrafiltration, Journal of Membrane Science, 229 (2004) 129-136

[87] Y. H. Zhao, Y. L. Qian, B. K. Zhu and Y. Y. Xu, Modification of porous poly(vinylidene fluoride) membrane using amphiphilic polymers with different structures in phase inversion process, Journal of Membrane Science, 310 (2008) 567-576

[88] Y. Q. Wang, Y. L. Su, Q. Sun, X. L. Ma and Z. Y. Jiang, Generation of anti-biofouling ultrafiltration membrane surface by blending novel branched amphiphilic polymers with polyethersulfone, Journal of Membrane Science, 286 (2006) 228-236

[89] Y. Q. Wang, T. Wang, Y. L. Su, F. B. Peng, H. Wu and Z. Y. Jiang, Remarkable reduction of irreversible fouling and improvement of the permeation properties of poly(ether sulfone) ultrafiltration membranes by blending with Pluronic F127, Langmuir, 21 (2005) 11856-11862

[90] C. Christy and S. Vermant, The state-of-the-art of filtration in recovery processes for biopharmaceutical production, Desalination, 147 (2002) 1-4

[91] F. T. Awadalla and A. Kumar, Opportunities for membrane technologies in the treatment of mining and mineral process streams and effluents, Separation Science and Technology, 29 (1994) 1231-1249

[92] K. B. Jirage and C. R. Martin, New developments in membrane-based separations, Trends in Biotechnology, 17 (1999) 197-200

[93] T. Burnouf and M. Radosevich, Nanofiltration of plasma-derived biopharmaceutical products, Haemophilia, 9 (2003) 24-37

[94] R. W. Baker, Membrane technology and applications, McGraw-Hill, New York, 2000

[95] K. B. Jirage, J. C. Hulteen and C. R. Martin, Nanotubule-based molecular-filtration membranes, Science, 278 (1997) 655-658

[96] S. F. Yu, S. B. Lee, M. Kang and C. R. Martin, Size-based protein separations in poly(ethylene glycol)-derivatized gold nanotubule membranes, Nano Letters, 1 (2001) 495-498

[97] K. F. Czaplewski, J. T. Hupp and R. Q. Snurr, Molecular squares as molecular sieves: Size-selective transport through porous-membrane-supported thin-film materials, Advanced Materials, 13 (2001) 1895-1897

[98] D. L. Gin, J. E. Bara, R. D. Noble and B. J. Elliott, Polymerized lyotropic liquid crystal assemblies for membrane applications, Macromolecular Rapid Communications, 29 (2008) 367-389

[99] M. H. Keefe, J. L. O'Donnell, R. C. Bailey, S. T. Nguyen and J. T. Hupp, Permeable, microporous polymeric membrane materials constructed from discrete molecular squares, Advanced Materials, 15 (2003) 1936-1939

[100] D. L. Gin, W. Q. Gu, B. A. Pindzola and W. J. Zhou, Polymerized lyotropic liquid crystal assemblies for materials applications, Accounts of Chemical Research, 34 (2001) 973-980

[101] M. Zhou, T. J. Kidd, R. D. Noble and D. L. Gin, Supported lyotropic liquid-crystal polymer membranes: Promising materials for molecular-size-selective aqueous nanofiltration, Advanced Materials, 17 (2005) 1850-1853

[102] K. V. Peinemann, V. Abetz and P. F. W. Simon, Asymmetric superstructure formed in a block copolymer via phase separation, Nature Materials, 6 (2007) 992-996

[103] S. Y. Yang, J. Park, J. Yoon, M. Ree, S. K. Jang and J. K. Kim, Virus filtration membranes prepared from nanoporous block copolymers with good dimensional stability under high pressures and excellent solvent resistance, Advanced Functional Materials, 18 (2008) 1371-1377

[104] T. Miyata, S. Obata and T. Uragami, Annealing effect of microphase-separated membranes containing poly(dimethylsiloxane) on their permselectivity for aqueous ethanol solutions, Macromolecules, 32 (1999) 8465-8475

[105] T. Miyata, S. Obata and T. Uragami, Morphological effects of microphase separation on the permselectivity for aqueous ethanol solutions of block and graft copolymer membranes containing poly(dimethylsiloxane), Macromolecules, 32 (1999) 3712-3720

[106] J. Y. Han, J. P. Fu and R. B. Schoch, Molecular sieving using nanofilters: Past, present and future, Lab on a Chip, 8 (2008) 23-33

[107] A. Kalbasi and L. Cisneros-Zevallos, Fractionation of monomeric and polymeric anthocyanins from concord grape (*vitis labrusca l.*) juice by membrane ultrafiltration, Journal of Agricultural and Food Chemistry, 55 (2007) 7036-7042

[108] A. Kumar, A. Srivastava, I. Y. Galaev and B. Mattiasson, Smart polymers: Physical forms and bioengineering applications, Progress in Polymer Science, 32 (2007) 1205-1237

[109] M. Ulbricht, Advanced functional polymer membranes, Polymer, 47 (2006) 2217-2262

[110] D. Lee, A. J. Nolte, A. L. Kunz, M. F. Rubner and R. E. Cohen, pH-induced hysteretic gating of track-etched polycarbonate membranes: Swelling/deswelling

behavior of polyelectrolyte multilayers in confined geometry, Journal of the American Chemical Society, 128 (2006) 8521-8529

[111] C. Geismann and M. Ulbricht, Photoreactive functionalization of poly(ethylene terephthalate) track-etched pore surfaces with "smart" polymer systems, Macromolecular Chemistry and Physics, 206 (2005) 268-281

[112] Y. Ito, M. Inaba, D. J. Chung and Y. Imanishi, Control of water permeation by pH and ionic-strength through a porous membrane having poly(carboxylic acid) surface-grafted, Macromolecules, 25 (1992) 7313-7316

[113] C. Geismann, A. Yaroshchuk and M. Ulbricht, Permeability and electrokinetic characterization of poly(ethylene terephthalate) capillary pore membranes with grafted temperature-responsive polymers, Langmuir, 23 (2007) 76-83

[114] A. Nykanen, M. Nuopponen, A. Laukkanen, S. P. Hirvonen, M. Rytela, O. Turunen, H. Tenhu, R. Mezzenga, O. Ikkala and J. Ruokolainen, Phase behavior and temperature-responsive molecular filters based on self-assembly of polystyrene-block-poly(n-isopropylacrylamide)-block-polystyrene, Macromolecules, 40 (2007) 5827-5834

[115] Y. S. Park, Y. Ito and Y. Imanishi, Permeation control through porous membranes immobilized with thermosensitive polymer, Langmuir, 14 (1998) 910-914

[116] G. V. R. Rao, M. E. Krug, S. Balamurugan, H. F. Xu, Q. Xu and G. P. Lopez, Synthesis and characterization of silica-poly(n-isopropylacrylamide) hybrid membranes: Switchable molecular filters, Chemistry of Materials, 14 (2002) 5075-5080

[117] V. Smuleac, D. A. Butterfield and D. Bhattacharyya, Permeability and separation characteristics of polypeptide-functionalized polycarbonate track-etched membranes, Chemistry of Materials, 16 (2004) 2762-2771

[118] L. Liang, X. D. Feng, L. Peurrung and V. Viswanathan, Temperature-sensitive membranes prepared by UV photopolymerization of n-isopropylacrylamide on a surface of porous hydrophilic polypropylene membranes, Journal of Membrane Science, 162 (1999) 235-246

[119] D. J. Chung, Y. Ito and Y. Imanishi, Preparation of porous membranes grafted with poly(spiropyran-containing methacrylate) and photocontrol of permeability, Journal of Applied Polymer Science, 51 (1994) 2027-2033

[120] Y. Ito, T. Ito, H. Takaba and S. Nakao, Development of gating membranes that are sensitive to the concentration of ethanol, Journal of Membrane Science, 261 (2005) 145-151

[121] Q. Fu, G. V. R. Rao, T. L. Ward, Y. F. Lu and G. P. Lopez, Thermoresponsive transport through ordered mesoporous silica/PNIPAAM copolymer membranes and microspheres, Langmuir, 23 (2007) 170-174

[122] D. W. Chung, S. Higuchi, M. Maeda and S. Inoue, pH-induced regulation of permselectivity of sugars by polymer membrane from polyvinyl-polypeptide graft copolymer, Journal of the American Chemical Society, 108 (1986) 5823-5826

[123] S. Higuchi, T. Mozawa, M. Maeda and S. Inoue, pH-induced regulation of the permeability of a polymer membrane with a transmembrane pathway prepared from a synthetic polypeptide, Macromolecules, 19 (1986) 2263-2267

[124] M. Maeda, M. Kimura, Y. Hareyama and S. Inoue, pH-dependent ion-transport across polymer membrane - pH-induced reversible conformational change of transmembrane poly(l-aspartic acid) domain in polymer membrane, Journal of the American Chemical Society, 106 (1984) 250-251

[125] M. Maeda, M. Aoyama and S. Inoue, Divalent cation-induced permeability regulation of polymer membrane with permeating pathway of a synthetic polypeptide, Makromolekulare Chemie-Macromolecular Chemistry and Physics, 187 (1986) 2137-2144

[126] S. Bekiranov, R. Bruinsma and P. Pincus, Solution behavior of polyethylene oxide in water as a function of temperature and pressure, Physical Review E, 55 (1997) 577-585

[127] B. Briscoe, P. Luckham and S. Zhu, Rheological study of poly(ethylene oxide) in aqueous salt solutions at high temperature and pressure, Macromolecules, 29 (1996) 6208-6211

[128] B. Briscoe, P. Luckham and S. Zhu, Rheological properties of poly(ethylene oxide) aqueous solutions, Journal of Applied Polymer Science, 70 (1998) 419-429

[129] B. Briscoe, P. Luckham and S. Zhu, On the effects of water solvency towards non-ionic polymers, Proceedings of the Royal Society of London Series a-Mathematical Physical and Engineering Sciences, 455 (1999) 737-756

[130] R. L. Cook, H. E. King and D. G. Peiffer, Pressure-induced crossover from good to poor solvent behavior for polyethylene oxide in water, Physical Review Letters, 69 (1992) 3072-3075

[131] E. E. Dormidontova, Role of competitive PEO-water and water-water hydrogen bonding in aqueous solution PEO behavior, Macromolecules, 35 (2002) 987-1001

[132] E. E. Dormidontova, Influence of end groups on phase behavior and properties of PEO in aqueous solutions, Macromolecules, 37 (2004) 7747-7761

[133] P. Gonzaleztello, F. Camacho and G. Blazquez, Density and viscosity of concentrated aqueous-solutions of polyethylene-glycol, Journal of Chemical and Engineering Data, 39 (1994) 611-614

[134] P. Gregory and M. B. Huglin, Viscosity of aqueous and alkaline-solutions of poly(ethylene oxide), Makromolekulare Chemie-Macromolecular Chemistry and Physics, 187 (1986) 1745-1755

[135] B. Hammouda and D. L. Ho, Insight into chain dimensions in PEO/water solutions, Journal of Polymer Science Part B-Polymer Physics, 45 (2007) 2196-2200

[136] D. L. Ho, B. Hammouda, S. R. Kline and W. R. Chen, Unusual phase behavior in mixtures of poly(ethylene oxide) and ethyl alcohol, Journal of Polymer Science Part B-Polymer Physics, 44 (2006) 557-564

[137] R. Kjellander and E. Florin, Water-structure and changes in thermal-stability of the system poly(ethylene oxide)-water, Journal of the Chemical Society-Faraday Transactions I, 77 (1981) 2053-2078

[138] A. Matsuyama and F. Tanaka, Theory of solvation-induced reentrant phase-separation in polymer-solutions, Physical Review Letters, 65 (1990) 341-344

[139] S. Saeki, N. Kuwahara, M. Nakata and M. Kaneko, Upper and lower critical solution temperatures in poly (ethyleneglycol) solutions, Polymer, 17 (1976) 685-689

[140] S. Saeki, N. Kuwahara, M. Nakata and M. Kaneko, Phase separation of poly(ethylene glycol) water salt systems, Polymer, 18 (1977) 1027-1031

[141] G. D. Smith and D. Bedrov, Roles of enthalpy, entropy, and hydrogen bonding in the lower critical solution temperature behavior of poly(ethylene oxide)/water solutions, Journal of Physical Chemistry B, 107 (2003) 3095-3097

[142] J. H. Choi, K. Fukushi and K. Yamamoto, Comparison of treatment efficiency of submerged nanofiltration membrane bioreactors using cellulose triacetate and polyamide membrane, Water Science and Technology, 51 (6-7) (2005) 305-312

[143] T. Wintgens, M. Gallenkemper and T. Melin, Endocrine disrupter removal from wastewater using membrane bioreactor and nanofiltration technology, Desalination, 146 (2002) 387-391

[144] T. F. Speth, A. M. Gusses and R. S. Summers, Evaluation of nanofiltration pretreatments for flux control, Desalination, 130 (2000) 31-44

[145] P. H. Hodgson, G. L. Leslie, R. P. Schneider, A. G. Fane, C. J. D. Fell and K. C. Marshall, Cake resistance and solute rejection in bacterial microfiltration - the role of the extracellular-matrix, Journal of Membrane Science, 79 (1993) 35-53

[146] S. Rosenberger, H. Evenblij, S. T. Poele, T. Wintgens and C. Laabs, The importance of liquid phase analyses to understand fouling in membrane assisted activated sludge processes - six case studies of different European research groups, Journal of Membrane Science, 263 (2005) 113-126

[147] N. Park, B. Kwon, I. S. Kim and J. W. Cho, Biofouling potential of various NF membranes with respect to bacteria and their soluble microbial products (SMP): Characterizations, flux decline, and transport parameters, Journal of Membrane Science, 258 (2005) 43-54

[148] G. P. Sheng and H. Q. Yu, Characterization of extracellular polymeric substances of aerobic and anaerobic sludge using three-dimensional excitation and emission matrix fluorescence spectroscopy, Water Research, 40 (2006) 1233-1239

[149] B. Jin, B. M. Wilen and P. Lant, Impacts of morphological, physical and chemical properties of sludge flocs on dewaterability of activated sludge, Chemical Engineering Journal, 98 (2004) 115-126

[150] B. Frolund, R. Palmgren, K. Keiding and P. H. Nielsen, Extraction of extracellular polymers from activated sludge using a cation exchange resin, Water Research, 30 (1996) 1749-1758

[151] M. Wahlgren and T. Arnebrant, Protein adsorption to solid surfaces, Trends in Biotechnology, 9 (1991) 201-208

[152] B. C. Robertson and A. L. Zydney, Protein adsorption in asymmetric ultrafiltration membranes with highly constricted pores, Journal of Colloid and Interface Science, 134 (1990) 563-575

[153] C. Jarusutthirak, G. Amy and J. P. Croue, Fouling characteristics of wastewater effluent organic matter (EfOM) isolates on NF and UF membranes, Desalination, 145 (2002) 247-255

[154] M. D. Afonso and R. Borquez, Nanofiltration of wastewaters from the fish meal industry, Desalination, 151 (2003) 131-138

[155] J. F. Lapointe, S. F. Gauthier, Y. Pouliot and C. Bouchard, Fouling of a nanofiltration membrane by a beta-lactoglobulin tryptic hydrolysate: Impact on the membrane sieving and electrostatic properties, Journal of Membrane Science, 253 (2005) 89-102

[156] J. M. K. Timmer, J. Kromkamp and T. Robbertsen, Lactic-acid separation from fermentation broths by reverse-osmosis and nanofiltration, Journal of Membrane Science, 92 (1994) 185-197

[157] P. Czekaj, F. Lopez and C. Guell, Membrane fouling by turbidity constituents of beer and wine: Characterization and prevention by means of infrasonic pulsing, Journal of Food Engineering, 49 (2001) 25-36

[158] M. Nystrom, L. Kaipia and S. Luque, Fouling and retention of nanofiltration membranes, Journal of Membrane Science, 98 (1995) 249-262

[159] Y. Ye, P. Le Clech, V. Chen, A. G. Fane and B. Jefferson, Fouling mechanisms of alginate solutions as model extracellular polymeric substances, Desalination, 175 (2005) 7-20

[160] A. R. Costa and M. N. de Pinho, Effect of membrane pore size and solution chemistry on the ultrafiltration of humic substances solutions, Journal of Membrane Science, 255 (2005) 49-56

[161] Y. Kaiya, Y. Itoh, S. Takizawa, K. Fujita and T. Tagawa, Analysis of organic matter causing membrane fouling in drinking water treatment, Water Science & Technology, 41 (10-11) (2000) 59-67

[162] J. A. Nilson and F. A. DiGiano, Influence of NOM composition on nanofiltration, Journal American Water Works Association, 88 (1996) 53-66

[163] J. W. Cho, G. Amy and J. Pellegrino, Membrane filtration of natural organic matter: Comparison of flux decline, nom rejection, and foulants during filtration with three UF membranes, Desalination, 127 (2000) 283-298

[164] M. Nystrom, K. Ruohomaki and L. Kaipia, Humic acid as a fouling agent in filtration, Desalination, 106 (1996) 79-87

[165] S. H. Yoon, C. H. Lee, K. J. Kim and A. G. Fane, Effect of calcium ion on the fouling of nanofilter by humic acid in drinking water production, Water Research, 32 (1998) 2180-2186

[166] Q. L. Li and M. Elimelech, Organic fouling and chemical cleaning of nanofiltration membranes: Measurements and mechanisms, Environmental Science & Technology, 38 (2004) 4683-4693

[167] A. R. Costa, M. N. De Pinho and M. Elimelech, Mechanisms of colloidal natural organic matter fouling in ultrafiltration, Journal of Membrane Science, 281 (2006) 716-725

[168] G. J. Wilson, A. Pruden, M. T. Suidan and A. D. Venosa, Biodegradation kinetics of MTBE in laboratory batch and continuous flow reactors, Journal of Environmental Engineering-Asce, 128 (2002) 824-829

[169] F. A. Holland and F. S. Chapman, Liquid mixing and processing in stirred tanks, Reinhold Pub. Corp., New York, 1966

[170] APHA, WEF and AWWA, Standard methods for the examination of water and wastewater, 20th edition, American Public Health Association, Washington, D.C., 1998

[171] E. D. Rhine, G. K. Sims, R. L. Mulvaney and E. J. Pratt, Improving the Berthelot reaction for determining ammonium in soil extracts and water, Soil Science Society of America Journal, 62 (1998) 473-480

[172] S. Inceoglu, S. C. Olugebefola, M. H. Acar and A. M. Mayes, Atom transfer radical polymerization using poly(vinylidene fluoride) as macroinitiator, Designed Monomers and Polymers, 7 (2004) 181-189

[173] W. S. Ang, S. Y. Lee and M. Elimelech, Chemical and physical aspects of cleaning of organic-fouled reverse osmosis membranes, Journal of Membrane Science, 272 (2006) 198-210

[174] S. Lee and M. Elimelech, Relating organic fouling of reverse osmosis membranes to intermolecular adhesion forces, Environmental Science & Technology, 40 (2006) 980-987

[175] P. C. Hiemenz and R. Rajagopalan, Principles of colloid and surface chemistry, Marcel Dekker, New York, 1997

[176] A. Seidel and M. Elimelech, Coupling between chemical and physical interactions in natural organic matter (NOM) fouling of nanofiltration membranes: Implications for fouling control, Journal of Membrane Science, 203 (2002) 245-255

[177] A. L. Menniti and E. Morgenroth, Linking floc structure to membrane fouling in membrane bioreactors, Abstracts of Papers of the American Chemical Society, 229 (2005) U633-U633

[178] H. Cheze-Lange, D. Beunard, P. Dhulster, D. Guillochon, A. M. Caze, M. Morcellet, N. Saude and G. A. Junter, Production of microbial alginate in a membrane bioreactor, Enzyme and Microbial Technology, 30 (2002) 656-661

[179] M. L. Ferrer, R. Duchowicz, B. Carrasco, J. G. de la Torre and A. U. Acuna, The conformation of serum albumin in solution: A combined phosphorescence depolarization-hydrodynamic modeling study, Biophysical Journal, 80 (2001) 2422-2430

[180] K. Matyjaszewski and J. H. Xia, Atom transfer radical polymerization, Chemical Reviews, 101 (2001) 2921-2990

[181] K. Matyjaszewski, T. Pintauer and S. Gaynor, Removal of copper-based catalyst in atom transfer radical polymerization using ion exchange resins, Macromolecules, 33 (2000) 1476-1478

[182] Y. Q. Shen, H. D. Tang and S. J. Ding, Catalyst separation in atom transfer radical polymerization, Progress in Polymer Science, 29 (2004) 1053-1078

[183] G. G. Odian, Principles of polymerization, Wiley-Interscience, Hoboken, N.J., 2004

[184] B. E. Read, Mechanical relaxation in some oxide polymers, Polymer, 3 (1962) 529-542

[185] A. S. Kenyon and M. J. Rayford, Mechanical relaxation processes in polyacrylonitrile polymers and copolymers, Journal of Applied Polymer Science, 23 (1979) 717-725

[186] B. van der Bruggen, B. Daems, D. Wilms and C. vandecasteele, Mechanisms of retention and flux decline for the nanofiltration of dye baths from the textile industry, Separation and Purification Technology, 22-23 (2001) 519-528

[187] W. Eykamp, Microfiltration and ultrafiltration, in *Membrane separation technology: Principles and applications,* R. D. Noble and S. A. Stern (eds), Elsevier Science, Amsterdam (1995)

[188] L. F. Hancock, Phase inversion membranes with an organized surface structure from mixtures of polysulfone and polysulfone poly(ethylene oxide) block copolymers, Journal of Applied Polymer Science, 66 (1997) 1353-1358

[189] L. F. Hancock, S. M. Fagan and M. S. Ziolo, Hydrophilic, semipermeable membranes fabricated with poly(ethylene oxide)-polysulfone block copolymer, Biomaterials, 21 (2000) 725-733

[190] N. A. Rahman, T. Sotani and H. Matsuyama, Effect of the addition of the surfactant tetronic 1307 on poly(ether sulfone) porous hollow-fiber membrane formation, Journal of Applied Polymer Science, 108 (2008) 3411-3418

[191] C. L. Lv, Y. L. Su, Y. Q. Wang, X. L. Ma, Q. Sun and Z. Y. Jiang, Enhanced permeation performance of cellulose acetate ultrafiltration membrane by incorporation of Pluronic F127, Journal of Membrane Science, 294 (2007) 68-74

[192] J. Y. Wang, Y. Y. Xu, L. P. Zhu, J. H. Li and B. K. Zhu, Amphiphilic ABA copolymers used for surface modification of polysulfone membranes, part 1: Molecular design, synthesis, and characterization, Polymer, 49 (2008) 3256-3264

[193] D. Rana, T. Matsuura and R. M. Narbaitz, Novel hydrophilic surface modifying macromolecules for polymeric membranes: Polyurethane ends capped by hydroxy group, Journal of Membrane Science, 282 (2006) 205-216

[194] L. S. Wan, Z. K. Xu and X. J. Huang, Asymmetric membranes fabricated from poly(acrylonitrile-co-n-vinyl-2-pyrrolidone)s with excellent biocompatibility, Journal of Applied Polymer Science, 102 (2006) 4577-4583

[195] M. Khayet, C. Y. Feng and T. Matsuura, Morphological study of fluorinated asymmetric polyetherimide ultrafiltration membranes by surface modifying macromolecules, Journal of Membrane Science, 213 (2003) 159-180

[196] D. G. Walton and A. M. Mayes, Entropically driven segregation in blends of branched and linear polymers, Physical Review E, 54 (1996) 2811-2815

[197] D. G. Walton, P. P. Soo, A. M. Mayes, S. J. S. Allgor, J. T. Fujii, L. G. Griffith, J. F. Ankner, H. Kaiser, J. Johansson, G. D. Smith, J. G. Barker and S. K. Satija, Creation of stable poly(ethylene oxide) surfaces on poly(methyl methacrylate) using blends of branched and linear polymers, Macromolecules, 30 (1997) 6947-6956

[198] Y. Chen, L. Ying, W. Yu, E. T. Kang and K. G. Neoh, Poly(vinylidene fluoride) with grafted poly(ethylene glycol) side chains via the RAFT-mediated process and pore size control of the copolymer membranes, Macromolecules, 36 (2003) 9451-9457

[199] Q. Peng, S. Q. Lu, D. Z. Chen, X. Q. Wu, P. F. Fan, R. Zhong and Y. W. Xu, Poly(vinylidene fluoride)-graft-poly (n-vinyl-2-pyrrolidone) copolymers prepared via a RAFT-mediated process and their use in antifouling and antibacterial membranes, Macromolecular Bioscience, 7 (2007) 1149-1159

[200] Q. Shi, Y. L. Su, S. P. Zhu, C. Li, Y. Y. Zhao and Z. Y. Jiang, A facile method for synthesis of PEGylated polyethersulfone and its application in fabrication of antifouling ultrafiltration membrane, Journal of Membrane Science, 303 (2007) 204-212

[201] X. L. Ma, Y. L. Su, Q. Sun, Y. Q. Wang and Z. Y. Jiang, Preparation of protein-adsorption-resistant polyethersulfone ultrafiltration membranes through surface segregation of amphiphilic comb copolymer, Journal of Membrane Science, 292 (2007) 116-124

[202] L. P. Zhu, Z. Yi, F. Liu, X. Z. Wei, B. K. Zhu and Y. Y. Xu, Amphiphilic graft copolymers based on ultrahigh molecular weight poly(styrene-alt-maleic anhydride) with poly(ethylene glycol) side chains for surface modification of polyethersulfone membranes, European Polymer Journal, 44 (2008) 1907-1914

[203] M. A. Rixman, D. Dean and C. Ortiz, Nanoscale intermolecular interactions between human serum albumin and low grafting density surfaces of poly(ethylene oxide), Langmuir, 19 (2003) 9357-9372

[204] Y. L. Su, C. Li, W. Zhao, Q. Shi, H. J. Wang, Z. Y. Jiang and S. P. Zhu, Modification of polyethersulfone ultrafiltration membranes with phosphorylcholine copolymer can remarkably improve the antifouling and permeation properties, Journal of Membrane Science, 322 (2008) 171-177

[205] S. H. Ye, J. Watanabe and K. Ishihara, Cellulose acetate hollow fiber membranes blended with phospholipid polymer and their performance for hemopurification, Journal of Biomaterials Science-Polymer Edition, 15 (2004) 981-1001

[206] X. J. Huang, Z. K. Xu, L. S. Wan, Z. G. Wang and J. L. Wang, Novel acrylonitrile-based copolymers containing phospholipid moieties: Synthesis and characterization, Macromolecular Bioscience, 5 (2005) 322-330

[207] J. Y. Wang, Y. Y. Xu, H. Xu, F. Zhang, Y. L. Qian and B. K. Zhu, Synthesis of an amphiphilic glucose-carrying graft copolymer and its use for membrane surface modification, Journal of Applied Polymer Science, 109 (2008) 2914-2923

[208] G. Beamson and D. Briggs, High resolution XPS of organic polymers: The scienta esca300 database, Wiley, Chichester [England]; New York, 1992

[209] T. L. Barr and S. Seal, Nature of the use of adventitious carbon as a binding-energy standard, Journal of Vacuum Science & Technology A-Vacuum Surfaces and Films, 13 (1995) 1239-1246

[210] S. T. Kang, A. Subramani, E. M. V. Hoek, M. A. Deshusses and M. R. Matsumoto, Direct observation of biofouling in cross-flow microfiltration: Mechanisms of deposition and release, Journal of Membrane Science, 244 (2004) 151-165

[211] K. Kato, E. Uchida, E. T. Kang, Y. Uyama and Y. Ikada, Polymer surface with graft chains, Progress in Polymer Science, 28 (2003) 209-259

[212] W. Zhang, M. Wahlgren and B. Sivik, Membrane characterization by the contact-angle technique 2. Characterization of UF-membranes and comparison between the captive bubble and sessile drop as methods to obtain water contact angles, Desalination, 72 (1989) 263-273

[213] M. Ulbricht, H. Matuschewski, A. Oechel and H. G. Hicke, Photo-induced graft polymerization surface modifications for the preparation of hydrophilic and low-protein-adsorbing ultrafiltration membranes, Journal of Membrane Science, 115 (1996) 31-47

[214] M. Ulbricht and A. Oechel, Photo-bromination and photo-induced graft polymerization as a two-step approach for surface modification of polyacrylonitrile ultrafiltration membranes, European Polymer Journal, 32 (1996) 1045-1054

[215] F. Q. Nie, Z. K. Xu, X. J. Huang, P. Ye and J. Wu, Acrylonitrile-based copolymer membranes containing reactive groups: Surface modification by the immobilization of

poly(ethylene glycol) for improving antifouling property and biocompatibility, Langmuir, 19 (2003) 9889-9895

[216] A. Roosjen, J. de Vries, H. C. van der Mei, W. Norde and H. J. Busscher, Stability and effectiveness against bacterial adhesion of poly(ethylene oxide) coatings in biological fluids, Journal of Biomedical Materials Research Part B-Applied Biomaterials, 73B (2005) 347-354

[217] X. W. Fan, L. J. Lin and P. B. Messersmith, Cell fouling resistance of polymer brushes grafted from Ti substrates by surface-initiated polymerization: Effect of ethylene glycol side chain length, Biomacromolecules, 7 (2006) 2443-2448

[218] A. Roosjen, H. J. Kaper, H. C. van der Mei, W. Norde and H. J. Busscher, Inhibition of adhesion of yeasts and bacteria by poly(ethylene oxide)-brushes on glass in a parallel plate flow chamber, Microbiology-Sgm, 149 (2003) 3239-3246

[219] S. Belfer, A. Bottino and G. Capannelli, Preparation and characterization of layered membranes constructed by sequential redox-initiated grafting onto polyacrylonitrile ultrafiltration membranes, Journal of Applied Polymer Science, 98 (2005) 509-520

[220] H. Miyama, H. Yoshida, Y. Nosaka and H. Tanzawa, Negatively charged polyacrylonitrile graft copolymer membrane for permeation and separation of plasma-proteins, Makromolekulare Chemie-Rapid Communications, 9 (1988) 57-61

[221] K. J. Kim, A. G. Fane and C. J. D. Fell, The performance of ultrafiltration membranes pretreated by polymers, Desalination, 70 (1988) 229-249

[222] W. Yuan and A. L. Zydney, Humic acid fouling during ultrafiltration, Environmental Science & Technology, 34 (2000) 5043-5050

[223] C. S. Hsu, S. H. Chen, R. M. Liou, M. Y. Hung and K. C. Yu, The effect of metal ions on humic acid removal and permeation properties in an ultrafiltration system, Journal of Environmental Science and Health Part A-Toxic/Hazardous Substances & Environmental Engineering, 38 (2003) 415-428

[224] I. H. Huisman, P. Pradanos and A. Hernandez, The effect of protein-protein and protein-membrane interactions on membrane fouling in ultrafiltration, Journal of Membrane Science, 179 (2000) 79-90

[225] E. M. Tracey and R. H. Davis, Protein fouling of track-etched polycarbonate microfiltration membrane, Journal of Colloid and Interface Science, 167 (1994) 104-116

[226] S. P. Palecek and A. L. Zydney, Intermolecular electrostatic interactions and their effect on flux and protein deposition during protein filtration, Biotechnology Progress, 10 (1994) 207-213

[227] Y. G. Park, Effect of an electric field during purification of protein using microfiltration, Desalination, 191 (2006) 404-410

[228] X. F. Wang, D. F. Fang, K. Yoon, B. S. Hsiao and B. Chu, High performance ultrafiltration composite membranes based on poly(vinyl alcohol) hydrogel coating on crosslinked nanofibrous poly(vinyl alcohol) scaffold, Journal of Membrane Science, 278 (2006) 261-268

[229] E. Ostuni, R. G. Chapman, R. E. Holmlin, S. Takayama and G. M. Whitesides, A survey of structure-property relationships of surfaces that resist the adsorption of protein, Langmuir, 17 (2001) 5605-5620

[230] Y. Masuda and T. Nakanishi, Ion-specific swelling behavior of poly(ethylene oxide) gel and the correlation to the intrinsic viscosity of the polymer in salt solutions, Colloid and Polymer Science, 280 (2002) 547-553

[231] A. Zaidi, K. Simms and S. Kok, The use of micro/ultrafiltration for the removal of oil and suspended solids from oilfield brines, Water Science & Technology, 25(10) (1992) 163-176

[232] L. G. Faksness, P. G. Grini and P. S. Daling, Partitioning of semi-soluble organic compounds between the water phase and oil droplets in produced water, Marine Pollution Bulletin, 48 (2004) 731-742

[233] B. A. Farnand and T. A. Krug, Oil removal from oilfield-produced water by cross flow ultrafiltration, Journal of Canadian Petroleum Technology, 28 (1989) 18-24

[234] C. A. Dyke and C. R. Bartels, Removal of organics from offshore produced waters using nanofiltration membrane technology, Environmental Progress, 9 (1990) 183-186

[235] T. Bilstad and E. Espedal, Membrane separation of produced water, Water Science & Technology, 34 (1996) 239-246

[236] F. T. Tao, S. Curtice, R. D. Hobbs, J. L. Sides, J. D. Wieser, C. A. Dyke, D. Tuohey and P. F. Pilger, Reverse-osmosis process successfully converts oil-field brine into fresh-water, Oil & Gas Journal, 91 (1993) 88-91

[237] U.S. Government Printing Office: Washington, DC, Protection of the environment, oil and gas extraction point source category, Code of Federal Regulations, Title 40, Part 435 (2001)

[238] N. Vlasopoulos, F. A. Memon, D. Butler and R. Murphy, Life cycle assessment of wastewater treatment technologies treating petroleum process waters, Science of the Total Environment, 367 (2006) 58-70

[239] C. C. Teodosiu, M. D. Kennedy, H. A. van Straten and J. C. Schippers, Evaluation of secondary refinery effluent treatment using ultrafiltration membranes, Water Research, 33 (1999) 2172-2180

[240] S. V. Zubarev, N. A. Alekseeva, V. N. Ivashentsev, G. P. Yavshits, V. I. Matyushkin, A. I. Bon and I. I. Shishova, Purification of waste-water in petroleum refining industries by membrane methods, Chemistry and Technology of Fuels and Oils, 25 (1989) 588-592

[241] S. Elmaleh and N. Ghaffor, Upgrading oil refinery effluents by cross-flow ultrafiltration, Water Science and Technology, 34 (1996) 231-238

[242] S. M. Santos and M. R. Wiesner, Ultrafiltration of water generated in oil and gas production, Water Environment Research, 69 (1997) 1120-1127

[243] M. Cakmakci, N. Kayaalp and I. Koyuncu, Desalination of produced water from oil production fields by membrane processes, Desalination, 222 (2008) 176-186

[244] J. R. Lu, X. L. Wang, B. T. Shan, X. M. Li and W. D. Wang, Analysis of chemical compositions contributable to chemical oxygen demand (COD) of oilfield produced water, Chemosphere, 62 (2006) 322-331

[245] F. N. Kemmer and Nalco Chemical Company., The Nalco water handbook, McGraw-Hill Book Co., New York, 1988

[246] D. L. Gallup, E. G. Isacoff and D. N. Smith, Use of Ambersorb(r) carbonaceous adsorbent for removal of BTEX compounds from oil-field produced water, Environmental Progress, 15 (1996) 197-203

[247] U.S. Government Printing Office: Washington, DC, Protection of the environment, petroleum refining point source category, Code of Federal Regulations, Title 40, Part 419 (1985)

180

[248] C. Murray-Gulde, J. E. Heatley, T. Karanfil, J. H. Rodgers and J. E. Myers, Performance of a hybrid reverse osmosis-constructed wetland treatment system for brackish oil field produced water, Water Research, 37 (2003) 705-713

[249] J. F. Hester and A. M. Mayes, Hydrophilic surface modification of polymer membranes via surface segregation., Abstracts of Papers of the American Chemical Society, 216 (1998) U630-U630

[250] D. Sehgal and I. K. Vijay, A method for the high-efficiency of water-soluble carbodiimide-mediated amidation, Analytical Biochemistry, 218 (1994) 87-91

[251] G. N. Whitesides, E. Ostuni, R. Chapman, M. Grunze and X. Y. Jiang, Sams and biofunctional surfaces: The "inert surface" problem, Abstracts of Papers of the American Chemical Society, 227 (2004) U354-U354

[252] Y. Y. Luk, M. Kato and M. Mrksich, Self-assembled monolayers of alkanethiolates presenting mannitol groups are inert to protein adsorption and cell attachment, Langmuir, 16 (2000) 9604-9608

[253] E. Ostuni, R. G. Chapman, M. N. Liang, G. Meluleni, G. Pier, D. E. Ingber and G. M. Whitesides, Self-assembled monolayers that resist the adsorption of proteins and the adhesion of bacterial and mammalian cells, Langmuir, 17 (2001) 6336-6343

[254] R. G. Chapman, E. Ostuni, M. N. Liang, G. Meluleni, E. Kim, L. Yan, G. Pier, H. S. Warren and G. M. Whitesides, Polymeric thin films that resist the adsorption of proteins and the adhesion of bacteria, Langmuir, 17 (2001) 1225-1233

[255] R. E. Holmlin, X. X. Chen, R. G. Chapman, S. Takayama and G. M. Whitesides, Zwitterionic SAMs that resist nonspecific adsorption of protein from aqueous buffer, Langmuir, 17 (2001) 2841-2850

[256] A. R. Statz, A. E. Barron and P. B. Messersmith, Protein, cell and bacterial fouling resistance of polypeptoid-modified surfaces: Effect of side-chain chemistry, Soft Matter, 4 (2008) 131-139

[257] A. R. Statz, R. J. Meagher, A. E. Barron and P. B. Messersmith, New peptidomimetic polymers for antifouling surfaces, Journal of the American Chemical Society, 127 (2005) 7972-7973

[258] D. O. H. Teare, W. C. E. Schofield, R. P. Garrod and J. P. S. Badyal, Poly(n-acryloylsarcosine methyl ester) protein-resistant surfaces, Journal of Physical Chemistry B, 109 (2005) 20923-20928

[259] W. Kuhlman, I. Taniguchi, L. G. Griffith and A. M. Mayes, Interplay between PEO tether length and ligand spacing governs cell spreading on RGD-modified PMMA-g-PEO comb copolymers, Biomacromolecules, 8 (2007) 3206-3213

[260] W. A. Kuhlman, E. A. Olivetti, L. G. Griffith and A. M. Mayes, Chain conformations at the surface of a polydisperse amphiphilic comb copolymer film, Macromolecules, 39 (2006) 5122-5126

[261] D. J. Irvine, A. V. G. Ruzette, A. M. Mayes and L. G. Griffith, Nanoscale clustering of RGD peptides at surfaces using comb polymers. 2. Surface segregation of comb polymers in polylactide, Biomacromolecules, 2 (2001) 545-556

[262] P. A. Kavakli and G. Guven, Removal of concentrated heavy metal ions from aqueous solutions using polymers with enriched amidoxime groups, Journal of Applied Polymer Science, 93 (2004) 1705-1710

[263] S. M. C. Ritchie and D. Bhattacharyya, Membrane-based hybrid processes for high water recovery and selective inorganic pollutant separation, Journal of Hazardous Materials, 92 (2002) 21-32

[264] I. Ozawa, K. Saito, K. Sugita, K. Sato, M. Akiba and T. Sugo, High-speed recovery of germanium in a convection-aided mode using functional porous hollow-fiber membranes, Journal of Chromatography A, 888 (2000) 43-49

[265] H. Kawakita, K. Uezu, S. Tsuneda, K. Saito, M. Tamada and T. Sugo, Recovery of Sb(V) using a functional-ligand-containing porous hollow-fiber membrane prepared by radiation-induced graft polymerization, Hydrometallurgy, 81 (2006) 190-196

[266] T. Saito, H. Kawakita, K. Uezu, S. Tsuneda, A. Hirata, K. Saito, M. Tamada and T. Sugo, Structure of polyol-ligand-containing polymer brush on the porous membrane for antimony(III) binding, Journal of Membrane Science, 236 (2004) 65-71

[267] H. A. Abd El-Rehim, E. A. Hegazy and A. E. Ali, Selective removal of some heavy metal ions from aqueous solution using treated polyethylene-g-styrene /maleic anhydride membranes, Reactive & Functional Polymers, 43 (2000) 105-116

[268] S. M. C. Ritchie, K. E. Kissick, L. G. Bachas, S. K. Sikdar, C. Parikh and D. Bhattacharyya, Polycysteine and other polyamino acid functionalized microfiltration membranes for heavy metal capture, Environmental Science & Technology, 35 (2001) 3252-3258

[269] S. Y. Nishiyama, K. Saito, K. Saito, K. Sugita, K. Sato, M. Akiba, T. Saito, S. Tsuneda, A. Hirata, M. Tamada and T. Sugo, High-speed recovery of antimony using chelating porous hollow-fiber membrane, Journal of Membrane Science, 214 (2003) 275-281

[270] C. Charcosset, Purification of proteins by membrane chromatography, Journal of Chemical Technology and Biotechnology, 71 (1998) 95-110

[271] E. Klein, Affinity membranes: A 10-year review, Journal of Membrane Science, 179 (2000) 1-27

[272] C. H. Bamford, K. G. Allamee, M. D. Purbrick and T. J. Wear, Studies of a novel membrane for affinity separations.1. Functionalization and protein coupling, Journal of Chromatography, 606 (1992) 19-31

[273] T. T. Ngo, Facile activation of sepharose hydroxyl-groups by 2-fluoro-1 methylpyridinium toluene-4-sulfonate - preparation of affinity and covalent chromatographic matrices, Bio-Technology, 4 (1986) 134-137

[274] S. M. A. Bueno, K. Haupt and M. A. Vijayalakshmi, Separation of immunoglobulin-g from human serum by pseudobioaffinity chromatography using immobilized l-histidine in hollow-fiber membranes, Journal of Chromatography B-Biomedical Applications, 667 (1995) 57-67

[275] D. Neugebauer, Graft copolymers with poly(ethylene oxide) segments, Polymer International, 56 (2007) 1469-1498

[276] Y. H. See-Toh, M. Silva and A. Livingston, Controlling molecular weight cut-off curves for highly solvent stable organic solvent nanofiltration (OSN) membranes, Journal of Membrane Science, 324 (2008) 220-232

[277] U. Razdan, S. V. Joshi and V. J. Shah, Novel membrane processes for separation of organics, Current Science, 85 (2003) 761-771

[278] P. Vandezande, L. E. M. Gevers and I. F. J. Vankelecom, Solvent resistant nanofiltration: Separating on a molecular level, Chemical Society Reviews, 37 (2008) 365-405

[279] Baker, R.W., Membrane Technology in *Encyclopedia of Polymer Science and Engineering*, H. F. Mark and J. I. Kroschwitz, (Eds.), Wiley, New York (1985)

[280] R. K. Kainthan, M. Gnanamani, M. Ganguli, T. Ghosh, D. E. Brooks, S. Maiti and J. N. Kizhakkedathu, Blood compatibility of novel water soluble hyperbranched polyglycerol-based multivalent cationic polymers and their interaction with DNA, Biomaterials, 27 (2006) 5377-5390

[281] B. Almarzoqi, A. V. George and N. S. Isaacs, The quarternization of tertiary-amines with dihalomethane, Tetrahedron, 42 (1986) 601-607

[282] A. L. A. Silva, I. Takase, R. P. Pereira and A. M. Rocco, Poly(styrene-co-acrylonitrile) based proton conductive membranes, European Polymer Journal, 44 (2008) 1462-1474

[283] T. Saito, B. D. Mather, P. J. Costanzo, F. L. Beyer and T. E. Long, Influence of site-specific sulfonation on acrylic graft copolymer morphology, Macromolecules, 41 (2008) 3503-3512

[284] N. Sasagawa, K. Saito, K. Sugita, S.-i. Kunori and T. Sugo, Ionic cross-linking of SO_3H-group-containing graft chains helps to capture lysozyme in a permeation mode, Journal of Chromatography A, 848 (1999) 161-168

Appendix A:

Representative ¹H-NMR Spectrum of PVDF-*g*-POEM

The ¹H-NMR characterization of poly(vinylidene fluoride)-*graft*-poly(ethylene oxide) methyl ether methacrylate (PVDF-*g*-POEM) was performed based on the protocol described in Hester *et al.*, Macromolecules 35 (2002) 7652-7661. A representative NMR spectrum and peak assignments are given in Figure A.1.
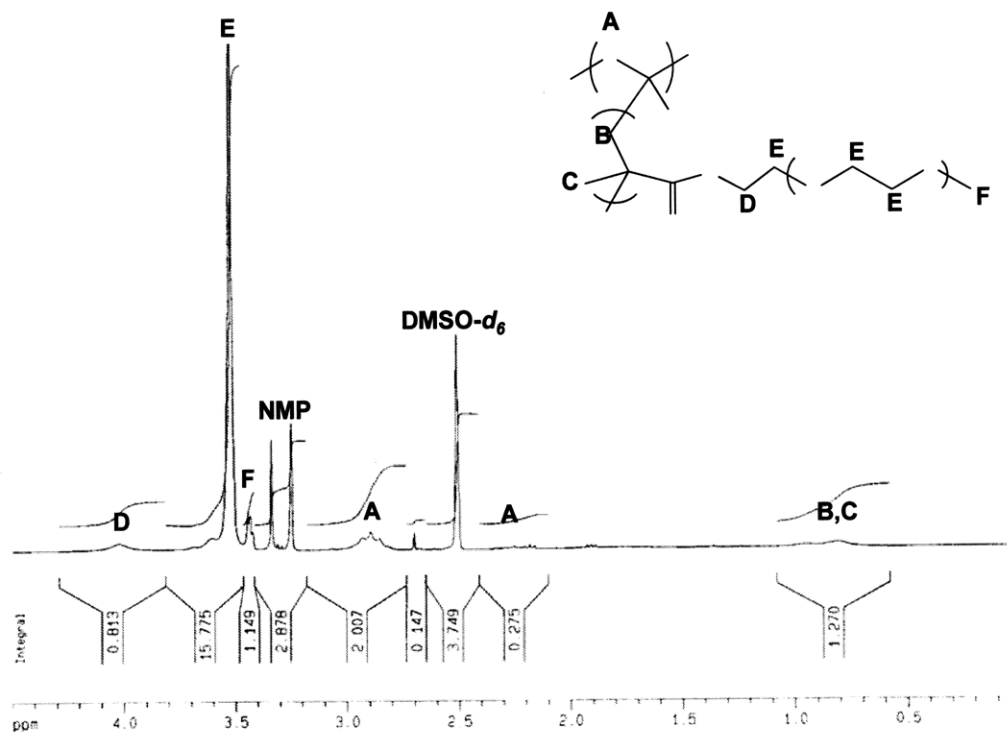
Figure A.1. Representative ¹H-NMR spectrum and peak assignments for PVDF-g-POEM

Appendix B:

Representative ^{1}H-NMR Spectrum of PAN-*g*-PEO

^{1}H-NMR characterization of PAN-*g*-PEO is described in Section 4.3.1 of this thesis. Figure B.1 shows a representative ^{1}H-NMR spectrum as well as the relevant peak assignments.
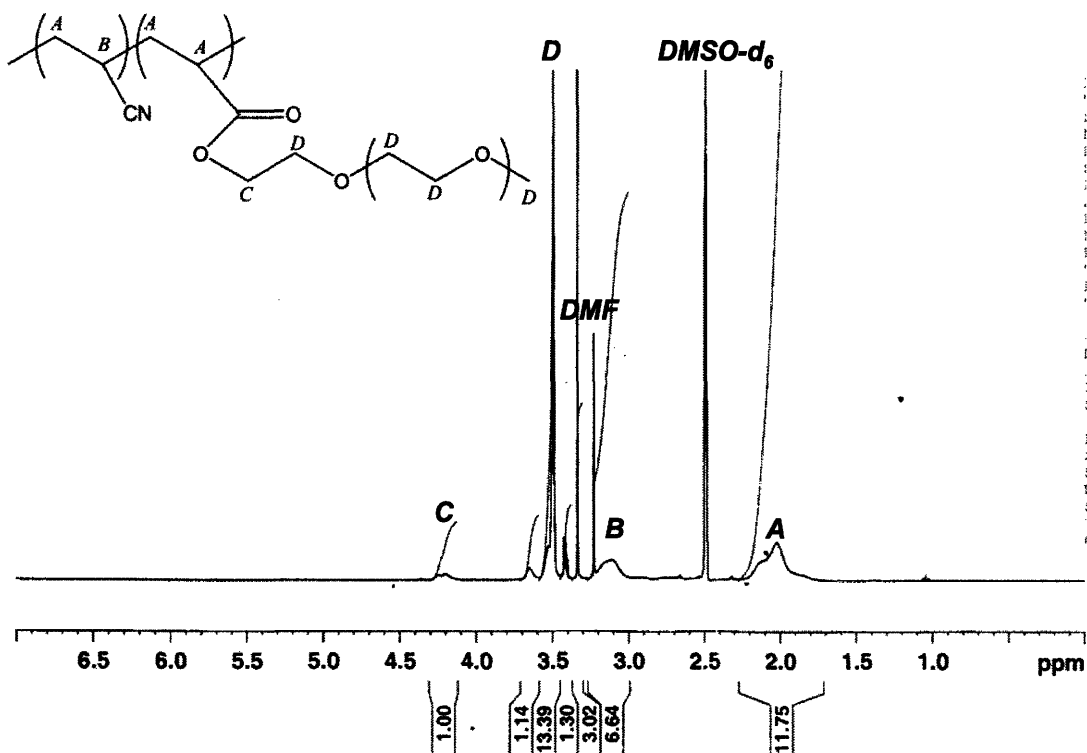

Figure B.1. Representative ^{1}H-NMR spectrum and peak assignments for PAN-g-PEO

Appendix C:

X-Ray Photoelectron Spectroscopy (XPS) data for PAN/PAN-*g*-PEO blend membranes

XPS was used to quantify the surface composition of PAN/PAN-*g*-PEO blend UF membranes (Chapter 5). For this purpose, a survey scan (0-1100 eV binding energy range, 160 eV pass energy) and a high-resolution scan of the C 1s peak (10 eV pass energy) were run for each sample. Table C.1 gives the N/C and O/C ratios calculated from the survey scan for each sample using the default relative surface factor (RSF) values of 0.278, 0.780 and 0.477 for C 1s, O 1s and N 1s peaks, respectively.

Table C.1. Elemental ratios of PAN/PAN-*g*-PEO blend membrane surfaces calculated from XPS survey scans

Membrane	Bulk PEO content (wt%)	O/C ratio	N/C ratio
PAN	0	0.072	0.227
P50-5	1.95	0.087	0.222
P50-10	3.9	0.091	0.206
P50-20	7.8	0.112	0.187
P25-20	5.8	0.078	0.212
P15-20	2.4	0.093	0.210
P50-100	39	0.186	0.146

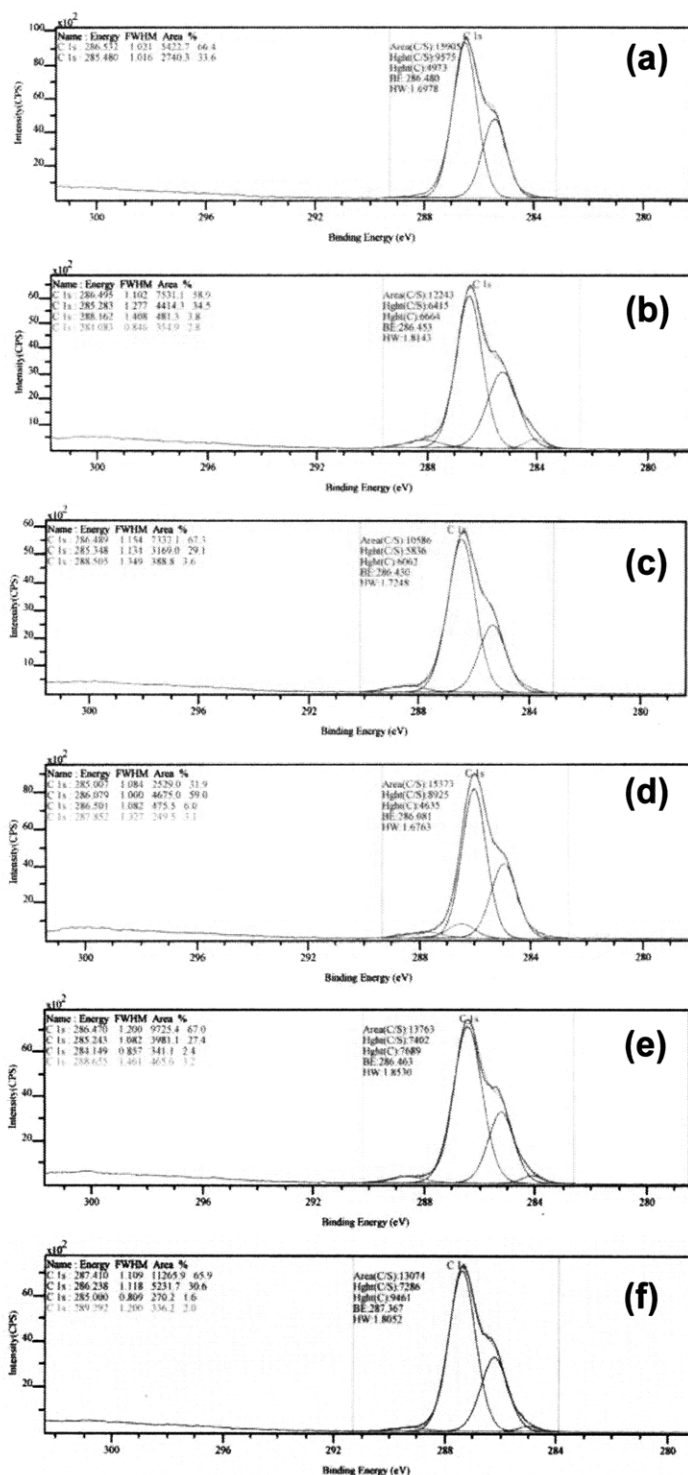High resolution scans of the C 1s peak for these membranes are given in Figure C.1.

Figure C.1. High resolution C 1s scans of PAN/PAN-g-PEO blend membranes (a)PAN, (b) P50-5, (c) P50-10, (d) P50-20, (e) P25-20, (f) P15-20

Biographical Note

EDUCATION

Massachusetts Institute of Technology, Cambridge, MA   2003-2009
Candidate for Ph.D. in Chemical Engineering, Program in Polymer Science and Technology.
Thesis: Amphiphilic Graft Copolymers for Improved Water Purification Membranes, GPA: 5.0/5.0
Thesis advisors: Prof. Anne M. Mayes and Prof. Michael F. Rubner
Estimated graduation date: December 2008

Middle East Technical University, Ankara, Turkey

Bachelor of Science in Chemical Engineering. GPA: 4.0/4.0   June 2002
Bachelor of Science in Chemistry. GPA: 4.0/4.0   January 2003

RESEARCH EXPERIENCE

Massachusetts Institute of Technology, Cambridge, MA
        2003-present
Research Assistant, Department of Materials Science and Engineering.
Thesis advisors: A.M. Mayes, M.F. Rubner

- Developed improved water purification membranes with higher permeabilities and fouling resistance, using principles of copolymer self-assembly.
- Achieved ultrafiltration membranes with complete resistance to irreversible fouling using a single-step casting process.
- Synthesized various graft copolymers, mainly using ATRP, free radical polymerization and copolymerization, macromonomer techniques, and polymer functionalization. Characterized synthesized polymers through NMR and GPC.
- Manufactured ultrafiltration and nanofiltration membranes using phase inversion and coating techniques. Characterized membrane structure by SEM, and membrane surface chemistry by XPS and contact angle.
- Tested ultrafiltration and nanofiltration membranes in dead-end configuration. Improved and systematized membrane manufacture and testing set-up.
- Collaborated with several contacts in the industry and other universities, in areas ranging from AFM methods to analyze the fouling resistance mechanisms, to membrane bioreactor and produced water filtration applications.

TEACHING EXPERIENCE

Massachusetts Institute of Technology, Cambridge, MA   February 2008
Guest Lecturer, Department of Mechanical Engineering
- Gave a guest lecture in Desalination class taught by Prof. Lienhart.
- Covered nanofiltration processes, membranes and applications, and membrane fouling

Massachusetts Institute of Technology, Cambridge, MA   Fall 2006
Instructor-G, Department of Chemical Engineering
- Taught Polymer Science Laboratory together with Prof. Hammond and Prof. Love

- Gave approximately one third of the lectures, contributed to class planning, prepared exam questions, graded exams.

Massachusetts Institute of Technology, Cambridge, MA   Fall 2006
Teaching Assistant, Department of Chemical Engineering
- Led lab section of Polymer Science Laboratory, graded reports, conducted review sessions.
- Redesigned experiment on ultrafiltration and membrane casting, including purchase and set-up of new lab equipment.

Massachusetts Institute of Technology, Cambridge, MA   2005-2006
Research Assistant, Department of Materials Science and Engineering
- Mentored two undergraduates during thesis work.

AWARDS AND ACHIEVEMENTS

- Best Student Oral Presentation, Engineering with Membranes 2008   May 2008
- Best Poster Award, MIT Materials Day   October 2007
- Best Poster Award, MIT Materials Day   October 2005
- Valedictorian among ~2000 graduates, Middle East Technical University June 2002
- Ranked 20th in >1.5 million students in national University Entrance Exam June 1998

PUBLICATIONS AND PATENTS

Peer-Reviewed Journal Articles

- A. Asatekin, E.A. Olivetti, A.M. Mayes, *Fouling resistant, high flux nanofiltration membranes from polyacrylonitrile-graft-poly(ethylene oxide)*, Journal of Membrane Science, submitted
- A. Asatekin, A.M. Mayes, *Oil industry wastewater treatment with fouling resistant membranes containing polyacrylonitrile-graft-poly(ethylene oxide)*, Environmental Science and Technology, submitted
- A. Asatekin, A.M. Mayes, *Responsive pore size properties of composite NF membranes based on PVDF graft copolymers*, Separation Science and Technology, submitted
- A. Asatekin, S. Kang, M. Elimelech and A.M. Mayes, *Anti-fouling ultrafiltration membranes containing polyacrylonitrile-graft-poly(ethylene oxide) comb copolymer additives*, Journal of Membrane Science, 298 (2007) 136-146
- S. Kang, A. Asatekin, A. M. Mayes and M. Elimelech, *Protein antifouling mechanisms of PAN UF membranes incorporating PAN-g-PEO*, Journal of Membrane Science, 296 (2007) 42-50
- A. Asatekin, A. Mennitti, S. Kang, M. Elimelech, E. Morgenroth and A. M. Mayes, *Antifouling nanofiltration membranes for membrane bioreactors from self-assembling graft copolymers*, Journal of Membrane Science, 285 (2006) 81-89
- E. A. Olivetti, J. H. Kim, D. R. Sadoway, A. Asatekin and A. M. Mayes, *Sol-gel synthesis of vanadium oxide within a block copolymer matrix*, Chemistry of Materials, 18 (2006) 2828-2833

Encyclopedia Section

- A. Asatekin, A.M. Mayes, *Polymer Filtration Membranes*, Encyclopedia of Polymer Science and Technology, submitted

Patent Application

- A.M. Mayes and A..Asatekin, *Fouling resistant membranes formed with polyacrylonitrile graft copolymers*. MIT Case No.12171, PCT application PCT/US2007/008797 filed April 10, 2007.

Conference Proceedings

- Asatekin, A., A.M. Mayes, *Performance of polyacrylonitrile-graft-poly(ethylene glycol) (PAN-g-PEG) containing ultrafiltration membranes*, Abstracts of Papers of the American Chemical Society, 235 (2008) ENVR 70
- Asatekin, A., A.M. Mayes, *Amphiphilic Graft Copolymers for High-Flux, Fouling Resistant Membranes for Ultrafiltration and Nanofiltration*, Abstracts of Papers of the American Chemical Society, 233 (2007) SUST 58
- Asatekin, A., A.M. Mayes, *Polyacrylonitrile-graft-poly(ethylene glycol) (PAN-g-PEG) for size-selective, fouling resistant nanofiltration (NF) membranes*, Abstracts of Papers of the American Chemical Society, 233 (2007) PMSE 383

INDUSTRY EXPERIENCE

Procter & Gamble European Technology Center, Brussels, Belgium   Summer 2001
Summer intern, Research & Development

- Evaluated and optimized laundry detergent performance for use in pretreatment.

Kordsa A.S. Nylon Yarn Production Plant, Izmit, Turkey   Summer 2000
Summer intern, Technical Department

- Monitored and investigated the causes of yarn breakage in spinning stage

SELECTED PRESENTATIONS

Invited Talks

- "Fouling resistant nanofiltration membranes with tunable subnanometer size selectivity", A. Asatekin, A.M. Mayes, Engineering with Membranes 2008 International Conference, Vale do lobo, Algarve, Portugal, May 27th, 2008
- "Amphiphilic comb copolymers for better water purification membranes", A. Asatekin, S. Kang, E. Olivetti, M. Elimelech, M.F. Rubner, A.M. Mayes, Millipore Research & Development Center, Bedford, MA, July 26th, 2007
- "Amphiphilic graft copolymers for fouling resistant membranes", A. Asatekin, A.M. Mayes, Middle East Technical University Department of Chemical Engineering seminar, Ankara, Turkey, June 26, 2006.

Contributed Oral Presentations

- "Performance of polyacrylonitrile-graft-poly(ethylene oxide) (PAN-g-PEO) containing ultrafiltration membranes", A. Asatekin, A.M. Mayes, American Chemical Society (ACS) 2008 Spring Meeting, New Orleans, LA, April 7, 2008.

- "Anti-fouling ultrafiltration membranes containing polyacrylonitrile-graft-poly(ethylene oxide) comb copolymer additives", A. Asatekin, S. Kang, M. Elimelech, M.F. Rubner, A.M. Mayes, Materials Research Society (MRS) 2007 Fall Meeting, Boston, MA, November 27, 2007.
- "Anti-fouling ultrafiltration membranes containing polyacrylonitrile-graft-poly(ethylene oxide) comb copolymer additives", A. Asatekin, S. Kang, M. Elimelech, M.F. Rubner, A.M. Mayes, North American Membrane Society (NAMS) 2007 Annual Meeting, Orlando, FL, May 14, 2007.
- "Amphiphilic Graft Copolymers for High-Flux, Fouling Resistant Membranes for Ultrafiltration and Nanofiltration", A. Asatekin, A.M. Mayes, ACS Spring 2007 Meeting, Chicago, IL, March 27, 2007.
- "Amphiphilic graft copolymers for nanofiltration membranes with tunable pore size", A. Asatekin, A.M. Mayes, MRS Fall 2006 Meeting, Boston, MA, November 28, 2006
- "Amphiphilic graft copolymers for fouling resistant membranes", A. Asatekin, A.M. Mayes, 1st National Polymer Science and Technology Conference, Ankara, Turkey, June 23, 2006.
- "Amphiphilic graft copolymers for high-flux fouling resistant membranes", A. Asatekin, A.M. Mayes, NAMS 2006 Annual Meeting, Chicago, IL, May 17, 2006.
- "Amphiphilic graft copolymers for high-flux, fouling resistant membranes", A. Asatekin, A.M. Mayes, WaterCAMPWS Symposium at MRS Spring Meeting, San Francisco, CA, April 17, 2006.

MEMBERSHIPS

American Chemical Society (ACS), Materials Research Society (MRS), North American Membrane Society (NAMS).